AOP ID and Title:

AOP 331: Increase in reactive oxygen species leading to growth inhibition via lipid peroxidation and cell death
Short Title: ROS leading to growth inhibition via LPO and cell death

Graphical Representation

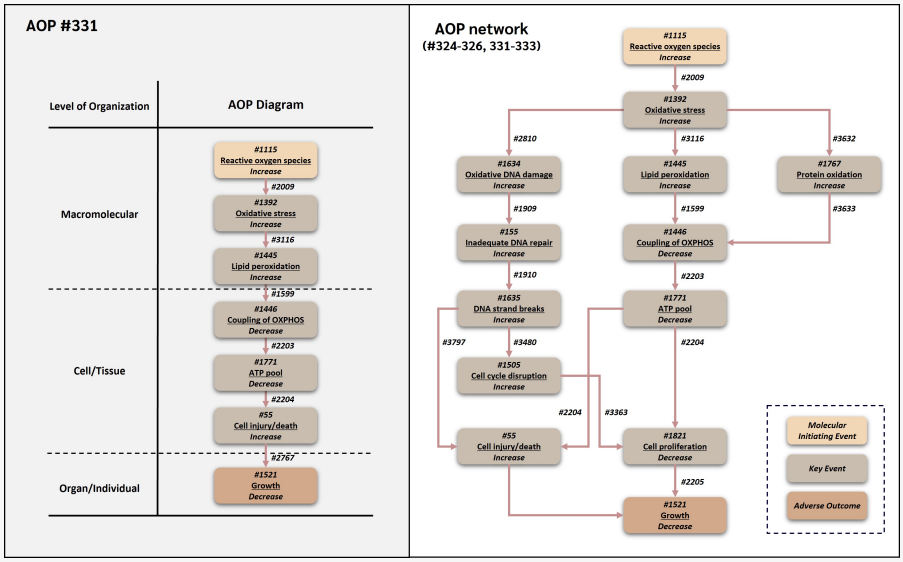

Authors

You Song, Li Xie, Knut Erik Tollefsen

Norwegian Institute for Water Research (NIVA), Sognsveien 72, 0855, Oslo, Norway

Status

Author status	OECD status	OECD project	SAAOP status
Under development: Not open for comment. Do not cite	Under Development		

Coaches

Shihori Tanabe

Abstract

This adverse outcome pathway (AOP 331) describes a linear route by which increased reactive oxygen species (ROS) can lead to decreased organismal growth through lipid peroxidation-mediated mitochondrial bioenergetic impairment and increased cell injury/death. In this AOP, increased ROS is treated operationally as the molecular initiating event because it represents the earliest common measurable redox perturbation shared by many chemical and non-chemical stressors within the broader ROS-growth AOP network. Increased ROS leads to oxidative stress, which promotes lipid peroxidation. Oxidative damage to membrane lipids can impair mitochondrial membrane integrity and coupling of oxidative phosphorylation (OXPHOS). Decreased OXPHOS coupling reduces ATP production, and insufficient ATP availability can compromise membrane homeostasis, ion transport, biosynthesis, stress-response capacity, and execution of regulated cell death pathways, ultimately resulting in increased cell injury/death. Increased loss of viable cells, particularly in developing, growing, or regenerating tissues and organisms, can contribute to decreased growth.

AOP 331 reuses and connects established AOP-Wiki components from several AOP contexts. The upstream ROS and oxidative stress segment is associated with AOP 478, in which deposition of energy leads to oxidative stress through increased free radical generation (AOP-Wiki, 2026a). The lipid peroxidation and mitochondrial bioenergetic segment is connected to the oxidative stress and mitochondrial impairment logic represented in the broader ROS-growth AOP network, while the KER from decreased coupling of OXPHOS to decreased ATP pool is directly associated with AOP 263, an OECD-published AOP that causally links uncoupling of OXPHOS to growth inhibition through ATP depletion and decreased cell proliferation (AOP-Wiki, 2026b; OECD, 2022; Song and Villeneuve, 2021). AOP 331 differs from AOP 326 by routing ATP depletion through increased cell injury/death rather than decreased cell proliferation. This terminal cellular injury module is supported by reuse of the broadly shared AOP-Wiki KE 'Increase, Cell injury/death' and by its occurrence in several AOPs, including AOPs 12, 13, 17, 38, and 48, where cell injury/death is used as an intermediate or downstream KE in neurotoxicity, oxidative stress, fibrosis, and excitotoxicity contexts (AOP-Wiki, 2026c-g). The AOP is relevant to environmental and human health contexts because ROS production, lipid peroxidation, mitochondrial ATP production, cell viability, and growth are conserved biological processes. It can support mechanistic interpretation of oxidative stress-mediated growth impairment, assay selection, chemical

prioritization, integrated approaches to testing and assessment (IATA), and quantitative AOP development for oxidative and mitochondrial toxicity.

Acknowledgement

This project was funded by the Research Council of Norway (RCN), grant no. RCN-315929 “EXPECT: In silico and experimental screening platform for characterizing environmental impact of industry development in the Arctic” (https://www.niva.no/en/projects/expect), the European Partnership for the Assessment of Risks from Chemicals (PARC) through European Union’s Horizon Europe research and innovation programme (Grant Agreement No 101057014, and supported by the NIVA Computational Toxicology Program, NCTP (https://www.niva.no/en/featured-pages/nctp, grant. No. RCN-342628).

AI disclosure

Artificial intelligence (AI) tools were used to support literature prioritization, review and AOP-Wiki page preparation in this work. AOP-helpFinder was used for automated literature mining, and ChatGPT (OpenAI) was used as an auxiliary tool for title and abstract screening, extraction of study metadata, and identification of potential weight-of-evidence indicators. AI-assisted outputs were used only to organize and prioritize information and were verified against the original sources by the authors before inclusion. Additional AI assistance was used for formatting, copy-editing, citation cross-checking, and harmonization of the AOP-Wiki pages. All scientific interpretations, weight-of-evidence judgments, final wording, and conclusions were determined and approved by the authors, who take full responsibility for the content and integrity of the work.

AOP Development Strategy

Context

ROS are continuously formed during aerobic metabolism and can also be generated in response to environmental stressors. At controlled levels, ROS participate in redox signaling, whereas excessive ROS can disturb redox homeostasis and initiate oxidative stress (Schieber and Chandel, 2014; Sies et al., 2017). Lipid membranes are important targets of oxidative attack because phospholipids containing polyunsaturated fatty acids can undergo radical-driven peroxidation. Lipid peroxidation generates lipid hydroperoxides and secondary reactive aldehydes, including malondialdehyde and 4-hydroxy-2-nonenal, which can propagate oxidative injury and alter membrane-associated protein and organelle function (Ayala et al., 2014).

AOP 331 was developed to represent the lipid peroxidation and cell injury/death-driven linear route within the broader ROS-growth AOP network. This route was selected because lipid peroxidation is a well-established consequence of oxidative stress and because mitochondrial membranes are central determinants of OXPHOS coupling. Peroxidative modification of mitochondrial membrane lipids can alter membrane fluidity, proton leak, respiratory control, and mitochondrial membrane potential, providing a mechanistically coherent bridge from oxidative stress to impaired ATP production (Murphy, 2009; Nicholls and Ferguson, 2013; Ouillon et al., 2021). ATP depletion is a well-established contributor to loss of cell viability because cellular survival depends on ATP-dependent ion gradients, membrane repair, protein turnover, stress-response pathways, and the execution of regulated death processes. Depletion of ATP can shift cells from adaptive responses to injury and death, and severe ATP loss can affect the mode of cell death (Leist et al., 1997; Bonora et al., 2012).

The AOP was also developed to take advantage of existing AOP-Wiki modularity. The upstream oxidative stress context is associated with AOP 478, while the OXPHOS-to-ATP KER is associated with AOP 263 (AOP-Wiki, 2026a,b; OECD, 2022). The cell injury/death KE is a highly reusable AOP-Wiki KE and appears across several established AOPs. AOP 17 explicitly includes oxidative stress leading to cell injury/death and also includes several KERs involving cell injury/death and neuroinflammation (AOP-Wiki, 2026e). AOP 48 includes mitochondrial dysfunction leading to cell injury/death in an excitotoxicity context (AOP-Wiki, 2026g). AOP 38 uses cell injury and cell death as key early tissue-level consequences of protein alkylation leading to fibrosis (AOP-Wiki, 2026f). AOPs 12 and 13 also use cell injury/death in neurodegeneration and synaptogenesis-related contexts (AOP-Wiki, 2026c,d). These associations support the reuse of Event 55 as a generic, modular cellular KE downstream of multiple upstream stressors and upstream of multiple adverse outcomes.

Strategy

AOP 331 was developed using the principles described in OECD AOP guidance, including modular description of KEs and KERs, reuse of existing AOP-Wiki content where appropriate, evidence evaluation using biological plausibility, empirical support, essentiality, and quantitative understanding, and clear description of the biological domain of applicability (OECD, 2018, 2021). The aim was to assemble a focused linear pathway from reusable AOP-Wiki elements rather than to create an isolated de novo pathway. This is important because AOP 331 is one branch of the broader ROS-growth AOP network and because its KEs overlap with oxidative stress, mitochondrial dysfunction, cellular energy metabolism, cell injury/death, and growth-related AOPs.

Reuse of existing AOP-Wiki content was considered at the outset. AOP 478 was reviewed because it provides an AOP-Wiki precedent for oxidative stress as a central KE downstream of free radical generation and energy deposition. AOP 263 was reviewed because it provides an OECD-published downstream bioenergetics module in which decreased coupling of OXPHOS leads to decreased ATP pool and subsequently growth inhibition, although in

AOP 263 the terminal cellular route proceeds through decreased cell proliferation rather than cell injury/death. AOPs 12, 13, 17, 38, and 48 were reviewed because they demonstrate repeated reuse of Event 55, 'Increase, Cell injury/death', across different biological contexts and provide support for treating cell injury/death as a modular KE that can connect distinct upstream mechanisms to downstream tissue or organism-level outcomes. AOP 296 was reviewed during development of the broader ROS-growth network to ensure that oxidative stress and macromolecular damage modules were harmonized with existing oxidative damage content, although AOP 331 specifically follows the lipid peroxidation and bioenergetic injury branch rather than the oxidative DNA damage branch.

The evidence base was assembled through an AI-human hybrid workflow. First, search terms were developed for each KE, including KE names, synonyms, endpoint names, assay terms, taxa, and representative stressors. AOP-helpFinder was used to search PubMed for co-occurrence between key events and related biological concepts, and the exported outputs included PMIDs, titles, abstracts, and matched KE terms (Carvaillo et al., 2019; Jornod et al., 2022). The exported records were subjected to overlap analysis to remove redundant hits and to filter taxa-related or clearly irrelevant literature.

Second, ChatGPT (OpenAI, San Francisco, CA, USA)-assisted screening was used as an auxiliary prioritization step. The LLM was used to pre-screen titles and abstracts, extract study metadata including stressor, species, biological system, dose or concentration, and exposure time, identify evidence types such as biological plausibility, empirical support, and essentiality, and flag weight-of-evidence indicators such as dose-response concordance, temporal concordance, incidence concordance, and intervention evidence. The LLM output was used to classify studies as high relevance, medium relevance, or low/not relevant. High-relevance studies were retrieved for full-text review, medium-relevance studies were reserved as supporting evidence, and low-relevance studies were documented as low priority or excluded.

Third, full-text review and expert curation were used to verify all evidence before inclusion in the AOP. LLM-assisted full-text review was used only to organize candidate evidence; all extracted information was checked manually against the original text. Expert review was then used to populate KER evidence tables with methods, endpoints, results, weight-of-evidence category, and references. Final weight-of-evidence evaluation was performed by expert judgment using biological plausibility, empirical support, essentiality, quantitative understanding, and identification of evidence gaps. Thus, the development process combined text-mining and AI-assisted evidence handling with human expert verification and final decision-making.

In parallel with this workflow, targeted searches were conducted to fill specific evidence gaps for ROS, oxidative stress, lipid peroxidation, mitochondrial membrane potential, OXPHOS coupling, ATP depletion, cytotoxicity, cell death, and growth inhibition. Studies were prioritized when they measured two or more KEs in the same biological system, reported dose or concentration and exposure time, or provided evidence relevant to dose-response, temporal, or incidence concordance. Mechanistic reviews and OECD reports were used primarily to support biological plausibility, while primary experimental studies were used to support empirical concordance wherever possible.

Summary of the AOP

Events

Molecular Initiating Events (MIE), Key Events (KE), Adverse Outcomes (AO)

Sequence	Type	Event ID	Title	Short name
	MIE	1115	Increase, Reactive oxygen species	Increase, ROS
	KE	1392	Increase, Oxidative Stress	Increase, Oxidative Stress
	KE	1445	Increase, Lipid peroxidation	Increase, LPO
	KE	1446	Decrease, Coupling of oxidative phosphorylation	Decrease, Coupling of OXPHOS
	KE	1771	Decrease, Adenosine triphosphate pool	Decrease, ATP pool
	KE	55	Increase, Cell injury/death	Cell injury/death
	AO	1521	Decrease, Growth	Decrease, Growth

Key Event Relationships

Upstream Event	Relationship Type	Downstream Event	Evidence	Quantitative Understanding
Increase, Reactive oxygen species	adjacent	Increase, Oxidative Stress	High	Moderate
Increase, Oxidative Stress	adjacent	Increase, Lipid peroxidation	High	Moderate
Increase, Lipid peroxidation	adjacent	Decrease, Coupling of oxidative phosphorylation	High	Moderate

Upstream Event	Relationship Type	Downstream Event	Evidence	Quantitative Understanding
Decrease, Coupling of oxidative phosphorylation	adjacent	Decrease, Adenosine triphosphate pool	High	High
Decrease, Adenosine triphosphate pool	adjacent	Increase, Cell injury/death	High	Moderate
Increase, Cell injury/death	adjacent	Decrease, Growth	High	Moderate

Stressors

Name	Evidence
Ultraviolet B radiation	High
Hydrogen peroxide	
Paraquat	
tert-Butyl hydroperoxide	
Heavy metals (cadmium, lead, copper, iron, nickel)	
Silver	
Silver nanoparticles	
Ionizing Radiation	

Overall Assessment of the AOP

The overall weight of evidence supporting AOP 331 is considered moderate. Biological plausibility is high for all six KERs in the pathway. The upstream oxidative stress, lipid peroxidation, and OXPHOS uncoupling sequence follows a well-established mechanistic logic, and the connection from ATP depletion to cell injury/death is supported by the fundamental dependence of cellular survival on adequate energy supply. The cell injury/death-to-growth relationship is reinforced by the broad reuse of Event 55 (Increase, Cell injury/death) as a modular KE across endorsed AOPs 12, 13, 17, 38, and 48 (AOP-Wiki, 2026a-e). The OXPHOS-to-ATP module is directly associated with OECD-endorsed AOP 263 and contributes high biological plausibility and strong quantitative understanding for this segment (OECD, 2022; Song and Villeneuve, 2021). Empirical support is high for the ROS-to-oxidative-stress and oxidative-stress-to-lipid-peroxidation relationships, moderate for the lipid-peroxidation-to-OXPHOS link, and moderate to high for the ATP-depletion-to-cell-death and OXPHOS-to-ATP relationships. The cell death-to-growth relationship has moderate empirical support, as direct concurrent measurement of cell injury/death and organismal growth is less common across the available literature. Essentiality is rated moderate to high overall, with the strongest direct evidence for the AOP 263 bioenergetics segment. Quantitative understanding is highest for the OXPHOS-to-ATP KER and low to moderate elsewhere. The main uncertainties are the quantitative thresholds governing the lipid-peroxidation-to-OXPHOS transition, the severity-dependent mode of cell death triggered by ATP depletion, and the extent to which cell injury/death versus reduced proliferation drives growth impairment in specific biological contexts. AOP 331 is most appropriate for mechanistic interpretation of cytotoxic growth impairment caused by oxidative lipid damage, IATA development, and chemical prioritisation (OECD, 2018; Becker et al., 2015).

Domain of Applicability

Life Stage Applicability

Life Stage	Evidence
All life stages	Moderate

Taxonomic Applicability

Term	Scientific Term	Evidence	Links
humans	Homo sapiens	High	NCBI
mammals	mammals	High	NCBI
fish	fish	High	NCBI
crustaceans	Daphnia magna	Moderate	NCBI
green algae	Ulva compressa	High	NCBI

Sex Applicability

Sex	Evidence
Unspecific	Moderate

The domain of applicability for AOP 331 is broad across aerobic eukaryotic organisms in which ROS generation, oxidative stress responses, lipid peroxidation, mitochondrial oxidative phosphorylation, ATP-dependent homeostasis, cell injury/death, and growth are biologically relevant. The AOP is most applicable to taxa and life stages in which

growth depends strongly on maintenance of viable cell number, tissue condition, and mitochondrial energy supply. This includes algae, aquatic invertebrates, fish embryos and juveniles, mollusks, and mammalian or human cell systems.

The stressor domain includes direct ROS generators, redox-cycling chemicals, metals, nanoparticles, mitochondrial toxicants, hypoxia-reoxygenation, and radiation. Because the MIE is defined operationally as increased ROS rather than as a chemical-specific molecular interaction, AOP 331 should be applied to stressors for which evidence supports increased ROS or oxidative stress and downstream concordance with lipid peroxidation, mitochondrial impairment, ATP depletion, cell injury/death, and decreased growth. Environmental factors such as oxygen availability, temperature, lipid composition, diet, nutrient status, and antioxidant capacity may modulate the pathway.

Essentiality of the Key Events

Essentiality is evaluated for the overall AOP based on whether preventing or modifying upstream KEs changes downstream KEs or the AO. Direct essentiality evidence is strongest for the OXPHOS to ATP relationship and for ATP dependence of cell viability. Essentiality for lipid peroxidation is biologically plausible and supported by intervention and association studies, but direct experiments showing that blocking lipid peroxidation prevents all downstream events are less common.

Key event	Essentiality	Rationale	Experimental manipulation evidence (KE knock-out / inhibition / rescue)	Uncertainties
Event 1115: Reactive oxygen species, increased	Moderate	ROS scavenging and antioxidant interventions frequently attenuate oxidative stress and downstream lipid peroxidation in oxidative stress models (Schieber and Chandel, 2014; Sies et al., 2017).	Indirect (stop/attenuation): antioxidant and ROS-scavenger pre-treatment reduces oxidative stress and downstream damage across oxidative-stress models (Schieber and Chandel, 2014; Sies et al., 2017). No selective single-source ROS knock-out is available.	ROS also participate in normal signaling; increased ROS does not always progress to adversity if compensation occurs.
Event 1392: Oxidative stress, increased	Moderate to high	Oxidative stress is required for lipid peroxidation when oxidant production exceeds antioxidant buffering. AOP 478 and AOP 17 support oxidative stress as a central KE downstream of free radical generation or decreased protection against oxidative stress (AOP-Wiki, 2026a,e).	Indirect: modulation of antioxidant capacity alters progression to oxidative macromolecular damage; oxidative stress is the curated hub KE in endorsed AOP 478 (AOP-Wiki, 2026a; Carrothers et al., 2025).	Oxidative stress is measured using several indirect biomarkers that may not be equivalent across systems.

Event 1445: Lipid peroxidation, increased	Moderate	Lipid peroxidation can alter membrane properties and generate reactive aldehydes that affect mitochondrial function (Ayala et al., 2014). Dietary PUFA studies in Daphnia show higher lipid peroxidation with lower mitochondrial membrane potential (Moore et al., 2023).	Indirect: antioxidant intervention attenuates lipid peroxidation in oxidative-stress models; direct block-and-rescue isolating LPO from other oxidative damage is uncommon (Murphy, 2009; Ouillon et al., 2021).	Direct blocking experiments are limited; lipid peroxidation may be both a cause and consequence of mitochondrial dysfunction.
Event 1446: Coupling of OXPHOS, decreased	High	The KER from decreased OXPHOS coupling to ATP depletion is associated with AOP 263, where restoration or removal of uncoupling supports a causal role for impaired coupling in ATP depletion (AOP-Wiki, 2026b; OECD, 2022; Song and Villeneuve, 2021).	Direct (rescue): removal of uncouplers or restoration of coupling recovers mitochondrial membrane potential and ATP in the endorsed AOP 263 module (AOP-Wiki, 2026b; OECD, 2022; Song and Villeneuve, 2021).	Mild uncoupling can sometimes reduce ROS generation and may be adaptive; severity and duration determine adversity.

Event 1771: ATP pool, decreased	High	ATP is required for maintenance of ion gradients, membrane repair, cellular stress responses, and execution of regulated cell death pathways. Severe ATP depletion is a well-established determinant of cell injury/death mode and severity (Leist et al., 1997; Bonora et al., 2012).	Indirect: ATP-restoration experiments reduce downstream injury/proliferation deficits; central KE in endorsed AOP 263 (Leist et al., 1997; Nicotera et al., 1998; OECD, 2022).	Compensatory glycolysis can buffer ATP depletion; total ATP may reflect changing cell number in some assays.
Event 55: Cell injury/death, increased	Moderate	Cell injury/death is a shared AOP-Wiki KE used in AOPs 12, 13, 17, 38, and 48. Loss of viable cells provides a plausible and broadly supported mechanism for reduced tissue or organismal growth (AOP-Wiki, 2026c-g).	Indirect: ATP restoration/maintenance reduces injury in some systems, indicating energy-status dependence (Leist et al., 1997; Nicotera et al., 1998); widely reused modular KE (AOPs 12, 13, 17, 38, 48).	Growth can also decrease through reduced proliferation, altered cell size, endocrine disruption, or energy allocation without overt cell death.
Event 1521: Growth, decreased (AO)	Not applicable (AO)	Growth is the adverse outcome and is regulatory relevant across algae, aquatic invertebrate, fish, amphibian, and plant test systems. AOP 263 provides precedent for using decreased growth as an AO in a mitochondrial bioenergetics AOP (OECD, 2022; Song and Villeneuve, 2021).	As the adverse outcome, essentiality is assessed for upstream KEs; AOP 263 provides precedent for decreased growth as an AO downstream of these modules (OECD, 2022; Song and Villeneuve, 2021).	Growth is integrative and can arise through multiple interacting mechanisms.

Weight of Evidence Summary

Evidence assessment is organized by KER. Calls follow OECD weight-of-evidence considerations for biological plausibility, empirical support, and quantitative understanding (OECD, 2018, 2021).

Biological plausibility of KERs

KER	Biological plausibility call	Rationale
Relationship 2009: ROS increase leads to oxidative stress increase	High	Oxidative stress reflects an imbalance between oxidant production and antioxidant capacity, and ROS are primary oxidant species in cellular redox biology (Schieber and Chandel, 2014; Sies et al., 2017). AOP 478 supports oxidative stress downstream of free radical generation (AOP-Wiki, 2026a).
Relationship 3116: oxidative stress increase leads to lipid peroxidation increase	High	ROS can initiate peroxidation of polyunsaturated fatty acids in membranes, generating lipid hydroperoxides and reactive aldehydes such as MDA and 4-HNE (Ayala et al., 2014; Sies et al., 2017).
Relationship 1599: lipid peroxidation increase leads to decreased coupling of OXPHOS	High	Mitochondrial coupling depends on inner mitochondrial membrane integrity. Lipid peroxidation can disrupt membrane properties, promote proton leak, alter membrane potential, and impair respiratory control (Murphy, 2009; Nicholls and Ferguson, 2013; Ouillon et al., 2021).
Relationship 2203: decreased coupling of OXPHOS leads to decreased ATP pool	High	This relationship is associated with AOP 263. OXPHOS coupling is a major determinant of ATP production in aerobic eukaryotic cells; reduced coupling lowers ATP synthesis efficiency (AOP-Wiki, 2026b; OECD, 2022; Song and Villeneuve, 2021).
Relationship 2768: decreased ATP pool leads to increased cell injury/death	High	ATP is required for survival, ion homeostasis, membrane repair, and regulated death processes. Severe ATP depletion can switch cellular outcomes toward necrosis or irreversible injury, while less severe depletion may permit apoptosis (Leist et al., 1997; Bonora et al., 2012).
Relationship 2767: increased cell injury/death leads to decreased growth	High	Growth depends on viable cell number, tissue integrity, and biomass accumulation. Increased cell death or injury reduces the cellular basis for growth and can impair tissue or organismal development (Conlon and Raff, 1999). Cell injury/death is reused across AOPs 12, 13, 17, 38, and 48 (AOP-Wiki, 2026c-g).

Empirical support for KERs

KER	Empirical support call	Rationale	Inconsistencies or evidence gaps
Relationship 2009: ROS increase leads to oxidative stress increase	High	Paraquat increased ROS and antioxidant enzyme responses in Chlorella vulgaris (Qian et al., 2009), and paraquat induced oxidative stress responses in Daphnia magna (Barata et al., 2005). AOP 478 reports extensive evidence linking free radical generation/energy deposition to oxidative stress (AOP-Wiki, 2026a).	ROS is often transient and measured indirectly; oxidative stress biomarkers vary across assays and taxa.

Relationship 3116: oxidative stress increase leads to lipid peroxidation increase	High	Copper increased antioxidant enzyme activity and MDA/TBARS in freshwater green microalgae (Knauert and Knauer, 2008). Paraquat induced lipid peroxidation in algae and Daphnia (Barata et al., 2005; Esperanza et al., 2015; Qian et al., 2009). Gamma radiation in Lemna minor induced a sequential oxidative stress to lipid peroxidation response upstream of mitochondrial membrane potential loss and cell death (Xie et al., 2019; Xie et al., 2022).	MDA/TBARS endpoints can lack specificity; lipid peroxidation and antioxidant responses may have different time courses.
Relationship 1599: lipid peroxidation increase leads to decreased coupling of OXPHOS	Moderate	Dietary PUFA manipulation in Daphnia showed higher lipid peroxidation associated with lower mitochondrial membrane potential (Moore et al., 2023). Cyclic hypoxia in Mya arenaria increased proton leak and reduced OXPHOS coupling efficiency, consistent with oxidative membrane damage effects on mitochondrial coupling (Ouillon et al., 2021). In Lemna minor, lipid peroxidation preceded mitochondrial membrane potential reduction under gamma radiation and 3,5-dichlorophenol exposure, supporting this link in an aquatic primary producer (Xie et al., 2018; Xie et al., 2019).	Direct studies measuring lipid peroxidation and OXPHOS coupling in the same exposure series are limited; mitochondrial dysfunction can also drive lipid peroxidation.
Relationship 2203: decreased coupling of OXPHOS leads to decreased ATP pool	High	AOP 263 reports strong evidence for this KER (AOP-Wiki, 2026b; OECD, 2022; Song and Villeneuve, 2021). Cadmium exposure in oysters reduced state 3 respiration and affected mitochondrial bioenergetics (Sokolova et al., 2005).	Compensatory glycolysis and altered metabolic demand can obscure total ATP changes.
Relationship 2768: decreased ATP pool leads to increased cell injury/death	Moderate to high	ATP depletion and cell death are linked in multiple cell systems. Intracellular ATP concentration influences the decision between apoptosis and necrosis (Leist et al., 1997). Calcium electroporation caused dose-dependent ATP depletion and cancer cell death (Hansen et al., 2015).	ATP assays may reflect both energy state and cell number; direct temporal separation of ATP depletion from cell death is needed.
Relationship 2767: increased cell injury/death leads to decreased growth	Moderate	In Daphnia, toxicant-induced physiological energy disruption and cell/tissue injury are associated with growth reduction (Knops et al., 2001). In bivalves, cadmium and temperature interactions caused cellular energy disruption, mortality, and reduced condition/growth-related outcomes (Cherkasov et al., 2006). Methanol-exposed mouse embryos showed growth reduction and elevated cell death (Abbott et al., 1995).	Growth can be reduced by mechanisms other than cell death; direct dose/time concordance between cell death and growth is not always measured.

Inconsistencies and uncertainties

The main uncertainty for AOP 331 is the quantitative strength and directionality of the lipid peroxidation to OXPHOS coupling relationship. Lipid peroxidation can impair mitochondrial membranes, but mitochondrial dysfunction can also enhance ROS generation and thereby increase lipid peroxidation. AOP 331 represents one biologically plausible and empirically supported direction within a broader feedback-prone network. Another uncertainty is that ATP depletion can lead to different cellular outcomes depending on severity and duration; moderate depletion may reduce proliferation or activate adaptive stress responses, whereas severe depletion promotes cell injury/death. Finally, growth is a multifactorial endpoint. Increased cell injury/death is an important contributor to impaired growth, but decreased growth can also arise through reduced proliferation, altered cell size, altered energy allocation, endocrine signaling, or developmental delay without overt cell death.

Quantitative Consideration

Quantitative understanding varies across the AOP. The relationship between OXPHOS coupling and ATP production has the strongest quantitative foundation, while the relationships linking oxidative stress to lipid peroxidation and cell injury/death to organismal growth are more often qualitative or semi-quantitative.

KER	Quantitative understanding call	Rationale
2009: ROS increase to oxidative stress increase	Low to moderate	ROS measurements are reactive, transient, and assay-dependent. Quantitative relationships can be defined within a specific assay, but generalizable prediction across taxa and stressors remains limited (Sies et al., 2017).
3116: oxidative stress increase to lipid peroxidation increase	Low to moderate	Dose-response relationships are reported for oxidative stress markers and lipid peroxidation, but lipid composition and assay differences strongly affect response magnitude (Ayala et al., 2014; Knauert and Knauer, 2008).
1599: lipid peroxidation increase to decreased OXPHOS coupling	Low to moderate	Quantitative associations exist between lipid peroxidation and mitochondrial membrane potential or coupling efficiency, but broadly generalizable models are not established (Moore et al., 2023; Ouillon et al., 2021).
2203: decreased OXPHOS coupling to decreased ATP pool	High	AOP 263 reports strong quantitative understanding, supported by bioenergetic theory and models linking mitochondrial coupling and ATP production (AOP-Wiki, 2026b; OECD, 2022; Song and Villeneuve, 2021).
2768: decreased ATP pool to increased cell injury/death	Moderate	ATP thresholds influence the type and severity of cell death, and quantitative relationships are reported in defined systems, but thresholds vary by cell type and exposure condition (Leist et al., 1997; Hansen et al., 2015).
2767: increased cell injury/death to decreased growth	Low to moderate	Quantitative linkage between cell loss and organismal growth is plausible and can be modeled in defined systems, but empirical cross-taxa response-response relationships remain limited (Conlon and Raff, 1999).

BMD/POD-anchored concordance

The following benchmark-dose/point-of-departure (BMD/POD) concordance table anchors AOP 331 to quantitative cross-KE ordering, in line with Handbook section 4C. The multiomics point-of-departure (moPOD) dataset for gamma-irradiated Daphnia magna (Song et al., 2023) provides POD magnitudes for increased ROS, decreased ATP, decreased OXPHOS coupling, and cell death, demonstrating the expected upstream-to-downstream POD ordering (more sensitive PODs upstream). The moPOD is presented as POD magnitude evidence, not as a causal re-ordering of KEs. The Lemna minor EDR50 range provides a whole-pathway apical anchor in an aquatic primary producer.

Key event (functional category)	POD metric	POD value (mGy/h)	POD ordering	Source
KE 1115: ROS, increased (mROS)	moPOD (multiomics POD)	0.4	1 (most sensitive)	Song et al., 2023

KE 1771: ATP pool, decreased	moPOD	2.5	2	Song et al., 2023
KE 1446: OXPHOS coupling, decreased (UPS/OXPHOS module)	moPOD	42.3	3	Song et al., 2023
KE 55: Cell injury/death (apoptosis)	moPOD	42.3	3 (least sensitive)	Song et al., 2023
Upstream KE chain → growth (Lemna minor, gamma)	EDR50 (growth)	31.5–54.8 (mGy/h)	whole-pathway apical	Xie et al., 2018, 2019, 2022

Considerations for Potential Applications of the AOP (optional)

AOP 331 can support mechanistic interpretation of growth impairment caused by oxidative stressors that induce lipid peroxidation, mitochondrial bioenergetic dysfunction, ATP depletion, and cell injury/death. The AOP is particularly relevant for hazard identification and chemical prioritization when evidence indicates increased ROS or oxidative stress together with lipid peroxidation, mitochondrial membrane potential changes, reduced respiratory control, ATP depletion, cytotoxicity, or growth inhibition. The AOP may also support IATA development by linking upstream NAM endpoints, such as ROS assays, lipid peroxidation markers, mitochondrial membrane potential, oxygen consumption rate, ATP content, cytotoxicity assays, and organismal growth measurements.

AOP 331 can support chemical grouping and read-across for stressors that share evidence of oxidative lipid damage, mitochondrial bioenergetic impairment, and ATP-associated cell injury. Because oxidative stress and lipid peroxidation are not chemical-specific, this AOP should not be used as a stand-alone basis for regulatory decisions. Instead, it should be applied as part of a weight-of-evidence framework that considers stressor mode of action, exposure context, assay specificity, taxonomic relevance, and concordance across multiple KEs. The AOP also highlights method-development needs, particularly standardized assays for lipid peroxidation, OXPHOS coupling, ATP depletion, and cell injury/death endpoints that can be connected quantitatively to apical growth outcomes.

References

Abbott BD, Harris MW, Birnbaum LS. 1995. Cell death in rat and mouse embryos exposed to methanol in whole embryo culture: evaluation of the role of the p53 tumor suppressor gene. Teratogenesis, Carcinogenesis, and Mutagenesis 15:147-169.

AOP-Wiki. 2026a. AOP 478: Deposition of energy leading to occurrence of cataracts. Collaborative Adverse Outcome Pathway Wiki. Available from: https://aopwiki.org/aops/478.

AOP-Wiki. 2026b. AOP 263: Uncoupling of oxidative phosphorylation leading to growth inhibition via decreased cell proliferation. Collaborative Adverse Outcome Pathway Wiki. Available from: https://aopwiki.org/aops/263.

AOP-Wiki. 2026c. AOP 12: Chronic binding of antagonist to N-methyl-D-aspartate receptors during brain development induces impairment of learning and memory abilities. Collaborative Adverse Outcome Pathway Wiki. Available from: https://aopwiki.org/aops/12.

AOP-Wiki. 2026d. AOP 13: Chronic binding of antagonist to N-methyl-D-aspartate receptors during brain development induces impairment of learning and memory abilities. Collaborative Adverse Outcome Pathway Wiki. Available from: https://aopwiki.org/aops/13.

AOP-Wiki. 2026e. AOP 17: Binding of electrophilic chemicals to SH/seleno-proteins involved in protection against oxidative stress leading to impairment of learning and memory. Collaborative Adverse Outcome Pathway Wiki. Available from: https://aopwiki.org/aops/17.

AOP-Wiki. 2026f. AOP 38: Protein alkylation leading to liver fibrosis. Collaborative Adverse Outcome Pathway Wiki. Available from: https://aopwiki.org/aops/38.

AOP-Wiki. 2026g. AOP 48: Binding of agonists to ionotropic glutamate receptors in adult brain causes excitotoxicity that mediates neuronal cell death, contributing to learning and memory impairment. Collaborative Adverse Outcome Pathway Wiki. Available from: https://aopwiki.org/aops/48.

AOP-Wiki. 2026h. AOP 296: Oxidative DNA damage leading to chromosomal aberrations and mutations. Collaborative Adverse Outcome Pathway Wiki. Available from: https://aopwiki.org/aops/296.

Ayala A, Munoz MF, Arguelles S. 2014. Lipid peroxidation: production, metabolism, and signaling mechanisms of malondialdehyde and 4-hydroxy-2-nonenal. Oxidative Medicine and Cellular Longevity 2014:360438.

Barata C, Varo I, Navarro JC, Arun S, Porte C. 2005. Antioxidant enzyme activities and lipid peroxidation in the freshwater cladoceran Daphnia magna exposed to redox cycling compounds. Comparative Biochemistry and Physiology Part C: Toxicology & Pharmacology 140:175-186.

Becker, R. A., Ankley, G. T., Edwards, S. W., Kennedy, S. W., Linkov, I., Meek, M. E., Sachana, M., Segner, H., Van der Burg, B., Villeneuve, D. L., Watanabe, H., & Barton-Maclaren, T. S. (2015). Increasing scientific confidence in adverse outcome pathways: Application of tailored Bradford-Hill considerations for evaluating weight of evidence. Regulatory Toxicology and Pharmacology, 72(3), 514-537. https://doi.org/10.1016/j.yrtph.2015.04.004

Bonora M, Bononi A, De Marchi E, Giorgi C, Lebiedzinska M, Marchi S, Patergnani S, Rimessi A, Suski JM, Wojtala A, Wieckowski MR, Kroemer G, Galluzzi L, Pinton P. 2012. Role of the c subunit of the FO ATP synthase in mitochondrial permeability transition. Cell Cycle 12:674-683.

Carrothers, E., et al. (2025). Adverse Outcome Pathway on Deposition of Energy Leading to Cataracts. OECD Series on Adverse Outcome Pathways, No. 40. OECD Publishing, Paris. https://doi.org/10.1787/5ad6b263-en

Carvaillo JC, Barouki R, Coumoul X, Audouze K. 2019. Linking bisphenol S to adverse outcome pathways using a combined text mining and systems biology approach. Environmental Health Perspectives 127:047005.

Cherkasov AS, Biswas PK, Ridings DM, Ringwood AH, Sokolova IM. 2006. Effects of acclimation temperature and cadmium exposure on cellular energy budgets in the marine mollusk Crassostrea virginica: linking cellular and mitochondrial responses. Journal of Experimental Biology 209:1274-1284.

Conlon I, Raff M. 1999. Size control in animal development. Cell 96:235-244.

Esperanza M, Cid A, Herrero C, Rioboo C. 2015. Acute effects of a prooxidant herbicide on the microalga Chlamydomonas reinhardtii: screening cytotoxicity and genotoxicity endpoints. Aquatic Toxicology 165:210-221.

Hansen EL, Sozer EB, Romeo S, Frandsen SK, Vernier PT, Gehl J. 2015. Dose-dependent ATP depletion and cancer cell death following calcium electroporation, relative effect of calcium concentration and electric field strength. PLoS ONE 10:e0122973.

Jornod F, Jaylet T, Blaha L, Sarigiannis D, Tamisier L, Audouze K. 2022. AOP-helpFinder webserver: a tool for comprehensive analysis of the literature to support adverse outcome pathways development. Bioinformatics 38:1173-1175.

Knauert S, Knauer K. 2008. The role of reactive oxygen species in copper toxicity to two freshwater green microalgae. Journal of Phycology 44:311-321.

Knops M, Altenburger R, Segner H. 2001. Alterations of physiological energetics, growth and reproduction of Daphnia magna under toxicant stress. Aquatic Toxicology 53:79-90.

Leist M, Single B, Castoldi AF, Kuhnle S, Nicotera P. 1997. Intracellular adenosine triphosphate concentration: a switch in the decision between apoptosis and necrosis. Journal of Experimental Medicine 185:1481-1486.

Moore TD, Martin-Creuzburg D, Yampolsky LY. 2023. Diet effects on longevity, heat tolerance, lipid peroxidation and mitochondrial membrane potential in Daphnia. Oecologia 202:151-163.

Murphy MP. 2009. How mitochondria produce reactive oxygen species. Biochemical Journal 417:1-13.

Nicholls DG, Ferguson SJ. 2013. Bioenergetics 4. London: Academic Press.

Nicotera P, Leist M, Ferrando-May E. 1998. Intracellular ATP, a switch in the decision between apoptosis and necrosis. Toxicology Letters 102-103:139-142. https://doi.org/10.1016/S0378-4274(98)00298-7

OECD. 2018. Users' handbook supplement to the guidance document for developing and assessing adverse outcome pathways. OECD Series on Adverse Outcome Pathways No. 1. Paris: OECD Publishing.

OECD. 2021. Guidance document for the scientific review of adverse outcome pathways. OECD Series on Testing and Assessment No. 344. Paris: OECD Publishing.

OECD. 2022. Uncoupling of oxidative phosphorylation leading to growth inhibition via decreased cell proliferation. OECD Series on Adverse Outcome Pathways No. 28. Paris: OECD Publishing.

Ouillon N, Sokolov EP, Otto S, Rehder G, Sokolova IM. 2021. Effects of variable oxygen regimes on mitochondrial bioenergetics and reactive oxygen species production in a marine bivalve, Mya arenaria. Journal of Experimental Biology 224:jeb237156.

Qian H, Chen W, Sun L, Jin Y, Liu W, Fu Z. 2009. Inhibitory effects of paraquat on photosynthesis and the response to oxidative stress in Chlorella vulgaris. Ecotoxicology 18:537-543.

Schieber M, Chandel NS. 2014. ROS function in redox signaling and oxidative stress. Current Biology 24:R453-R462.

Sies H, Berndt C, Jones DP. 2017. Oxidative stress. Annual Review of Biochemistry 86:715-748.

Sokolova IM, Sokolov EP, Ponnappa KM. 2005. Cadmium exposure affects mitochondrial bioenergetics and gene expression of key mitochondrial proteins in the eastern oyster Crassostrea virginica Gmelin (Bivalvia: Ostreidae). Aquatic Toxicology 73:242-255.

Song Y, Villeneuve DL. 2021. Uncoupling of oxidative phosphorylation leading to growth inhibition via decreased cell proliferation. Environmental Toxicology and Chemistry 40:2951-2963.

Song Y, Zheng K, Brede DA, Gomes T, Xie L, Kassaye Y, Salbu B, Tollefsen KE. 2023. Multiomics point of

departure (moPOD) modeling supports an adverse outcome pathway network for ionizing radiation. Environ Sci Technol 57:3198-3205. https://doi.org/10.1021/acs.est.2c04917

Xie L, Gomes T, Solhaug KA, Song Y, Tollefsen KE. 2018. Linking mode of action of the model respiratory and photosynthesis uncoupler 3,5-dichlorophenol to adverse outcomes in Lemna minor. Aquatic Toxicology 197:98-108. https://doi.org/10.1016/j.aquatox.2018.02.005

Xie L, Solhaug KA, Song Y, Brede DA, Lind OC, Salbu B, Tollefsen KE. 2019. Modes of action and adverse effects of gamma radiation in an aquatic macrophyte Lemna minor. Science of the Total Environment 680:23-34. https://doi.org/10.1016/j.scitotenv.2019.05.016

Xie L, Song Y, Petersen K, Solhaug KA, Lind OC, Brede DA, Salbu B, Tollefsen KE. 2022. Ultraviolet B modulates gamma radiation-induced stress responses in Lemna minor at multiple levels of biological organisation. Science of the Total Environment 846:157457. https://doi.org/10.1016/j.scitotenv.2022.157457

Appendix 1

List of MIEs in this AOP

Event: 1115: Increase, Reactive oxygen species

Short Name: Increase, ROS

Event Component

Process	Object	Action
reactive oxygen species biosynthetic process	reactive oxygen species	increased

AOPs Including This Key Event

AOP ID and Name	Event Type
Aop:186 - unknown MIE leading to renal failure and mortality	KeyEvent
Aop:213 - Inhibition of fatty acid beta oxidation leading to nonalcoholic steatohepatitis (NASH)	KeyEvent
Aop:303 - Frustrated phagocytosis-induced lung cancer	KeyEvent
Aop:383 - Inhibition of Angiotensin-converting enzyme 2 leading to liver fibrosis	KeyEvent
Aop:382 - Angiotensin II type 1 receptor (AT1R) agonism leading to lung fibrosis	KeyEvent
Aop:384 - Hyperactivation of ACE/Ang-II/AT1R axis leading to chronic kidney disease	KeyEvent
Aop:396 - Deposition of ionizing energy leads to population decline via impaired meiosis	KeyEvent
Aop:409 - Frustrated phagocytosis leads to malignant mesothelioma	KeyEvent
Aop:413 - Oxidation and antagonism of reduced glutathione leading to mortality via acute renal failure	KeyEvent
Aop:416 - Aryl hydrocarbon receptor activation leading to lung cancer through IL-6 toxicity pathway	KeyEvent
Aop:418 - Aryl hydrocarbon receptor activation leading to impaired lung function through AHR-ARNT toxicity pathway	KeyEvent
Aop:386 - Deposition of ionizing energy leading to population decline via inhibition of photosynthesis	KeyEvent
Aop:387 - Deposition of ionising energy leading to population decline via mitochondrial dysfunction	KeyEvent
Aop:319 - Binding to ACE2 leading to lung fibrosis	KeyEvent
Aop:451 - Interaction with lung resident cell membrane components leads to lung cancer	KeyEvent
Aop:476 - Adverse Outcome Pathways diagram related to PBDEs associated male reproductive toxicity	MolecularInitiatingEvent
Aop:492 - Glutathione conjugation leading to reproductive dysfunction via oxidative stress	KeyEvent
Aop:497 - ERa inactivation alters mitochondrial functions and insulin signalling in skeletal muscle and leads to insulin resistance and metabolic syndrome	KeyEvent
Aop:500 - Activation of MEK-ERK1/2 leads to deficits in learning and cognition via ROS and apoptosis	KeyEvent
Aop:505 - Reactive Oxygen Species (ROS) formation leads to cancer via inflammation pathway	MolecularInitiatingEvent
Aop:513 - Reactive Oxygen (ROS) formation leads to cancer via Peroxisome proliferation-activated receptor (PPAR) pathway	MolecularInitiatingEvent
Aop:521 - Essential element imbalance leads to reproductive failure via oxidative stress	KeyEvent
Aop:540 - Oxidative Stress in the Fish Ovary Leads to Reproductive Impairment via Reduced Vitellogenin Production	MolecularInitiatingEvent

AOP ID and Name	Event Type
Aop:462 - Activation of reactive oxygen species leading the atherosclerosis	MolecularInitiatingEvent
Aop:299 - Deposition of energy leading to population decline via DNA oxidation and follicular atresia	KeyEvent
Aop:311 - Deposition of energy leading to population decline via DNA oxidation and oocyte apoptosis	KeyEvent
Aop:331 - Increase in reactive oxygen species leading to growth inhibition via lipid peroxidation and cell death	MolecularInitiatingEvent
Aop:327 - Excessive reactive oxygen species production leading to mortality (1)	MolecularInitiatingEvent
Aop:328 - Excessive reactive oxygen species production leading to mortality (2)	MolecularInitiatingEvent
Aop:329 - Excessive reactive oxygen species production leading to mortality (3)	MolecularInitiatingEvent
Aop:330 - Excessive reactive oxygen species production leading to mortality (4)	MolecularInitiatingEvent
Aop:26 - Calcium-mediated neuronal ROS production and energy imbalance	KeyEvent
Aop:534 - Succinate dehydrogenase (SDH) inhibition leads to oxidative stress	KeyEvent
Aop:273 - Mitochondrial complex inhibition leading to liver injury	KeyEvent
Aop:488 - Increased reactive oxygen species production leading to decreased cognitive function	MolecularInitiatingEvent
Aop:298 - Increase in reactive oxygen species (ROS) leading to human treatment-resistant gastric cancer	MolecularInitiatingEvent
Aop:27 - Cholestatic Liver Injury induced by Inhibition of the Bile Salt Export Pump (ABCB11)	KeyEvent
Aop:511 - The AOP framework on ROS-mediated oxidative stress induced vascular disrupting effects	MolecularInitiatingEvent
Aop:207 - NADPH oxidase and P38 MAPK activation leading to reproductive failure in Caenorhabditis elegans	KeyEvent
Aop:423 - Toxicological mechanisms of hepatocyte apoptosis through the PARP1 dependent cell death pathway	MolecularInitiatingEvent
Aop:481 - AOPs of amorphous silica nanoparticles: ROS-mediated oxidative stress increased respiratory dysfunction and diseases.	MolecularInitiatingEvent
Aop:282 - Adverse outcome pathway on photochemical toxicity initiated by light exposure	MolecularInitiatingEvent
Aop:569 - Decreased DNA methylation of FAM50B/PTCHD3 leading to IQ loss of children via PI3K-Akt pathway	KeyEvent
Aop:595 - Emerging OPFRS reproductive outcome pathway	MolecularInitiatingEvent
Aop:596 - Excessive reactive oxygen species leading to growth inhibition via protein oxidation and cell injury/death	MolecularInitiatingEvent
Aop:598 - Excessive reactive oxygen species leading to growth inhibition via protein oxidation and reduced cell proliferation	MolecularInitiatingEvent
Aop:599 - Excessive reactive oxygen species leading to growth inhibition via fatty acid oxidation and cell injury/death	MolecularInitiatingEvent
Aop:600 - Excessive reactive oxygen species leading to growth inhibition via fatty acid oxidation and reduced cell growth	MolecularInitiatingEvent
Aop:601 - Excessive reactive oxygen species leading to growth inhibition via fatty acid oxidation and reduced cell proliferation	MolecularInitiatingEvent
Aop:602 - Excessive reactive oxygen species leading to growth inhibition via oxidative DNA damage	MolecularInitiatingEvent
Aop:603 - Excessive reactive oxygen species leading to growth inhibition via protein oxidation and cell cycle disruption	MolecularInitiatingEvent
Aop:608 - Thyroid Hormone Excess Leading to Reduced, Swimming Performance via Hypomyelination	KeyEvent
Aop:613 - Peroxisome proliferator-activated receptor alpha activation leading to early life stage mortality via increased reactive oxygen species production	KeyEvent
Aop:622 - Calcineurin inhibitor induced nephrotoxicity leading to kidney failure	KeyEvent
Aop:636 - Increase in reactive oxygen species (ROS) leading to human amyotrophic lateral sclerosis (ALS)	MolecularInitiatingEvent
Aop:638 - Co-exposure to microplastics and cadmium leading to progression from NAFLD to liver tumorigenesis	MolecularInitiatingEvent
Aop:472 - DNA adduct formation leading to kidney failure	KeyEvent
Aop:324 - Increase in reactive oxygen species leading to growth inhibition via oxidative DNA damage and cell cycle disruption	MolecularInitiatingEvent
Aop:325 - Increase in reactive oxygen species leading to growth inhibition via oxidative DNA damage and cell death	MolecularInitiatingEvent
Aop:326 - Increase in reactive oxygen species leading to growth inhibition via lipid peroxidation and decreased cell proliferation	MolecularInitiatingEvent
Aop:332 - Increase in reactive oxygen species leading to growth inhibition via protein oxidation and decreased cell proliferation	MolecularInitiatingEvent

AOP ID and Name	Event Type
Aop:333 - Increase in reactive oxygen species leading to growth inhibition via protein oxidation and cell death	MolecularInitiatingEvent
Aop:647 - ROS formation leading to growth inhibition modulated by the Keap1–Nrf2 antioxidant response	MolecularInitiatingEvent

Biological Context

Level of Biological Organization

Cellular

Cell term

Cell term

cell

Organ term

Organ term

organ

Domain of Applicability

Taxonomic Applicability

Term	Scientific Term	Evidence	Links
Vertebrates	Vertebrates	High	NCBI
human	Homo sapiens	Moderate	NCBI
human and other cells in culture	human and other cells in culture	Moderate	NCBI
mouse	Mus musculus	Moderate	NCBI
crustaceans	Daphnia magna	High	NCBI
Lemna minor	Lemna minor	High	NCBI
zebrafish	Danio rerio	High	NCBI

Life Stage Applicability

Life Stage	Evidence
All life stages	High

Sex Applicability

Sex	Evidence
Unspecific	High
Mixed	High

ROS is a normal constituent found in all organisms, *lifestages, and sexes.*

Key Event Description

Biological State: increased reactive oxygen species (ROS)

Biological compartment: an entire cell -- may be cytosolic, may also enter organelles.

Reactive oxygen species (ROS) are O_2- derived molecules that can be both free radicals (e.g. superoxide, hydroxyl, peroxyl, alcoxyl) and non-radicals (hypochlorous acid, ozone and singlet oxygen) (Bedard and Krause 2007; Ozcan and Ogun 2015). ROS production occurs naturally in all kinds of tissues inside various cellular compartments, such as mitochondria and peroxisomes (Drew and Leeuwenburgh 2002; Ozcan and Ogun 2015). Furthermore, these molecules have an important function in the regulation of several biological processes – they might act as antimicrobial agents or triggers of animal gamete activation and capacitation (Goud et al. 2008; Parrish 2010; Bisht et al. 2017).
However, in environmental stress situations (exposure to radiation, chemicals, high temperatures) these molecules have its levels drastically increased, and overly interact with macromolecules, namely nucleic acids, proteins, carbohydrates and lipids, causing cell and tissue damage (Brieger et al. 2012; Ozcan and Ogun 2015).

Reactive oxygen species (ROS) refers to the chemical species superoxide, hydrogen peroxide, and their secondary reactive products. In the biological context, ROS are signaling molecules with important roles in cell energy metabolism, cell proliferation, and fate. Therefore, balancing ROS levels at the cellular and tissue level is an important part of many biological processes. Disbalance, mainly an increase in ROS levels, can cause cell dysfunction and irreversible cell damage.

ROS are produced from both exogenous stressors and normal endogenous cellular processes, such as the mitochondrial electron transport chain (ETC). Inhibition of the ETC can result in the accumulation of ROS. Exposure to chemicals, heavy metal ions, or ionizing radiation can also result in increased production of ROS. Chemicals and heavy metal ions can deplete cellular antioxidants reducing the cell's ability to control cellular ROS and resulting in the accumulation of ROS. Cellular antioxidants include glutathione (GSH), protein sulfhydryl groups, superoxide dismutase (SOD).

ROS are radicals, ions, or molecules that have a single unpaired electron in their outermost shell of electrons, which can be categorized into two groups: free oxygen radicals and non-radical ROS [Liou et al., 2010].

<Free oxygen radicals>

superoxide	$O_2\cdot^-$
hydroxyl radical	·OH
nitric oxide	NO·
organic radicals	R·
peroxyl radicals	ROO·
alkoxyl radicals	RO·
thiyl radicals	RS·
sulfonyl radicals	ROS·
thiyl peroxyl radicals	RSOO·
disulfides	RSSR

<Non-radical ROS>

hydrogen peroxide	H_2O_2
singlet oxygen	$^1O_2$
ozone/trioxygen	O_3
organic hydroperoxides	ROOH
hypochlorite	ClO^-
peroxynitrite	$ONOO^-$
nitrosoperoxycarbonate anion	$O{=}NOOCO_2^-$
nitrocarbonate anion	$O_2NOCO_2^-$
dinitrogen dioxide	N_2O_2
nitronium	NO_2^+
highly reactive lipid- or carbohydrate-derived carbonyl compounds	

Potential sources of ROS include NADPH oxidase, xanthine oxidase, mitochondria, nitric oxide synthase, cytochrome P450, lipoxygenase/cyclooxygenase, and monoamine oxidase [Granger et al., 2015]. ROS are generated through NADPH oxidases consisting of $p47^{phox}$ and $p67^{phox}$. ROS are generated through xanthine oxidase activation in sepsis [Ramos et al., 2018]. Arsenic produces ROS [Zhang et al., 2011]. Mitochondria-targeted paraquat and metformin mediate ROS production [Chowdhury et al., 2020]. ROS are generated by bleomycin [Lu et al., 2010]. Radiation induces dose-dependent ROS production [Ji et al., 2019].

ROS are generated in the course of cellular respiration, metabolism, cell signaling, and inflammation [Dickinson and Chang 2011; Egea et al. 2017]. Hydrogen peroxide is also made by the endoplasmic reticulum in the course of protein folding. Nitric oxide (NO) is produced at the highest levels by nitric oxide synthase in endothelial cells and phagocytes. NO production is one of the main mechanisms by which phagocytes kill bacteria [Wang et al., 2017]. The other species are produced by reactions with superoxide or peroxide, or by other free radicals or enzymes.

ROS activity is principally local. Most ROS have short half-lives, ranging from nano- to milliseconds, so diffusion is limited, while reactive nitrogen species (RNS) nitric oxide or peroxynitrite can survive long enough to diffuse across membranes [Calcerrada et al. 2011]. Consequently, local concentrations of ROS are much higher than average cellular concentrations, and signaling is typically controlled by colocalization with redox buffers [Dickinson and Chang 2011; Egea et al. 2017].

Although their existence is limited temporally and spatially, ROS interact with other ROS or with other nearby molecules to produce more ROS and participate in a feedback loop to amplify the ROS signal, which can increase RNS. Both ROS and RNS also move into neighboring cells, and ROS can increase intracellular ROS signaling in neighboring cells [Egea et al. 2017].

In the primary event, photoreactive chemicals are excited by the absorption of photon energy. The energy of the photoactivated chemicals transfer to oxygen and then generates the reactive oxygen species (ROS), including superoxide (O_2^-) via type I reaction and singlet oxygen ($^1O_2$) via type II reaction, as principal intermediate species in phototoxic reaction (Foote, 1991, Onoue et al. , 2009).

How it is Measured or Detected

Photocolorimetric assays (Sharma et al. 2017; Griendling et al. 2016) or through commercial kits purchased from specialized companies.

Yuan, Yan, et al., (2013) described ROS monitoring by using H_2-DCF-DA, a redox-sensitive fluorescent dye. Briefly, the harvested cells were incubated with H_2-DCF-DA (50 µmol/L final concentration) for 30 min in the dark at 37°C. After treatment, cells were immediately washed twice, re-suspended in PBS, and analyzed on a BD-FACS Aria flow cytometry. ROS generation was based on fluorescent intensity which was recorded by excitation at 504 nm and emission at 529 nm.

Lipid peroxidation (LPO) can be measured as an indicator of oxidative stress damage Yen, Cheng Chien, et al., (2013).

Chattopadhyay, Sukumar, et al. (2002) assayed the generation of free radicals within the cells and their extracellular release in the medium by addition of yellow NBT salt solution (Park et al., 1968). Extracellular release of ROS converted NBT to a purple colored

formazan. The cells were incubated with 100 ml of 1 mg/ml NBT solution for 1 h at 37 °C and the product formed was assayed at 550 nm in an Anthos 2001 plate reader. The observations of the ‘cell-free system’ were confirmed by cytological examination of parallel set of explants stained with chromogenic reactions for NO and ROS.

On the basis of the pathogenesis of drug-induced phototoxicity, a reactive oxygen species (ROS) assay was proposed to evaluate the phototoxic risk of chemicals. The ROS assay can monitor generation of ROS, such as singlet oxygen and superoxide, from photoirradiated chemicals, and the ROS data can be used to evaluate the photoreactivity of chemicals (Onoue et al. , 2014, Onoue et al. , 2013, Onoue and Tsuda, 2006). The ROS assay is a recommended approach by guidelines to evaluate the phototoxic risk of chemicals (ICH, 2014, PCPC, 2014).

<Direct detection>

Many fluorescent compounds can be used to detect ROS, some of which are specific, and others are less specific.

ROS can be detected by fluorescent probes such as *p*-methoxy-phenol derivative [Ashoka et al., 2020].

Chemiluminescence analysis can detect the superoxide, where some probes have a wider range for detecting hydroxyl radical, hydrogen peroxide, and peroxynitrite [Fuloria et al., 2021].

ROS in the blood can be detected using superparamagnetic iron oxide nanoparticles (SPION)-based biosensor [Lee et al., 2020].

Hydrogen peroxide (H_2O_2) can be detected with a colorimetric probe, which reacts with H_2O_2 in a 1:1 stoichiometry to produce a bright pink colored product, followed by the detection with a standard colorimetric microplate reader with a filter in the 540-570 nm range.

The levels of ROS can be quantified using multiple-step amperometry using a stainless steel counter electrode and non-leak Ag|AgCl reference node [Flaherty et al., 2017].

Singlet oxygen can be measured by monitoring the bleaching of *p*-nitrosodimethylaniline at 440 nm using a spectrophotometer with imidazole as a selective acceptor of singlet oxygen [Onoue et al., 2014].

<Indirect Detection>

Alternative methods involve the detection of redox-dependent changes to cellular constituents such as proteins, DNA, lipids, or glutathione [Dickinson and Chang 2011; Wang et al. 2013; Griendling et al. 2016]. However, these methods cannot generally distinguish between the oxidative species behind the changes and cannot provide good resolution for the kinetics of oxidative activity.

References

Akai, K., et al. (2004). "Ability of ferric nitrilotriacetate complex with three pH-dependent conformations to induce lipid peroxidation." Free Radic Res. Sep;38(9):951-62. doi: 10.1080/1071576042000261945

Ashoka, A. H., et al. (2020). "Recent Advances in Fluorescent Probes for Detection of HOCl and HNO." ACS omega, 5(4), 1730-1742. doi:10.1021/acsomega.9b03420

B.H. Park, S.M. Fikrig, E.M. Smithwick Infection and nitroblue tetrazolium reduction by neutrophils: a diagnostic aid Lancet, 2 (1968), pp. 532-534

Bedard, Karen, and Karl-Heinz Krause. 2007. “The NOX Family of ROS-Generating NADPH Oxidases: Physiology and Pathophysiology.” Physiological Reviews 87 (1): 245–313.

Bisht, Shilpa, Muneeb Faiq, Madhuri Tolahunase, and Rima Dada. 2017. “Oxidative Stress and Male Infertility.” Nature Reviews. Urology 14 (8): 470–85.

Brieger, K., S. Schiavone, F. J. Miller Jr, and K-H Krause. 2012. “Reactive Oxygen Species: From Health to Disease.” Swiss Medical Weekly 142 (August): w13659.

Calcerrada, P., et al. (2011). "Nitric oxide-derived oxidants with a focus on peroxynitrite: molecular targets, cellular responses and therapeutic implications." Curr Pharm Des 17(35): 3905-3932.

Chattopadhyay, Sukumar, et al. "Apoptosis and necrosis in developing brain cells due to arsenic toxicity and protection with antioxidants." Toxicology letters 136.1 (2002): 65-76.

Chowdhury, A. R., et al. (2020). "Mitochondria-targeted paraquat and metformin mediate ROS production to induce multiple pathways of retrograde signaling: A dose-dependent phenomenon." Redox Biol. doi: 10.1016/j.redox.2020.101606. PMID: 32604037; PMCID: PMC7327929.

Dickinson, B. C. and Chang C. J. (2011). "Chemistry and biology of reactive oxygen species in signaling or stress responses." Nature chemical biology 7(8): 504-511.

Drew, Barry, and Christiaan Leeuwenburgh. 2002. “Aging and the Role of Reactive Nitrogen Species.” Annals of the New York Academy of Sciences 959 (April): 66–81.

Egea, J., et al. (2017). "European contribution to the study of ROS: A summary of the findings and prospects for the future from the COST action BM1203 (EU-ROS)." Redox biology 13: 94-162.

Flaherty, R. L., et al. (2017). "Glucocorticoids induce production of reactive oxygen species/reactive nitrogen species and DNA damage through an iNOS mediated pathway in breast cancer." Breast Cancer Research, 19(1), 1–13. https://doi.org/10.1186/s13058-017-0823-8

Foote CS. Definition of type I and type II photosensitized oxidation. Photochem Photobiol. 1991;54:659.

Fuloria, S., et al. (2021). "Comprehensive Review of Methodology to Detect Reactive Oxygen Species (ROS) in Mammalian Species and Establish Its Relationship with Antioxidants and Cancer." Antioxidants (Basel, Switzerland) 10(1) 128.

doi:10.3390/antiox10010128

Go, Y. M. and Jones, D. P. (2013). "The redox proteome." J Biol Chem 288(37): 26512-26520.

Goud, Anuradha P., Pravin T. Goud, Michael P. Diamond, Bernard Gonik, and Husam M. Abu-Soud. 2008. “Reactive Oxygen Species and Oocyte Aging: Role of Superoxide, Hydrogen Peroxide, and Hypochlorous Acid.” Free Radical Biology & Medicine 44 (7): 1295–1304.

Granger, D. N. and Kvietys, P. R. (2015). "Reperfusion injury and reactive oxygen species: The evolution of a concept" Redox Biol. doi: 10.1016/j.redox.2015.08.020. PMID: 26484802; PMCID: PMC4625011.

Griendling, K. K., et al. (2016). "Measurement of Reactive Oxygen Species, Reactive Nitrogen Species, and Redox-Dependent Signaling in the Cardiovascular System: A Scientific Statement From the American Heart Association." Circulation research 119(5): e39-75.

Griendling, Kathy K., Rhian M. Touyz, Jay L. Zweier, Sergey Dikalov, William Chilian, Yeong-Renn Chen, David G. Harrison, Aruni Bhatnagar, and American Heart Association Council on Basic Cardiovascular Sciences. 2016. “Measurement of Reactive Oxygen Species, Reactive Nitrogen Species, and Redox-Dependent Signaling in the Cardiovascular System: A Scientific Statement From the American Heart Association.” Circulation Research 119 (5): e39–75.

ICH. ICH Guideline S10 Guidance on Photosafety Evaluation of Pharmaceuticals.: International Council on Harmonisation of Technical Requirements for Registration of Pharmaceuticals for Human Use; 2014.

Itziou, A., et al. (2011). "In vivo and in vitro effects of metals in reactive oxygen species production, protein carbonylation, and DNA damage in land snails Eobania vermiculata." Archives of Environmental Contamination and Toxicology, 60(4), 697–707. https://doi.org/10.1007/s00244-010-9583-5

Ji, W. O., et al. "Quantitation of the ROS production in plasma and radiation treatments of biotargets." Sci Rep. 2019 Dec 27;9(1):19837. doi: 10.1038/s41598-019-56160-0. PMID: 31882663; PMCID: PMC6934759.

Kruk, J. and Aboul-Enein, H. Y. (2017). "Reactive Oxygen and Nitrogen Species in Carcinogenesis: Implications of Oxidative Stress on the Progression and Development of Several Cancer Types." Mini-Reviews in Medicinal Chemistry, 17:11. doi:10.2174/1389557517666170228115324

Lee, D. Y., et al. (2020). "PEGylated Bilirubin-coated Iron Oxide Nanoparticles as a Biosensor for Magnetic Relaxation Switching-based ROS Detection in Whole Blood." Theranostics, 10(5), 1997-2007. doi:10.7150/thno.39662

Li, Z., et al. (2020). "Inhibition of MiR-25 attenuates doxorubicin-induced apoptosis, reactive oxygen species production and DNA damage by targeting pten." International Journal of Medical Sciences, 17(10), 1415–1427. https://doi.org/10.7150/ijms.41980

Liou, G. Y. and Storz, P. "Reactive oxygen species in cancer." Free Radic Res. 2010 May;44(5):479-96. doi:10.3109/10715761003667554. PMID: 20370557; PMCID: PMC3880197.

Lu, Y., et al. (2010). "Phosphatidylinositol-3-kinase/akt regulates bleomycin-induced fibroblast proliferation and collagen production." American journal of respiratory cell and molecular biology, 42(4), 432–441. https://doi.org/10.1165/rcmb.2009-0002OC

Onoue, S., et al. (2013). "Establishment and intra-/inter-laboratory validation of a standard protocol of reactive oxygen species assay for chemical photosafety evaluation." J Appl Toxicol. 33(11):1241-50. doi: 10.1002/jat.2776. Epub 2012 Jun 13. PMID: 22696462.

Onoue S, Hosoi K, Toda T, Takagi H, Osaki N, Matsumoto Y, et al. Intra-/inter-laboratory validation study on reactive oxygen species assay for chemical photosafety evaluation using two different solar simulators. Toxicology in vitro : an international journal published in association with BIBRA. 2014;28:515-23.

Onoue S, Hosoi K, Wakuri S, Iwase Y, Yamamoto T, Matsuoka N, et al. Establishment and intra-/inter-laboratory validation of a standard protocol of reactive oxygen species assay for chemical photosafety evaluation. Journal of applied toxicology : JAT. 2013;33:1241-50.

Onoue S, Kawamura K, Igarashi N, Zhou Y, Fujikawa M, Yamada H, et al. Reactive oxygen species assay-based risk assessment of drug-induced phototoxicity: classification criteria and application to drug candidates. J Pharm Biomed Anal. 2008;47:967-72.

Onoue S, Seto Y, Gandy G, Yamada S. Drug-induced phototoxicity; an early*in vitro* identification of phototoxic potential of new drug entities in drug discovery and development. Current drug safety. 2009;4:123-36.

Onoue S, Tsuda Y. Analytical studies on the prediction of photosensitive/phototoxic potential of pharmaceutical substances. Pharmaceutical research. 2006;23:156-64.

Ozcan, Ayla, and Metin Ogun. 2015. “Biochemistry of Reactive Oxygen and Nitrogen Species.” In Basic Principles and Clinical Significance of Oxidative Stress, edited by Sivakumar Joghi Thatha Gowder. Rijeka: IntechOpen.

Parrish, A. R. 2010. “2.27 - Hypoxia/Ischemia Signaling.” In Comprehensive Toxicology (Second Edition), edited by Charlene A. McQueen, 529–42. Oxford: Elsevier.

PCPC. PCPC 2014 safety evaluation guidelines; Chapter 7: Evaluation of Photoirritation and Photoallergy potential. Personal Care Products Council; 2014.

Ramos, M. F. P., et al. (2018). "Xanthine oxidase inhibitors and sepsis." Int J Immunopathol Pharmacol. 32:2058738418772210. doi:10.1177/2058738418772210

Ravanat, J. L., et al. (2014). "Radiation-mediated formation of complex damage to DNA: a chemical aspect overview." Br J Radiol 87(1035): 20130715.

Schutzendubel, A. and Polle, A. (2002). "Plant responses to abiotic stresses: heavy metal-induced oxidative stress and protection by mycorrhization." Journal of Experimental Botany, 53(372), 1351–1365. https://doi.org/10.1093/jexbot/53.372.1351

Seto Y, Kato M, Yamada S, Onoue S. Development of micellar reactive oxygen species assay for photosafety evaluation of poorly water-soluble chemicals. Toxicology in vitro : an international journal published in association with BIBRA. 2013;27:1838-46.

Sharma, Gunjan, Nishant Kumar Rana, Priya Singh, Pradeep Dubey, Daya Shankar Pandey, and Biplob Koch. 2017. “p53 Dependent Apoptosis and Cell Cycle Delay Induced by Heteroleptic Complexes in Human Cervical Cancer Cells.” Biomedicine & Pharmacotherapy = Biomedecine & Pharmacotherapie 88 (April): 218–31.

Silva, R., et al. (2019). "Light exposure during growth increases riboflavin production, reactive oxygen species accumulation and DNA damage in Ashbya gossypii riboflavin-overproducing strains." FEMS Yeast Research, 19(1), 1–7. https://doi.org/10.1093/femsyr/foy114

Tsuchiya K, et al. (2005). "Oxygen radicals photo-induced by ferric nitrilotriacetate complex." Biochim Biophys Acta. 1725(1):111-9. doi:10.1016/j.bbagen.2005.05.001

Wang, J., et al. (2017). "Glucocorticoids Suppress Antimicrobial Autophagy and Nitric Oxide Production and Facilitate Mycobacterial Survival in Macrophages." Scientific reports, 7(1), 982. https://doi.org/10.1038/s41598-017-01174-9

Wang, X., et al. (2013). "Imaging ROS signaling in cells and animals." Journal of molecular medicine 91(8): 917-927.

Yen, Cheng Chien, et al. "Inorganic arsenic causes cell apoptosis in mouse cerebrum through an oxidative stress-regulated signaling pathway." Archives of toxicology 85 (2011): 565-575.

Yuan, Yan, et al. "Cadmium-induced apoptosis in primary rat cerebral cortical neurons culture is mediated by a calcium signaling pathway." PloS one 8.5 (2013): e64330.

Zhang, Z., et al. (2011). "Reactive oxygen species mediate arsenic induced cell transformation and tumorigenesis through Wnt/β-catenin pathway in human colorectal adenocarcinoma DLD1 cells. " Toxicology and Applied Pharmacology, 256(2), 114-121. doi:10.1016/j.taap.2011.07.016

List of Key Events in the AOP

Event: 1392: Increase, Oxidative Stress

Short Name: Increase, Oxidative Stress

Event Component

Process	Object	Action
oxidative stress		increased

AOPs Including This Key Event

AOP ID and Name	Event Type
Aop:220 - Cyp2E1 Activation Leading to Liver Cancer	KeyEvent
Aop:17 - Binding of electrophilic chemicals to SH(thiol)-group of proteins and /or to seleno-proteins involved in protection against oxidative stress during brain development leads to impairment of learning and memory	KeyEvent
Aop:284 - Binding of electrophilic chemicals to SH(thiol)-group of proteins and /or to seleno-proteins involved in protection against oxidative stress leads to chronic kidney disease	KeyEvent
Aop:377 - Dysregulated prolonged Toll Like Receptor 9 (TLR9) activation leading to Multi Organ Failure involving Acute Respiratory Distress Syndrome (ARDS)	KeyEvent
Aop:411 - Oxidative stress Leading to Decreased Lung Function	MolecularInitiatingEvent
Aop:424 - Oxidative stress Leading to Decreased Lung Function via CFTR dysfunction	MolecularInitiatingEvent
Aop:425 - Oxidative Stress Leading to Decreased Lung Function via Decreased FOXJ1	MolecularInitiatingEvent
Aop:429 - A cholesterol/glucose dysmetabolism initiated Tau-driven AOP toward memory loss (AO) in sporadic Alzheimer's Disease with plausible MIE's plug-ins for environmental neurotoxicants	KeyEvent
Aop:452 - Adverse outcome pathway of PM-induced respiratory toxicity	KeyEvent
Aop:464 - Calcium overload in dopaminergic neurons of the substantia nigra leading to parkinsonian motor deficits	KeyEvent
Aop:470 - Deposition of energy leads to abnormal vascular remodeling	KeyEvent
Aop:478 - Deposition of energy leading to occurrence of cataracts	KeyEvent
Aop:479 - Mitochondrial complexes inhibition leading to left ventricular function decrease via increased myocardial oxidative stress	KeyEvent
Aop:481 - AOPs of amorphous silica nanoparticles: ROS-mediated oxidative stress increased respiratory dysfunction and diseases.	KeyEvent
Aop:482 - Deposition of energy leading to occurrence of bone loss	KeyEvent
Aop:483 - Deposition of Energy Leading to Learning and Memory Impairment	KeyEvent
Aop:505 - Reactive Oxygen Species (ROS) formation leads to cancer via inflammation pathway	KeyEvent
Aop:521 - Essential element imbalance leads to reproductive failure via oxidative stress	KeyEvent

AOP ID and Name	Event Type
Aop:26 - Calcium-mediated neuronal ROS production and energy imbalance	AdverseOutcome
Aop:488 - Increased reactive oxygen species production leading to decreased cognitive function	KeyEvent
Aop:396 - Deposition of ionizing energy leads to population decline via impaired meiosis	KeyEvent
Aop:437 - Inhibition of mitochondrial electron transport chain (ETC) complexes leading to kidney toxicity	KeyEvent
Aop:535 - Binding and activation of GPER leading to learning and memory impairments	KeyEvent
Aop:171 - Chronic cytotoxicity of the serous membrane leading to pleural/peritoneal mesotheliomas in the rat.	KeyEvent
Aop:138 - Organic anion transporter (OAT1) inhibition leading to renal failure and mortality	KeyEvent
Aop:177 - Cyclooxygenase 1 (COX1) inhibition leading to renal failure and mortality	KeyEvent
Aop:186 - unknown MIE leading to renal failure and mortality	KeyEvent
Aop:200 - Estrogen receptor activation leading to breast cancer	KeyEvent
Aop:444 - Ionizing radiation leads to reduced reproduction in Eisenia fetida via reduced spermatogenesis and cocoon hatchability	KeyEvent
Aop:447 - Kidney failure induced by inhibition of mitochondrial electron transfer chain through apoptosis, inflammation and oxidative stress pathways	KeyEvent
Aop:476 - Adverse Outcome Pathways diagram related to PBDEs associated male reproductive toxicity	KeyEvent
Aop:497 - ERa inactivation alters mitochondrial functions and insulin signalling in skeletal muscle and leads to insulin resistance and metabolic syndrome	KeyEvent
Aop:457 - Succinate dehydrogenase inhibition leading to increased insulin resistance through reduction in circulating thyroxine	KeyEvent
Aop:459 - AhR activation in the thyroid leading to Subsequent Adverse Neurodevelopmental Outcomes in Mammals	KeyEvent
Aop:507 - Nrf2 inhibition leading to vascular disrupting effects via inflammation pathway	KeyEvent
Aop:509 - Nrf2 inhibition leading to vascular disrupting effects through activating apoptosis signal pathway and mitochondrial dysfunction	KeyEvent
Aop:510 - Demethylation of PPAR promotor leading to vascular disrupting effects	KeyEvent
Aop:511 - The AOP framework on ROS-mediated oxidative stress induced vascular disrupting effects	KeyEvent
Aop:538 - Adverse outcome pathway of PFAS-induced vascular disrupting effects via activating oxidative stress related pathways	KeyEvent
Aop:260 - CYP2E1 activation and formation of protein adducts leading to neurodegeneration	KeyEvent
Aop:450 - Inhibition of AChE and activation of CYP2E1 leading to sensory axonal peripheral neuropathy and mortality	KeyEvent
Aop:501 - Excessive iron accumulation leading to neurological disorders	KeyEvent
Aop:540 - Oxidative Stress in the Fish Ovary Leads to Reproductive Impairment via Reduced Vitellogenin Production	KeyEvent
Aop:471 - Neuron defect induced early behavioral change	KeyEvent
Aop:31 - Oxidation of iron in hemoglobin leading to hematotoxicity	KeyEvent
Aop:534 - Succinate dehydrogenase (SDH) inhibition leads to oxidative stress	AdverseOutcome
Aop:462 - Activation of reactive oxygen species leading the atherosclerosis	KeyEvent
Aop:331 - Increase in reactive oxygen species leading to growth inhibition via lipid peroxidation and cell death	KeyEvent
Aop:595 - Emerging OPFRS reproductive outcome pathway	KeyEvent
Aop:596 - Excessive reactive oxygen species leading to growth inhibition via protein oxidation and cell injury/death	KeyEvent
Aop:598 - Excessive reactive oxygen species leading to growth inhibition via protein oxidation and reduced cell proliferation	KeyEvent
Aop:599 - Excessive reactive oxygen species leading to growth inhibition via fatty acid oxidation and cell injury/death	KeyEvent
Aop:600 - Excessive reactive oxygen species leading to growth inhibition via fatty acid oxidation and reduced cell growth	KeyEvent
Aop:601 - Excessive reactive oxygen species leading to growth inhibition via fatty acid oxidation and reduced cell proliferation	KeyEvent
Aop:602 - Excessive reactive oxygen species leading to growth inhibition via oxidative DNA damage	KeyEvent
Aop:603 - Excessive reactive oxygen species leading to growth inhibition via protein oxidation and cell cycle disruption	KeyEvent

AOP ID and Name	Event Type
Aop:608 - Thyroid Hormone Excess Leading to Reduced, Swimming Performance via Hypomyelination	KeyEvent
Aop:616 - organic UV filter and its Photoproducts reproductive toxicity pathways	KeyEvent
Aop:622 - Calcineurin inhibitor induced nephrotoxicity leading to kidney failure	KeyEvent
Aop:625 - Increased 11β-Hydroxysteroid dehydrogenase type 1 activity leading to MASLD progression via insulin resistance-associated oxidative stress	KeyEvent
Aop:628 - Increased 11β-Hydroxysteroid dehydrogenase type 1 activity leading to MASLD progression via lipogenesis-associated oxidative stress	KeyEvent
Aop:472 - DNA adduct formation leading to kidney failure	KeyEvent
Aop:642 - Intestinal FXR inhibition leading to steatohepatitis via gut-liver axis dysregulation	KeyEvent
Aop:324 - Increase in reactive oxygen species leading to growth inhibition via oxidative DNA damage and cell cycle disruption	KeyEvent
Aop:325 - Increase in reactive oxygen species leading to growth inhibition via oxidative DNA damage and cell death	KeyEvent
Aop:326 - Increase in reactive oxygen species leading to growth inhibition via lipid peroxidation and decreased cell proliferation	KeyEvent
Aop:332 - Increase in reactive oxygen species leading to growth inhibition via protein oxidation and decreased cell proliferation	KeyEvent
Aop:333 - Increase in reactive oxygen species leading to growth inhibition via protein oxidation and cell death	KeyEvent
Aop:645 - Binding and activation of AhR lead to cardiovascular aging	KeyEvent
Aop:646 - Binding and activation of AhR/PPARγ lead to lipid metabolism disorders	KeyEvent
Aop:647 - ROS formation leading to growth inhibition modulated by the Keap1–Nrf2 antioxidant response	KeyEvent
Aop:636 - Increase in reactive oxygen species (ROS) leading to human amyotrophic lateral sclerosis (ALS)	KeyEvent

Stressors

Name
Acetaminophen
Chloroform
furan
Platinum
Aluminum
Cadmium
Mercury
Uranium
Arsenic
Silver
Manganese
Nickel
Zinc
nanoparticles

Biological Context

Level of Biological Organization
Molecular

Domain of Applicability

Taxonomic Applicability

Term	Scientific Term	Evidence	Links
rodents	rodents	High	NCBI
Homo sapiens	Homo sapiens	High	NCBI

Term	Scientific Term	Evidence	Links

Life Stage Applicability

Life Stage	Evidence
All life stages	High

Sex Applicability

Sex	Evidence
Mixed	High

Taxonomic applicability: Occurrence of oxidative stress is not species specific.

Life stage applicability: Occurrence of oxidative stress is not life stage specific.

Sex applicability: Occurrence of oxidative stress is not sex specific.

Evidence for perturbation by prototypic stressor: There is evidence of the increase of oxidative stress following perturbation from a variety of stressors including exposure to ionizing radiation and altered gravity (Bai et al., 2020; Ungvari et al., 2013; Zhang et al., 2009).

Key Event Description

Oxidative stress is defined as an imbalance in the production of reactive oxygen species (ROS) and antioxidant defenses. High levels of oxidizing free radicals can be very damaging to cells and molecules within the cell. As a result, the cell has important defense mechanisms to protect itself from ROS. For example, Nrf2 is a transcription factor and master regulator of the oxidative stress response. During periods of oxidative stress, Nrf2-dependent changes in gene expression are important in regaining cellular homeostasis (Nguyen, et al., 2009) and can be used as indicators of the presence of oxidative stress in the cell.

In addition to the directly damaging actions of ROS, cellular oxidative stress also changes cellular activities on a molecular level. Redox sensitive proteins have altered physiology in the presence and absence of ROS, which is caused by the oxidation of sulfhydryls to disulfides on neighboring amino acids (Antelmann & Helmann 2011). Importantly Keap1, the negative regulator of Nrf2, is regulated in this manner (Itoh, et al. 2010).

ROS also undermine the mitochondrial defense system from oxidative damage. The antioxidant systems consist of superoxide dismutase, catalase, glutathione peroxidase and glutathione reductase, as well as antioxidants such as α-tocopherol and ubiquinol, or antioxidant vitamins and minerals including vitamin E, C, carotene, lutein, zeaxanthin, selenium, and zinc (Fletcher, 2010). The enzymes, vitamins and minerals catalyze the conversion of ROS to non-toxic molecules such as water and O2. However, these antioxidant systems are not perfect and endogenous metabolic processes and/or exogenous oxidative influences can trigger cumulative oxidative injuries to the mitochondria, causing a decline in their functionality and efficiency, which further promotes cellular oxidative stress (Balasubramanian, 2000; Ganea & Harding, 2006; Guo et al., 2013; Karimi et al., 2017).

However, an emerging viewpoint suggests that ROS-induced modifications may not be as detrimental as previously thought, but rather contribute to signaling processes (Foyer et al., 2017).

Sources of ROS Production

Direct Sources: Direct sources involve the deposition of energy onto water molecules, breaking them into active radical species. When ionizing radiation hits water, it breaks it into hydrogen (H*) and hydroxyl (OH*) radicals by destroying its bonds. The hydrogen will create hydroxyperoxyl free radicals (HO2*) if oxygen is available, which can then react with another of itself to form hydrogen peroxide (H2O2) and more O2 (Elgazzar and Kazem, 2015). Antioxidant mechanisms are also affected by radiation, with catalase (CAT) and peroxidase (POD) levels rising as a result of exposure (Seen et al. 2018; Ahmad et al. 2021).

Indirect Sources: An indirect source of ROS is the mitochondria, which is one of the primary producers in eukaryotic cells (Powers et al., 2008). As much as 2% of the electrons that should be going through the electron transport chain in the mitochondria escape, allowing them an opportunity to interact with surrounding structures. Electron-oxygen reactions result in free radical production, including the formation of hydrogen peroxide (H2O2) (Zhao et al., 2019). The electron transport chain, which also creates ROS, is activated by free adenosine diphosphate (ADP), O2, and inorganic phosphate (Pi) (Hargreaves et al. 2020; Raimondi et al. 2020; Vargas-Mendoza et al. 2021). The first and third complexes of the transport chain are the most relevant to mammalian ROS production (Raimondi et al., 2020). The mitochondria has its own set of DNA and it is a prime target of oxidative damage (Guo et al., 2013). ROS is also produced through nicotinamide adenine dinucleotide phosphate oxidase (Nox) stimulation, an event commenced by angiotensin II, a product/effector of the renin-angiotensin system (Nguyen Dinh Cat et al. 2013; Forrester et al. 2018). Other ROS producers include xanthine oxidase, immune cells (macrophage, neutrophils, monocytes, and eosinophils), phospholipase A2 (PLA2), monoamine oxidase (MAO), and carbon-based nanomaterials (Powers et al. 2008; Jacobsen et al. 2008; Vargas-Mendoza et al. 2021).

How it is Measured or Detected

Oxidative Stress: Direct measurement of ROS is difficult because ROS are unstable. The presence of ROS can be assayed indirectly by measurement of cellular antioxidants, or by ROS-dependent cellular damage. Listed below are common methods for detecting the KE, however there may be other comparable methods that are not listed

- Detection of ROS by chemiluminescence (https://www.sciencedirect.com/science/article/abs/pii/S0165993606001683)
- Detection of ROS by chemiluminescence is also described in OECD TG 495 to assess phototoxic potential.
- Glutathione (GSH) depletion. GSH can be measured by assaying the ratio of reduced to oxidized glutathione (GSH:GSSG) using a commercially available kit (e.g., http://www.abcam.com/gshgssg-ratio-detection-assay-kit-fluorometric-green-

ab138881.html).
- TBARS. Oxidative damage to lipids can be measured by assaying for lipid peroxidation using TBARS (thiobarbituric acid reactive substances) using a commercially available kit.
- 8-oxo-dG. Oxidative damage to nucleic acids can be assayed by measuring 8-oxo-dG adducts (for which there are a number of ELISA based commercially available kits),or HPLC, described in Chepelev et al. (Chepelev, et al. 2015).

Molecular Biology: Nrf2. Nrf2's transcriptional activity is controlled post-translationally by oxidation of Keap1. Assay for Nrf2 activity include:

- Immunohistochemistry for increases in Nrf2 protein levels and translocation into the nucleus Western blot for increased Nrf2 protein levels
- Western blot of cytoplasmic and nuclear fractions to observe translocation of Nrf2 protein from the cytoplasm to the nucleus qPCR of Nrf2 target genes (e.g., Nqo1, Hmox-1, Gcl, Gst, Prx, TrxR, Srxn), or by commercially available pathway-based qPCR array (e.g., oxidative stress array from SABiosciences)
- Whole transcriptome profiling by microarray or RNA-seq followed by pathway analysis (in IPA, DAVID, metacore, etc.) for enrichment of the Nrf2 oxidative stress response pathway (e.g., Jackson et al. 2014)
- OECD TG422D describes an ARE-Nrf2 Luciferase test method

In general, there are a variety of commercially available colorimetric or fluorescent kits for detecting Nrf2 activation.

Assay Type & Measured Content	**Description**	**Dose Range Studied**	**Assay Characteristics (Length/Ease of use/Accuracy)**
ROS Formation in the Mitochondria assay (Shaki et al., 2012)	"The mitochondrial ROS measurement was performed flow cytometry using DCFH-DA. Briefly, isolated kidney mitochondria were incubated with UA (0, 50, 100 and 200 µM) in respiration buffer containing (0.32 mM sucrose, 10mM Tris, 20 mM Mops, 50 µM EGTA, 0.5 mM MgCl2, 0.1 mM KH2PO4 and 5 mM sodium succinate) [32]. In the interval times of 5, 30 and 60 min following the UA addition, a sample was taken and DCFH-DA was added (final concentration, 10 µM) to mitochondria and was then incubated for 10 min.Uranyl acetate-induced ROS generation in isolated kidney mitochondria were determined through the flow cytometry (Partec, Deutschland) equipped with a 488-nm argon ion laser and supplied with the Flomax software and the signals were obtained using a 530-nm bandpass filter (FL-1 channel). Each determination is based on the mean fluorescence intensity of 15,000 counts."	0, 50,100 and 200 µM of Uranyl Acetate	Long/ Easy High accuracy
Mitochondrial Antioxidant Content Assay Measuring GSH content (Shaki et al., 2012)	"GSH content was determined using DTNB as the indicator and spectrophotometer method for the isolated mitochondria. The mitochondrial fractions (0.5 mg protein/ml) were incubated with various concentrations of uranyl acetate for 1 h at 30 °C and then 0.1 ml of mitochondrial fractions was added into 0.1 mol/l of phosphate buffers and 0.04% DTNB in a total volume of 3.0 ml (pH 7.4). The developed yellow color was read at 412 nm on a spectrophotometer (UV-1601 PC, Shimadzu, Japan). GSH content was expressed as µg/mg protein."	0, 50, 100, or 200 µM Uranyl Acetate	
H2O2 Production Assay Measuring H2O2 Production in isolated mitochondria (Heyno et al., 2008)	"Effect of CdCl2 and antimycin A (AA) on H2O2 production in isolated mitochondria from potato. H2O2 production was measured as scopoletin oxidation. Mitochondria were incubated for 30 min in the measuring buffer (see the Materials and Methods) containing 0.5 mM succinate as an electron donor and 0.2 µM mesoxalonitrile 3-chlorophenylhydrazone (CCCP) as an uncoupler, 10 U horseradish peroxidase and 5 µM scopoletin."	0, 10, 30 µM Cd2+ 2 µM antimycin A	
Flow Cytometry ROS & Cell Viability (Kruiderig et al., 1997)	"For determination of ROS, samples taken at the indicated time points were directly transferred to FACScan tubes. Dih123 (10 mM, final concentration) was added and cells were incubated at 37°C in a humidified atmosphere (95% air/5% CO2) for 10 min. At t 5 9, propidium iodide (10 mM, final concentration) was added, and cells were analyzed by flow cytometry at 60 ml/min. Nonfluorescent Dih123 is cleaved by ROS to fluorescent R123 and detected by the FL1 detector as described above for Dc (Van de Water 1995)""For determination of ROS, samples taken at the indicated time points were directly transferred to FACScan tubes. Dih123 (10 mM, final concentration) was added and cells were incubated at 37°C in a humidified atmosphere (95% air/5% CO2) for 10 min. At t 5 9, propidium iodide (10 mM, final concentration) was added, and cells were analyzed by flow cytometry at 60 ml/min. Nonfluorescent Dih123 is cleaved by ROS to fluorescent R123 and detected by the FL1 detector as described above for Dc (Van de Water 1995)"		Strong/easy medium
DCFH-DA Assay Detection of hydrogen peroxide production (Yuan et al., 2016)	Intracellular ROS production was measured using DCFH-DA as a probe. Hydrogen peroxide oxidizes DCFH to DCF. The probe is hydrolyzed intracellularly to DCFH carboxylate anion. No direct reaction with H2O2 to form fluorescent production.	0-400 µM	Long/ Easy High accuracy

H2-DCF-DAAssay Detection of superoxide production (Thiebault etal., 2007)	This dye is a stable nonpolar compound which diffuses readily into the cells and yields H2-DCF. Intracellular OH or ONOO- react with H2-DCF when cells contain peroxides, to form the highly fluorescent compound DCF, which effluxes the cell. Fluorescence intensity of DCF is measured using a fluorescence spectrophotometer.	0–600 µM	Long/ Easy High accuracy
CM-H2DCFDA Assay (Eruslanov & Kusmartsev, 2009)	The dye (CM-H2DCFDA) diffuses into the cell and is cleaved by esterases, the thiol reactive chlormethyl group reacts with intracellular glutathione which can be detected using flow cytometry.		Long/Easy/ High Accuracy

Method of Measurement	**References**	**Description**	**OECD-Approved Assay**
Chemiluminescence	(Lu, C. et al., 2006; Griendling, K. K., et al., 2016)	ROS can induce electron transitions in molecules, leading to electronically excited products. When the electrons transition back to ground state, chemiluminescence is emitted and can be measured. Reagents such as luminol and lucigenin are commonly used to amplify the signal.	No
Spectrophotometry	(Griendling, K. K., et al., 2016)	NO has a short half-life. However, if it has been reduced to nitrite (NO2-), stable azocompounds can be formed via the Griess Reaction, and further measured by spectrophotometry.	No
Direct or Spin Trapping-Based electron paramagnetic resonance (EPR) Spectroscopy	(Griendling, K. K., et al., 2016)	The unpaired electrons (free radicals) found in ROS can be detected with EPR and is known as electron paramagnetic resonance. A variety of spin traps can be used.	No
Nitroblue Tetrazolium Assay	(Griendling, K. K., et al., 2016)	The Nitroblue Tetrazolium assay is used to measure O2.− levels. O2.− reduces nitroblue tetrazolium (a yellow dye) to formazan (a blue dye), and can be measured at 620 nm.	No
Fluorescence analysis of dihydroethidium (DHE) or Hydrocyans	(Griendling, K. K., et al., 2016)	Fluorescence analysis of DHE is used to measure O2.− levels. O2.− is reduced to O2 as DHE is oxidized to 2-hydroxyethidium, and this reaction can be measured by fluorescence. Similarly, hydrocyans can be oxidized by any ROS, and measured via fluorescence.	No
Amplex Red Assay	(Griendling, K. K., et al., 2016)	Fluorescence analysis to measure extramitochondrial or extracellular H2O2 levels. In the presence of horseradish peroxidase and H2O2, Amplex Red is oxidized to resorufin, a fluorescent molecule measurable by plate reader.	No
Dichlorodihydrofluorescein Diacetate (DCFH-DA)	(Griendling, K. K., et al., 2016)	An indirect fluorescence analysis to measure intracellular H2O2 levels. H2O2 interacts with peroxidase or heme proteins, which further react with DCFH, oxidizing it to dichlorofluorescein (DCF), a fluorescent product.	No
HyPer Probe	(Griendling, K. K., et al., 2016)	Fluorescent measurement of intracellular H2O2 levels. HyPer is a genetically encoded fluorescent sensor that can be used for in vivo and in situ imaging.	No
Cytochrome c Reduction Assay	(Griendling, K. K., et al., 2016)	The cytochrome c reduction assay is used to measure O2.− levels. O O2.− is reduced to O2 as ferricytochrome c is oxidized to ferrocytochrome c, and this reaction can be measured by an absorbance increase at 550 nm.	No
Proton-electron double-resonance imaging (PEDRI)	(Griendling, K. K., et al., 2016)	The redox state of tissue is detected through nuclear magnetic resonance/magnetic resonance imaging, with the use of a nitroxide spin probe or biradical molecule.	No
Glutathione (GSH) depletion	(Biesemann, N. et al., 2018)	A downstream target of the Nrf2 pathway is involved in GSH synthesis. As an indication of oxidation status, GSH can be measured by assaying the ratio of reduced to oxidized glutathione (GSH:GSSG) using a commercially available kit (e.g., http://www.abcam.com/gshgssg-ratio-detection-assay-kit-fluorometric-green-ab138881.html).	No
Thiobarbituric acid reactive substances (TBARS)	(Griendling, K. K., et al., 2016)	Oxidative damage to lipids can be measured by assaying for lipid peroxidation with TBARS using a commercially available kit.	No

Protein oxidation (carbonylation)	(Azimzadeh et al., 2017; Azimzadeh et al., 2015; Ping et al., 2020)	Can be determined with ELISA or a commercial assay kit. Protein oxidation can indicate the level of oxidative stress.	No
Seahorse XFp Analyzer	Leung et al. 2018	The Seahorse XFp Analyzer provides information on mitochondrial function, oxidative stress, and metabolic dysfunction of viable cells by measuring respiration (oxygen consumption rate; OCR) and extracellular pH (extracellular acidification rate; ECAR).	No

Molecular Biology: Nrf2. Nrf2's transcriptional activity is controlled post-translationally by oxidation of Keap1. Assays for Nrf2 activity include:

Method of Measurement	References	Description	OECD-Approved Assay
Immunohistochemistry	(Amsen, D., de Visser, K. E., and Town, T., 2009)	Immunohistochemistry for increases in Nrf2 protein levels and translocation into the nucleus	No
qPCR	(Forlenza et al., 2012)	qPCR of Nrf2 target genes (e.g., Nqo1, Hmox-1, Gcl, Gst, Prx, TrxR, Srxn), or by commercially available pathway-based qPCR array (e.g., oxidative stress array from SABiosciences)	No
Whole transcriptome profiling via microarray or via RNA-seq followed by a pathway analysis	(Jackson, A. F. et al., 2014)	Whole transcriptome profiling by microarray or RNA-seq followed by pathway analysis (in IPA, DAVID, metacore, etc.) for enrichment of the Nrf2 oxidative stress response pathway	No

Update - non-endorsed (by You Song, 02/09/2026)

ToxCast/Tox21 assays (invitrodb v4.3): ATG_NRF2_ARE_CIS; Tox21_ARE_BLA_Agonist_ratio; TOX21_ARE_KS_LUC_Agonist; LTEA_HepaRG_NFE2L2; LTEA_HepaRG_GCLC; LTEA_HepaRG_CAT

References

Ahmad, S. et al. (2021), "60Co-γ Radiation Alters Developmental Stages of Zeugodacus cucurbitae (Diptera: Tephritidae) Through Apoptosis Pathways Gene Expression", Journal Insect Science, Vol. 21/5, Oxford University Press, Oxford, https://doi.org/10.1093/jisesa/ieab080

Antelmann, H. and J. D. Helmann (2011), "Thiol-based redox switches and gene regulation.", Antioxidants & Redox Signaling, Vol. 14/6, Mary Ann Leibert Inc., Larchmont, https://doi.org/10.1089/ars.2010.3400

Amsen, D., de Visser, K. E., and Town, T. (2009), "Approaches to determine expression of inflammatory cytokines", in Inflammation and Cancer, Humana Press, Totowa, https://doi.org/10.1007/978-1-59745-447-6_5

Azimzadeh, O. et al. (2015), "Integrative Proteomics and Targeted Transcriptomics Analyses in Cardiac Endothelial Cells Unravel Mechanisms of Long-Term Radiation-Induced Vascular Dysfunction", Journal of Proteome Research, Vol. 14/2, American Chemical Society, Washington, https://doi.org/10.1021/pr501141b

Azimzadeh, O. et al. (2017), "Proteome analysis of irradiated endothelial cells reveals persistent alteration in protein degradation and the RhoGDI and NO signalling pathways", International Journal of Radiation Biology, Vol. 93/9, Informa, London, https://doi.org/10.1080/09553002.2017.1339332

Azzam, E. I. et al. (2012), "Ionizing radiation-induced metabolic oxidative stress and prolonged cell injury", Cancer Letters, Vol. 327/1-2, Elsevier, Ireland, https://doi.org/10.1016/j.canlet.2011.12.012

Bai, J. et al. (2020), "Irradiation-induced senescence of bone marrow mesenchymal stem cells aggravates osteogenic differentiation dysfunction via paracrine signaling", American Journal of Physiology - Cell Physiology, Vol. 318/5, American Physiological Society, Rockville, https://doi.org/10.1152/ajpcell.00520.2019.

Balasubramanian, D (2000), "Ultraviolet radiation and cataract", Journal of ocular pharmacology and therapeutics, Vol. 16/3, Mary Ann Liebert Inc., Larchmont, https://doi.org/10.1089/jop.2000.16.285.

Biesemann, N. et al., (2018), "High Throughput Screening of Mitochondrial Bioenergetics in Human Differentiated Myotubes Identifies Novel Enhancers of Muscle Performance in Aged Mice", Scientific Reports, Vol. 8/1, Nature Portfolio, London, https://doi.org/10.1038/s41598-018-27614-8.

Elgazzar, A. and N. Kazem. (2015), "Chapter 23: Biological effects of ionizing radiation" in The Pathophysiologic Basis of Nuclear Medicine, Springer, New York, pp. 540-548

Eruslanov, E., & Kusmartsev, S. (2010). Identification of ROS using oxidized DCFDA and flow-cytometry. Methods in molecular biology ,N.J., Vol. 594, https://doi.org/10.1007/978-1-60761-411-1_4

Fletcher, A. E (2010), "Free radicals, antioxidants and eye diseases: evidence from epidemiological studies on cataract and age-related macular degeneration", Ophthalmic Research, Vol. 44, Karger International, Basel, https://doi.org/10.1159/000316476.

Forlenza, M. et al. (2012), "The use of real-time quantitative PCR for the analysis of cytokine mRNA levels" in Cytokine Protocols, Springer, New York, https://doi.org/10.1007/978-1-61779-439-1_2

Forrester, S.J. et al. (2018), "Angiotensin II Signal Transduction: An Update on Mechanisms of Physiology and Pathophysiology", Physiological Reviews, Vol. 98/3, American Physiological Society, Rockville, https://doi.org/10.1152/physrev.00038.201

Foyer, C. H., A. V. Ruban, and G. Noctor (2017), “Viewing oxidative stress through the lens of oxidative signalling rather than damage”, Biochemical Journal, Vol. 474/6, Portland Press, England, https://doi.org/10.1042/BCJ20160814

Ganea, E. and J. J. Harding (2006), “Glutathione-related enzymes and the eye”, Current eye research, Vol. 31/1, Informa, London, https://doi.org/10.1080/02713680500477347.

Griendling, K. K. et al. (2016), “Measurement of reactive oxygen species, reactive nitrogen species, and redox-dependent signaling in the cardiovascular system: a scientific statement from the American Heart Association”, Circulation research, Vol. 119/5, Lippincott Williams & Wilkins, Philadelphia, https://doi.org/10.1161/RES.0000000000000110

Guo, C. et al. (2013), “Oxidative stress, mitochondrial damage and neurodegenerative diseases”, Neural regeneration research, Vol. 8/21, Publishing House of Neural Regeneration Research, China, https://doi.org/10.3969/j.issn.1673-5374.2013.21.009

Hargreaves, M., and L. L. Spriet (2020), “Skeletal muscle energy metabolism during exercise.”, Nature Metabolism, Vol. 2, Nature Portfolio, London, https://doi.org/10.1038/s42255-020-0251-4

Hladik, D. and S. Tapio (2016), “Effects of ionizing radiation on the mammalian brain”, Mutation Research/Reviews in Mutation Research, Vol. 770, Elsevier, Amsterdam, https://doi.org/10.1016/j.mrrev.2016.08.003

Itoh, K., J. Mimura and M. Yamamoto (2010), “Discovery of the negative regulator of Nrf2, Keap1: a historical overview”, Antioxidants & Redox Signaling, Vol. 13/11, Mary Ann Leibert Inc., Larchmont, https://doi.org/10.1089/ars.2010.3222

Jackson, A.F. et al. (2014), “Case study on the utility of hepatic global gene expression profiling in the risk assessment of the carcinogen furan.”, Toxicology and Applied Pharmacology, Vol. 274/11, Elsevier, Amsterdam, https://doi.org/10.1016/j.taap.2013.10.019

Jacobsen, N.R. et al. (2008), “Genotoxicity, cytotoxicity, and reactive oxygen species induced by single-walled carbon nanotubes and C60 fullerenes in the FE1-MutaTM Mouse lung epithelial cells”, Environmental and Molecular Mutagenesis, Vol. 49/6, John Wiley & Sons, Inc., Hoboken, https://doi.org/10.1002/em.20406

Karimi, N. et al. (2017), “Radioprotective effect of hesperidin on reducing oxidative stress in the lens tissue of rats”, International Journal of Pharmaceutical Investigation, Vol. 7/3, Phcog Net, Bengaluru, https://doi.org/10.4103/jphi.JPHI_60_17.

Leung, D.T.H., and Chu, S. (2018), “Measurement of Oxidative Stress: Mitochondrial Function Using the Seahorse System” In: Murthi, P., Vaillancourt, C. (eds) Preeclampsia. Methods in Molecular Biology, vol 1710. Humana Press, New York, NY. https://doi.org/10.1007/978-1-4939-7498-6_22

Lu, C., G. Song, and J. Lin (2006), “Reactive oxygen species and their chemiluminescence-detection methods”, TrAC Trends in Analytical Chemistry, Vol. 25/10, Elsevier, Amsterdam, https://doi.org/10.1016/j.trac.2006.07.007

Nguyen Dinh Cat, A. et al. (2013), “Angiotensin II, NADPH oxidase, and redox signaling in the vasculature”, Antioxidants & redox signaling, Vol. 19/10, Mary Ann Liebert, Larchmont, https://doi.org/10.1089/ars.2012.4641

Ping, Z. et al. (2020), “Oxidative Stress in Radiation-Induced Cardiotoxicity”, Oxidative Medicine and Cellular Longevity, Vol. 2020, Hindawi, https://doi.org/10.1155/2020/3579143

Powers, S.K. and M.J. Jackson. (2008), “Exercise-Induced Oxidative Stress: Cellular Mechanisms and Impact on Muscle Force Production”, Physiological Reviews, Vol. 88/4, American Physiological Society, Rockville, https://doi.org/10.1152/physrev.00031.2007

Raimondi, V., F. Ciccarese and V. Ciminale. (2020), “Oncogenic pathways and the electron transport chain: a dangeROS liason”, British Journal of Cancer, Vol. 122/2, Nature Portfolio, London, https://doi.org/10.1038/s41416-019-0651-y

Seen, S. and L. Tong. (2018), “Dry eye disease and oxidative stress”, Acta Ophthalmologica, Vol. 96/4, John Wiley & Sons, Inc., Hoboken, https://doi.org/10.1111/aos.13526

Ungvari, Z. et al. (2013), “Ionizing Radiation Promotes the Acquisition of a Senescence-Associated Secretory Phenotype and Impairs Angiogenic Capacity in Cerebromicrovascular Endothelial Cells: Role of Increased DNA Damage and Decreased DNA Repair Capacity in Microvascular Radiosensitivity”, The Journals of Gerontology Series A: Biological Sciences and Medical Sciences, Vol. 68/12, Oxford University Press, Oxford, https://doi.org/10.1093/gerona/glt057.

Vargas-Mendoza, N. et al. (2021), “Oxidative Stress, Mitochondrial Function and Adaptation to Exercise: New Perspectives in Nutrition”, Life, Vol. 11/11, Multidisciplinary Digital Publishing Institute, Basel, https://doi.org/10.3390/life11111269

Wang, H. et al. (2019), “Radiation-induced heart disease: a review of classification, mechanism and prevention”, International Journal of Biological Sciences, Vol. 15/10, Ivyspring International Publisher, Sydney, https://doi.org/10.7150/ijbs.35460

Zhang, R. et al. (2009), “Blockade of AT1 receptor partially restores vasoreactivity, NOS expression, and superoxide levels in cerebral and carotid arteries of hindlimb unweighting rats”, Journal of applied physiology, Vol. 106/1, American Physiological Society, Rockville, https://doi.org/10.1152/japplphysiol.01278.2007.

Zhao, R. Z. et al. (2019), “Mitochondrial electron transport chain, ROS generation and uncoupling”, International journal of molecular medicine, Vol. 44/1, Spandidos Publishing Ltd., Athens, https://doi.org/10.3892/ijmm.2019.4188

Event: 1445: Increase, Lipid peroxidation

Short Name: Increase, LPO

Event Component

Process	Object	Action

Process	Object	Action
lipid oxidation	polyunsaturated fatty acid	increased

AOPs Including This Key Event

AOP ID and Name	Event Type
Aop:329 - Excessive reactive oxygen species production leading to mortality (3)	KeyEvent
Aop:413 - Oxidation and antagonism of reduced glutathione leading to mortality via acute renal failure	KeyEvent
Aop:492 - Glutathione conjugation leading to reproductive dysfunction via oxidative stress	KeyEvent
Aop:521 - Essential element imbalance leads to reproductive failure via oxidative stress	KeyEvent
Aop:331 - Increase in reactive oxygen species leading to growth inhibition via lipid peroxidation and cell death	KeyEvent
Aop:615 - Suppression of Keap1 cysteine oxidation leading to liver inflammation	KeyEvent
Aop:326 - Increase in reactive oxygen species leading to growth inhibition via lipid peroxidation and decreased cell proliferation	KeyEvent
Aop:647 - ROS formation leading to growth inhibition modulated by the Keap1–Nrf2 antioxidant response	KeyEvent

Biological Context

Level of Biological Organization
Molecular

Cell term

Cell term
cell

Organ term

Organ term
organ

Domain of Applicability

Taxonomic Applicability

Term	Scientific Term	Evidence	Links
fish	fish	Moderate	NCBI
mammals	mammals	High	NCBI

Life Stage Applicability

Life Stage	Evidence
All life stages	High

Sex Applicability

Sex	Evidence
Unspecific	High

The biological domain of applicability for this KE is broad because lipid membranes and oxidizable fatty acids are widely conserved biological features. The event is applicable wherever lipid substrates susceptible to oxidation are present and where oxidants can access those substrates. The KE is therefore relevant across many biological systems, including unicellular algae, invertebrates, fish, mammals and human-derived cells. The current evidence base is strongest in mammalian systems because lipid peroxidation chemistry and analytical methods have been extensively studied there, but ecotoxicological evidence supports relevance in algae, crustaceans, mollusks and fish.

The KE is not intrinsically limited by sex or life stage. However, the magnitude of lipid peroxidation and its downstream consequences may be modified by lipid composition, antioxidant capacity, oxygen availability, temperature, metabolic rate, nutritional status, metal availability, and exposure duration. Organisms or tissues enriched in polyunsaturated fatty acids, exposed to high oxygen flux, or experiencing antioxidant depletion may be particularly susceptible. In photosynthetic organisms, lipid peroxidation may also occur in chloroplast and thylakoid membranes; in animals, mitochondria and plasma membranes are common sites of interest.

Within the ROS-growth AOP network, this KE is especially relevant as a molecular damage event linking oxidative stress to impaired mitochondrial membrane function, decreased coupling of oxidative phosphorylation, reduced ATP production, cell injury, and decreased growth. Nevertheless, this KE should remain modular: it may be reused in other AOPs whenever increased lipid oxidation products are measured as a consequence of oxidative stress or other lipid-damaging perturbations.

Key Event Description

Lipid peroxidation is an oxidative degradation process affecting lipids, particularly polyunsaturated fatty acids in cellular and organelle membranes. The process is initiated when oxidants, including free radicals and reactive oxygen species, abstract hydrogen atoms from susceptible lipid chains. This generates lipid radicals that react with molecular oxygen to form lipid peroxyl radicals and lipid hydroperoxides. These products can propagate chain reactions, producing additional oxidized lipids and secondary reactive aldehydes such as malondialdehyde (MDA), 4-hydroxy-2-nonenal (4-HNE), and related hydroxyalkenals (Esterbauer et al., 1991; Yin et al., 2011; Ayala et al., 2014).

As a key event, increased lipid peroxidation represents a measurable increase in oxidized lipid products relative to an appropriate control state. The event may reflect direct oxidative damage to membrane lipids, increased formation of lipid hydroperoxides, increased accumulation of MDA or 4-HNE, or increased abundance of specific oxidized phospholipid or fatty acid species. Because lipid peroxidation products can alter membrane fluidity, permeability and signaling, the event is relevant both as a marker of oxidative damage and as a potential contributor to downstream mitochondrial dysfunction, loss of membrane integrity, cytotoxicity and impaired growth (Esterbauer et al., 1991; Uchida, 2003; Ayala et al., 2014).

This KE should be described independently of any specific upstream or downstream event. In an AOP context, lipid peroxidation is commonly downstream of oxidative stress and upstream of events related to decreased mitochondrial coupling, cellular injury, or altered membrane-dependent biological processes. However, the KE itself is defined only by the increased lipid oxidation state and its measurable biochemical products.

How it is Measured or Detected

No OECD Test Guideline is currently dedicated specifically to measurement of lipid peroxidation as a standalone endpoint. Nevertheless, the KE can be measured using several well-established biochemical and analytical methods. Scientific confidence is highest when methods quantify specific lipid peroxidation products or oxidized lipid species directly, and lower when nonspecific colorimetric assays are used without appropriate controls or confirmatory methods.

Measurement approach	Endpoint measured	Representative method names	Scientific confidence and limitations
TBARS / MDA assays	Thiobarbituric acid reactive substances, often interpreted as MDA or MDA-like products	TBARS assay; spectrophotometric or fluorometric MDA assays	Widely used and sensitive, but not fully specific because TBA can react with compounds other than MDA. Best used as a screening or comparative indicator of lipid peroxidation, particularly when supported by extraction, HPLC separation or additional markers (Buege and Aust, 1978; Ohkawa et al., 1979; Janero, 1990; Draper and Hadley, 1990).
4-HNE and hydroxyalkenal assays	4-hydroxy-2-nonenal and related reactive aldehydes	ELISA, immunoblotting of HNE-protein adducts, HPLC or LC-MS quantification	Mechanistically informative because 4-HNE is a major bioactive lipid peroxidation product. Antibody-based methods can detect protein adducts, whereas chromatographic or mass spectrometric methods improve specificity (Esterbauer et al., 1991; Uchida, 2003; Ayala et al., 2014).

Measurement approach	Endpoint measured	Representative method names	Scientific confidence and limitations
Lipid hydroperoxide assays	Primary lipid hydroperoxides	FOX assay; iodometric assays; commercial lipid hydroperoxide kits	Useful for detecting relatively early lipid peroxidation products. Hydroperoxides can be unstable and sample handling is critical. FOX-based methods provide a simple approach for lipid hydroperoxide detection (Jiang et al., 1992).
Chromatography and mass spectrometry	Specific oxidized fatty acids, oxidized phospholipids, oxylipins or oxidized lipid classes	HPLC, GC, LC-MS/MS, lipidomics	High specificity and quantitative power when standards and validated workflows are available. These methods can distinguish individual oxidized lipid species and are preferred for detailed mechanistic studies (Yin et al., 2011; Li et al., 2019).
Fluorescent probes and imaging	Oxidation-sensitive fluorescent signal in cellular lipids	BODIPY 581/591 C11 and related lipid oxidation probes	Useful for cell-based or imaging applications and spatial localization, but probe specificity, photoxidation and calibration must be considered. Best used with complementary biochemical or analytical endpoints.

References

AOP-Wiki. 2026. Key Event 1445: Increase, Lipid peroxidation. AOP-Wiki. Available at: https://aopwiki.org/events/1445. Accessed 14 May 2026.

Alam MR, Ehiguese FO, Vitale D, Martín-Díaz ML. 2022. Oxidative stress response to hydrogen peroxide exposure of Mytilus galloprovincialis and Ruditapes philippinarum: reduced embryogenesis success and altered biochemical response of sentinel marine bivalve species. Environmental Chemistry and Ecotoxicology 4:97-105.

Ayala A, Munoz MF, Arguelles S. 2014. Lipid peroxidation: production, metabolism, and signaling mechanisms of malondialdehyde and 4-hydroxy-2-nonenal. Oxidative Medicine and Cellular Longevity 2014:360438. https://doi.org/10.1155/2014/360438.

Belaid C, Sbartai I. 2021. Assessing the effects of Thiram to oxidative stress responses in a freshwater bioindicator cladoceran (Daphnia magna). Chemosphere 268:128808. https://doi.org/10.1016/j.chemosphere.2020.128808.

Buege JA, Aust SD. 1978. Microsomal lipid peroxidation. Methods in Enzymology 52:302-310. https://doi.org/10.1016/S0076-6879(78)52032-6.

Cong B, Liu C, Wang L, Chai Y. 2020. The impact on antioxidant enzyme activity and related gene expression following adult zebrafish (Danio rerio) exposure to dimethyl phthalate. Animals 10(4):717. https://doi.org/10.3390/ani10040717.

Draper HH, Hadley M. 1990. Malondialdehyde determination as index of lipid peroxidation. Methods in Enzymology 186:421-431. https://doi.org/10.1016/0076-6879(90)86135-I.

Esperanza M, Cid A, Herrero C, Rioboo C. 2015. Acute effects of a prooxidant herbicide on the microalga Chlamydomonas reinhardtii: screening cytotoxicity and genotoxicity endpoints. Aquatic Toxicology 165:210-221. https://doi.org/10.1016/j.aquatox.2015.06.004.

Esterbauer H, Schaur RJ, Zollner H. 1991. Chemistry and biochemistry of 4-hydroxynonenal, malonaldehyde and related aldehydes. Free Radical Biology and Medicine 11(1):81-128. https://doi.org/10.1016/0891-5849(91)90192-6.

Janero DR. 1990. Malondialdehyde and thiobarbituric acid-reactivity as diagnostic indices of lipid peroxidation and peroxidative tissue injury. Free Radical Biology and Medicine 9(6):515-540. https://doi.org/10.1016/0891-5849(90)90131-2.

Jiang ZY, Hunt JV, Wolff SP. 1992. Ferrous ion oxidation in the presence of xylenol orange for detection of lipid hydroperoxide in low density lipoprotein. Analytical Biochemistry 202(2):384-389. https://doi.org/10.1016/0003-2697(92)90122-N.

Knauert S, Knauer K. 2008. The role of reactive oxygen species in copper toxicity to two freshwater green algae. Journal of Phycology 44(2):311-319. https://doi.org/10.1111/j.1529-8817.2008.00471.x.

Li L, Zhong S, Shen X, Li Q, Xu W, Tao Y, Yin H. 2019. Recent development on liquid chromatography-mass

spectrometry analysis of oxidized lipids. Free Radical Biology and Medicine 144:16-34. https://doi.org/10.1016/j.freeradbiomed.2019.06.006.

Moore TD, Martin-Creuzburg D, Yampolsky LY. 2023. Diet effects on longevity, heat tolerance, lipid peroxidation and mitochondrial membrane potential in Daphnia. Oecologia 202(1):151-163. https://doi.org/10.1007/s00442-023-05382-1.

Ohkawa H, Ohishi N, Yagi K. 1979. Assay for lipid peroxides in animal tissues by thiobarbituric acid reaction. Analytical Biochemistry 95(2):351-358. https://doi.org/10.1016/0003-2697(79)90738-3.

Ouillon N, Sokolov EP, Otto S, Rehder G, Sokolova IM. 2021. Effects of variable oxygen regimes on mitochondrial bioenergetics and reactive oxygen species production in a marine bivalve, Mya arenaria. Journal of Experimental Biology 224(4):jeb237156. https://doi.org/10.1242/jeb.237156.

Tseng YC, Chen RD, Lucassen M, Schmidt MM, Dringen R, Abele D, Hwang PP. 2011. Exploring uncoupling proteins and antioxidant mechanisms under acute cold exposure in brains of fish. PLoS ONE 6(3):e18180. https://doi.org/10.1371/journal.pone.0018180.

Uchida K. 2003. 4-Hydroxy-2-nonenal: a product and mediator of oxidative stress. Progress in Lipid Research 42(4):318-343. https://doi.org/10.1016/S0163-7827(03)00014-6.

Yin H, Xu L, Porter NA. 2011. Free radical lipid peroxidation: mechanisms and analysis. Chemical Reviews 111(10):5944-5972. https://doi.org/10.1021/cr200084z.

Event: 1446: Decrease, Coupling of oxidative phosphorylation

Short Name: Decrease, Coupling of OXPHOS

Event Component

Process	Object	Action
proton binding	mitochondrion	increased
oxidative phosphorylation uncoupler activity	mitochondrion	increased
regulation of mitochondrial membrane potential	mitochondrion	decreased

AOPs Including This Key Event

AOP ID and Name	Event Type
Aop:267 - Uncoupling of oxidative phosphorylation leading to growth inhibition via glucose depletion	MolecularInitiatingEvent
Aop:263 - Uncoupling of oxidative phosphorylation leading to growth inhibition via decreased cell proliferation	MolecularInitiatingEvent
Aop:264 - Uncoupling of oxidative phosphorylation leading to growth inhibition via ATP depletion associated cell death	MolecularInitiatingEvent
Aop:265 - Uncoupling of oxidative phosphorylation leading to growth inhibition via increased cytosolic calcium	MolecularInitiatingEvent
Aop:266 - Uncoupling of oxidative phosphorylation leading to growth inhibition via decreased Na-K ATPase activity	MolecularInitiatingEvent
Aop:268 - Uncoupling of oxidative phosphorylation leading to growth inhibition via mitochondrial swelling	MolecularInitiatingEvent
Aop:534 - Succinate dehydrogenase (SDH) inhibition leads to oxidative stress	KeyEvent
Aop:331 - Increase in reactive oxygen species leading to growth inhibition via lipid peroxidation and cell death	KeyEvent
Aop:596 - Excessive reactive oxygen species leading to growth inhibition via protein oxidation and cell injury/death	KeyEvent
Aop:598 - Excessive reactive oxygen species leading to growth inhibition via protein oxidation and reduced cell proliferation	KeyEvent
Aop:612 - Peroxisome proliferator-activated receptor alpha activation leading to early life stage mortality via reduced adenosine triphosphate	KeyEvent
Aop:613 - Peroxisome proliferator-activated receptor alpha activation leading to early life stage mortality via increased reactive oxygen species production	KeyEvent
Aop:326 - Increase in reactive oxygen species leading to growth inhibition via lipid peroxidation and decreased cell proliferation	KeyEvent
Aop:332 - Increase in reactive oxygen species leading to growth inhibition via protein oxidation and decreased cell proliferation	KeyEvent

AOP ID and Name	Event Type
Aop:333 - Increase in reactive oxygen species leading to growth inhibition via protein oxidation and cell death	KeyEvent

Stressors

Name
2,4-Dinitrophenol
Carbonyl cyanide-p-trifluoromethoxyphenylhydrazone
Carbonyl cyanide m-chlorophenyl hydrazone
Pentachlorophenol
Triclosan
Emodin
Malonoben

Biological Context

Level of Biological Organization
Cellular

Cell term

Cell term
cell

Domain of Applicability

Taxonomic Applicability

Term	Scientific Term	Evidence	Links
zebrafish	Danio rerio	High	NCBI
human	Homo sapiens	High	NCBI
mouse	Mus musculus	High	NCBI
rat	Rattus norvegicus	High	NCBI
Lemna minor	Lemna minor	High	NCBI

Life Stage Applicability

Life Stage	Evidence
Embryo	High
Juvenile	High
Adult, reproductively mature	Moderate

Sex Applicability

Sex	Evidence
Unspecific	High

Taxonomic applicability domain

This key event is in general considered applicable to most eukaryotes, as the mitochondrion and oxidative phosphorylation are highly conserved (Roger 2017).

Life stage applicability domain

This key event is considered applicable to all life stages, as ATP synthesis by oxidative phosphorylation is an essential biological process for most living organisms.

Sex applicability domain

This key event is considered sex-unspecific, as both males and females use oxidative phosphorylation as a main process to generate ATP.

Key Event Description

Decreased coupling of oxidative phosphorylation (OXPHOS), or uncoupling of OXPHOS, describes dissipation of protonmotive force (PMF) across the inner mitochondrial membrane (IMM) by environmental stressors. In eukaryotes, the mitochondrial electron transport chain mediates a series of redox reactions to create a PMF across the IMM. The PMF is used as energy to drive adenosine triphosphate (ATP) synthesis through phosphorylation of adenosine diphosphate (ADP). These processes are coupled and referred to as OXPHOS. A number of chemicals can dissipate the PMF, leading to uncoupling of OXPHOS. This key event describes the main outcome of the interactions between an uncoupler and the transmembrane PMF. An uncoupler can bind to a proton in the mitochondrial inter membrane space, transport the proton to the matrix side of the IMM, release the proton and move back to the inter membrane space. These processes are repeated until the transmembrane PMF is dissipated. This KE is therefore a lumped term of these processes and represents the final consequence of the interactions.

How it is Measured or Detected

Uncoupling of oxidative phosphorylation can be indicated by reduced mitochondrial membrane potential, increased proton leak and/or increased oxygen consumption rate.

- Mitochondrial membrane potential can be determined using ToxCast high-throughput screening bioassays such as “APR_HepG2_MitoMembPot”, “APR_Hepat_MitoFxnI”, and “APR_Mitochondrial_membrane_potential”, and the Tox21 high-throughput screening assay “tox21-mitotox-p1”.
- Mitochondrial membrane potential can also be measured using commercially available fluorescent probes such as TMRM (tetramethylrhodamine, methyl ester, perchlorate), TMRE (tetramethylrhodamine, ethyl ester, perchlorate) and JC-1 (Perry 2011).
- Proton leak and oxygen consumption rate can be measured using a high-resolution respirometry (Affourtit 2018) or a Seahorse XF analyzer (Divakaruni 2014).

References

Affourtit C, Wong H-S, Brand MD. 2018. Measurement of proton leak in isolated mitochondria. In Palmeira CM, Moreno AJ, eds, *Mitochondrial Bioenergetics: Methods and Protocols*. Springer New York, New York, NY, pp 157-170.

Attene-Ramos MS, Huang R, Sakamuru S, Witt KL, Beeson GC, Shou L, Schnellmann RG, Beeson CC, Tice RR, Austin CP, Xia M. 2013. Systematic study of mitochondrial toxicity of environmental chemicals using quantitative high throughput screening. *Chemical Research in Toxicology* 26:1323-1332. DOI: 10.1021/tx4001754.

Attene-Ramos MS, Huang RL, Michael S, Witt KL, Richard A, Tice RR, Simeonov A, Austin CP, Xia MH. 2015. Profiling of the Tox21 chemical collection for mitochondrial function to identify compounds that acutely decrease mitochondrial membrane potential. *Environ Health Persp* 123:49-56. DOI: 10.1289/ehp.1408642.

Divakaruni AS, Paradyse A, Ferrick DA, Murphy AN, Jastroch M. 2014. Chapter Sixteen - Analysis and Interpretation of Microplate-Based Oxygen Consumption and pH Data. In Murphy AN, Chan DC, eds, *Methods in Enzymology*. Vol 547. Academic Press, pp 309-354.

Dreier DA, Denslow ND, Martyniuk CJ. 2019. Computational *in vitro* toxicology uncovers chemical structures impairing mitochondrial membrane potential. *J Chem Inf Model* 59:702-712. DOI: 10.1021/acs.jcim.8b00433.

Escher BI, Schwarzenbach RP. 2002. Mechanistic studies on baseline toxicity and uncoupling of organic compounds as a basis for modeling effective membrane concentrations in aquatic organisms. *Aquatic Sciences* 64:20-35. DOI: 10.1007/s00027-002-8052-2.

Legradi J, Dahlberg A-K, Cenijn P, Marsh G, Asplund L, Bergman Å, Legler J. 2014. Disruption of Oxidative Phosphorylation (OXPHOS) by Hydroxylated Polybrominated Diphenyl Ethers (OH-PBDEs) Present in the Marine Environment. *Environmental Science & Technology* 48:14703-14711. DOI: 10.1021/es5039744.

Naven RT, Swiss R, Klug-Mcleod J, Will Y, Greene N. 2012. The development of structure-activity relationships for mitochondrial dysfunction: Uncoupling of oxidative phosphorylation. *Toxicol Sci* 131:271-278. DOI: 10.1093/toxsci/kfs279.

Perry SW, Norman JP, Barbieri J, Brown EB, Gelbard HA. 2011. Mitochondrial membrane potential probes and the proton gradient: a practical usage guide. *BioTechniques* 50:98-115. DOI: 10.2144/000113610.

Roger AJ, Munoz-Gomez SA, Kamikawa R. 2017. The origin and diversification of mitochondria.*Curr Biol* 27:R1177-R1192. DOI: 10.1016/j.cub.2017.09.015.

Russom CL, Bradbury SP, Broderius SJ, Hammermeister DE, Drummond RA. 1997. Predicting modes of toxic action from chemical structure: Acute toxicity in the fathead minnow (Pimephales promelas). *Environ Toxicol Chem* 16:948-967. DOI: https://doi.org/10.1002/etc.5620160514.

Schultz TW, Cronin MTD. 1997. Quantitative structure-activity relationships for weak acid respiratory uncouplers to Vibrio fisheri. *Environ Toxicol Chem* 16:357-360. DOI: https://doi.org/10.1002/etc.5620160235.

Shim J, Weatherly LM, Luc RH, Dorman MT, Neilson A, Ng R, Kim CH, Millard PJ, Gosse JA. 2016. Triclosan is a mitochondrial uncoupler in live zebrafish. *J Appl Toxicol* 36:1662-1667. DOI: 10.1002/jat.3311.

Sugiyama Y, Shudo T, Hosokawa S, Watanabe A, Nakano M, Kakizuka A. 2019. Emodin, as a mitochondrial uncoupler, induces strong decreases in adenosine triphosphate (ATP) levels and proliferation of B16F10 cells, owing to their poor glycolytic reserve. *Genes to Cells* 24:569-584. DOI: https://doi.org/10.1111/gtc.12712.

Terada H. 1990. Uncouplers of oxidative phosphorylation. *Environ Health Perspect* 87:213-218. DOI: 10.1289/ehp.9087213.

Troger F, Delp J, Funke M, van der Stel W, Colas C, Leist M, van de Water B, Ecker GF. 2020. Identification of mitochondrial toxicants by combined in silico and in vitro studies – A structure-based view on the adverse outcome pathway. *Computational Toxicology* 14:100123. DOI: https://doi.org/10.1016/j.comtox.2020.100123.

Weatherly LM, Shim J, Hashmi HN, Kennedy RH, Hess ST, Gosse JA. 2016. Antimicrobial agent triclosan is a proton ionophore

uncoupler of mitochondria in living rat and human mast cells and in primary human keratinocytes. *Journal of Applied Toxicology* 36:777-789. DOI: https://doi.org/10.1002/jat.3209.

Xia M, Huang R, Shi Q, Boyd WA, Zhao J, Sun N, Rice JR, Dunlap PE, Hackstadt AJ, Bridge MF, Smith MV, Dai S, Zheng W, Chu PH, Gerhold D, Witt KL, DeVito M, Freedman JH, Austin CP, Houck KA, Thomas RS, Paules RS, Tice RR, Simeonov A. 2018. Comprehensive analyses and prioritization of Tox21 10K chemicals affecting mitochondrial function by in-depth mechanistic studies. *Environ Health Perspect* 126:077010. DOI: 10.1289/EHP2589.

Event: 1771: Decrease, Adenosine triphosphate pool

Short Name: Decrease, ATP pool

Event Component

Process	Object	Action
ATP biosynthetic process	ATP	decreased

AOPs Including This Key Event

AOP ID and Name	Event Type
Aop:328 - Excessive reactive oxygen species production leading to mortality (2)	KeyEvent
Aop:329 - Excessive reactive oxygen species production leading to mortality (3)	KeyEvent
Aop:264 - Uncoupling of oxidative phosphorylation leading to growth inhibition via ATP depletion associated cell death	KeyEvent
Aop:263 - Uncoupling of oxidative phosphorylation leading to growth inhibition via decreased cell proliferation	KeyEvent
Aop:290 - Mitochondrial ATP synthase antagonism leading to growth inhibition (1)	KeyEvent
Aop:291 - Mitochondrial ATP synthase antagonism leading to growth inhibition (2)	KeyEvent
Aop:286 - Mitochondrial complex III antagonism leading to growth inhibition (1)	KeyEvent
Aop:287 - Mitochondrial complex III antagonism leading to growth inhibition (2)	KeyEvent
Aop:266 - Uncoupling of oxidative phosphorylation leading to growth inhibition via decreased Na-K ATPase activity	KeyEvent
Aop:331 - Increase in reactive oxygen species leading to growth inhibition via lipid peroxidation and cell death	KeyEvent
Aop:596 - Excessive reactive oxygen species leading to growth inhibition via protein oxidation and cell injury/death	KeyEvent
Aop:598 - Excessive reactive oxygen species leading to growth inhibition via protein oxidation and reduced cell proliferation	KeyEvent
Aop:599 - Excessive reactive oxygen species leading to growth inhibition via fatty acid oxidation and cell injury/death	KeyEvent
Aop:600 - Excessive reactive oxygen species leading to growth inhibition via fatty acid oxidation and reduced cell growth	KeyEvent
Aop:601 - Excessive reactive oxygen species leading to growth inhibition via fatty acid oxidation and reduced cell proliferation	KeyEvent
Aop:612 - Peroxisome proliferator-activated receptor alpha activation leading to early life stage mortality via reduced adenosine triphosphate	KeyEvent
Aop:326 - Increase in reactive oxygen species leading to growth inhibition via lipid peroxidation and decreased cell proliferation	KeyEvent
Aop:332 - Increase in reactive oxygen species leading to growth inhibition via protein oxidation and decreased cell proliferation	KeyEvent
Aop:333 - Increase in reactive oxygen species leading to growth inhibition via protein oxidation and cell death	KeyEvent

Stressors

Name
Carbonyl cyanide-p-trifluoromethoxyphenylhydrazone
Carbonyl cyanide m-chlorophenyl hydrazone
2,4-Dinitrophenol
Malonoben
Pentachlorophenol
Triclosan
Emodin

Biological Context

Level of Biological Organization

Cellular

Cell term

Cell term

cell

Domain of Applicability

Taxonomic Applicability

Term	Scientific Term	Evidence	Links
zebrafish	Danio rerio	High	NCBI
human	Homo sapiens	High	NCBI
rat	Rattus norvegicus	High	NCBI
mouse	Mus musculus	High	NCBI
Lemna minor	Lemna minor	High	NCBI

Life Stage Applicability

Life Stage	Evidence
Embryo	High
Juvenile	High
Adult, reproductively mature	Moderate

Sex Applicability

Sex	Evidence
Unspecific	High

Taxonomic applicability domain

This key event is in general considered applicable to all eukaryotes utilizing ATP as a direct source of energy and signaling molecule.

Life stage applicability domain

This key event is considered applicable to all life stages, as all developmental stages require energy supply to maintain necessary physiological processes.

Sex applicability domain

This key event is considered sex-unspecific, as both males and females use ATP as an essential energy molecule.

Key Event Description

Decreased adenosine triphosphate (ATP) pool describes the loss of balance between ATP synthesis and ATP consumption, leading to reduced total ATP. As a primary form of biological energy, ATP is used by many biological processes (Bonora 2012). Decrease in ATP level normally attributes to metabolic disorders in major ATP synthetic pathways, such as mitochondrial oxidative phosphorylation, fatty acid β-oxidation, glycolysis and plant photophosphorylation.

How it is Measured or Detected

-The ATP pool in cells or tissue can be quantified using a well-established ATP bioluminescent assay (Lemasters 1978; Wibom 1990). Assay principles: ATP can react with luciferase and luciferin from firefly and the luminescence emitted from the reaction is proportional to the ATP concentration:

ATP + D-Luciferin + O_2 è Oxyluciferin + AMP + PPi + CO_2 + Light

-ToxCast high-throughput screening bioassays, such as “NCCT_HEK293T_CellTiterGLO” and “NIS_HEK293T_CTG_Cytotoxicity” can be used to measure this KE.

References

Bonora M, Patergnani S, Rimessi A, De Marchi E, Suski JM, Bononi A, Giorgi C, Marchi S, Missiroli S, Poletti F, Wieckowski MR, Pinton P.

2012. ATP synthesis and storage. *Purinergic Signalling* 8:343-357. DOI: 10.1007/s11302-012-9305-8.

Lemasters JJ, Hackenbrock CR. 1978. [4] Firefly luciferase assay for ATP production by mitochondria.*Methods in Enzymology*. Vol 57. Academic Press, pp 36-50.

Wibom R, Lundin A, Hultman E. 1990. A sensitive method for measuring ATP-formation in rat muscle mitochondria.*Scandinavian Journal of Clinical and Laboratory Investigation* 50:143-152. DOI: 10.1080/00365519009089146.

Event: 55: Increase, Cell injury/death

Short Name: Cell injury/death

Event Component

Process	Object	Action
cell death		increased

AOPs Including This Key Event

AOP ID and Name	Event Type
Aop:48 - Binding of agonists to ionotropic glutamate receptors in adult brain causes excitotoxicity that mediates neuronal cell death, contributing to learning and memory impairment.	KeyEvent
Aop:13 - Chronic binding of antagonist to N-methyl-D-aspartate receptors (NMDARs) during brain development induces impairment of learning and memory abilities	KeyEvent
Aop:38 - Protein Alkylation leading to Liver Fibrosis	KeyEvent
Aop:12 - Chronic binding of antagonist to N-methyl-D-aspartate receptors (NMDARs) during brain development leads to neurodegeneration with impairment in learning and memory in aging	KeyEvent
Aop:144 - Endocytic lysosomal uptake leading to liver fibrosis	KeyEvent
Aop:17 - Binding of electrophilic chemicals to SH(thiol)-group of proteins and /or to seleno-proteins involved in protection against oxidative stress during brain development leads to impairment of learning and memory	KeyEvent
Aop:278 - IKK complex inhibition leading to liver injury	KeyEvent
Aop:281 - Acetylcholinesterase Inhibition Leading to Neurodegeneration	KeyEvent
Aop:273 - Mitochondrial complex inhibition leading to liver injury	KeyEvent
Aop:377 - Dysregulated prolonged Toll Like Receptor 9 (TLR9) activation leading to Multi Organ Failure involving Acute Respiratory Distress Syndrome (ARDS)	KeyEvent
Aop:265 - Uncoupling of oxidative phosphorylation leading to growth inhibition via increased cytosolic calcium	KeyEvent
Aop:264 - Uncoupling of oxidative phosphorylation leading to growth inhibition via ATP depletion associated cell death	KeyEvent
Aop:266 - Uncoupling of oxidative phosphorylation leading to growth inhibition via decreased Na-K ATPase activity	KeyEvent
Aop:268 - Uncoupling of oxidative phosphorylation leading to growth inhibition via mitochondrial swelling	KeyEvent
Aop:479 - Mitochondrial complexes inhibition leading to left ventricular function decrease via increased myocardial oxidative stress	KeyEvent
Aop:490 - Co-activation of IP3R and RyR leads to reduced IQ and increased socio-economic burden through non-cholinergic mechanisms	KeyEvent
Aop:494 - AhR activation leading to liver fibrosis	KeyEvent
Aop:530 - Endocytotic lysosomal uptake leads to intestinal barrier disruption	KeyEvent
Aop:331 - Increase in reactive oxygen species leading to growth inhibition via lipid peroxidation and cell death	KeyEvent
Aop:596 - Excessive reactive oxygen species leading to growth inhibition via protein oxidation and cell injury/death	KeyEvent
Aop:599 - Excessive reactive oxygen species leading to growth inhibition via fatty acid oxidation and cell injury/death	KeyEvent
Aop:624 - Increased 11β-Hydroxysteroid dehydrogenase type 1 activity leading to MASLD progression via insulin resistance-associated mitochondrial dysfunction	KeyEvent
Aop:625 - Increased 11β-Hydroxysteroid dehydrogenase type 1 activity leading to MASLD progression via insulin resistance-associated oxidative stress	KeyEvent
Aop:626 - Increased 11β-Hydroxysteroid dehydrogenase type 1 activity leading to MASLD progression via insulin resistance-associated endoplasmic reticulum stress	KeyEvent
Aop:627 - Increased 11β-Hydroxysteroid dehydrogenase type 1 activity leading to MASLD progression via lipogenesis-associated mitochondrial dysfunction	KeyEvent
Aop:628 - Increased 11β-Hydroxysteroid dehydrogenase type 1 activity leading to MASLD progression via lipogenesis-associated oxidative stress	KeyEvent

AOP ID and Name	Event Type
Aop:629 - Increased 11β-Hydroxysteroid dehydrogenase type 1 activity leading to MASLD progression via lipogenesis-associated endoplasmic reticulum stress	KeyEvent
Aop:325 - Increase in reactive oxygen species leading to growth inhibition via oxidative DNA damage and cell death	KeyEvent
Aop:333 - Increase in reactive oxygen species leading to growth inhibition via protein oxidation and cell death	KeyEvent
Aop:647 - ROS formation leading to growth inhibition modulated by the Keap1–Nrf2 antioxidant response	KeyEvent

Biological Context

Level of Biological Organization
Cellular

Cell term

Cell term
eukaryotic cell

Domain of Applicability

Taxonomic Applicability

Term	Scientific Term	Evidence	Links
human	Homo sapiens	High	NCBI
human and other cells in culture	human and other cells in culture	High	NCBI
Rattus norvegicus	Rattus norvegicus	High	NCBI
mouse	Mus musculus	High	NCBI

Life Stage Applicability

Life Stage	Evidence
All life stages	

Sex Applicability

Sex	Evidence
Unspecific	

Cell death is an universal event occurring in cells of any species (Fink and Cookson,2005).

Key Event Description

Two types of cell death can be distinguished by morphological features, although it is likely that these are two ends of a spectrum with possible intermediate forms. Apoptosis involves shrinkage, nuclear disassembly, and fragmentation of the cell into discrete bodies with intact plasma membranes. These are rapidly phagocytosed by neighbouring cells. An important feature of apoptosis is the requirement for adenosine triphosphate (ATP) to initiate the execution phase. In contrast, necrotic cell death is characterized by cell swelling and lysis. This is usually a consequence of profound loss of mitochondrial function and resultant ATP depletion, leading to loss of ion homeostasis, including volume regulation, and increased intracellular Ca2+. The latter activates a number of nonspecific hydrolases (i.e., proteases, nucleases, and phospholipases) as well as calcium dependent kinases. Activation of calpain I, the Ca2+-dependent cysteine protease cleaves the death-promoting Bcl-2 family members Bid and Bax which translocate to mitochondrial membranes, resulting in release of truncated apoptosis-inducing factor (tAIF), cytochrome c and endonuclease in the case of Bid and cytocrome c in the case of Bax. tAIF translocates to cell nuclei, and together with cyclophilin A and phosphorylated histone H2AX (γH2AX) is responsible for DNA cleavage, a feature of programmed necrosis. Activated calpain I has also been shown to cleave the plasma membrane Na+–Ca2+ exchanger, which leads to build-up of intracellular Ca2+, which is the source of additional increased intracellular Ca2+. Cytochrome c in cellular apoptosis is a component of the apoptosome.

DNA damage activates nuclear poly(ADP-ribose) polymerase-1(PARP-1), a DNA repair enzyme. PARP-1 forms poly(ADP-ribose) polymers, to repair DNA, but when DNA damage is extensive, PAR accumulates, exits cell nuclei and travels to mitochondrial membranes, where it, like calpain I, is involved in AIF release from mitochondria. A fundamental distinction between necrosis and apoptosis is the loss of plasma membrane integrity; this is integral to the former but not the latter. As a consequence, lytic release of cellular constituents promotes a local inflammatory reaction, whereas the rapid removal of apoptotic bodies minimizes such a reaction. The distinction between the two modes of death is easily accomplished in vitro but not in vivo. Thus, although claims that certain drugs induce apoptosis have been made, these are relatively unconvincing. DNA fragmentation can occur in necrosis, leading to positive TUNEL staining (see explanation below). Conversely, when apoptosis is massive, it can exceed the capacity for rapid phagocytosis, resulting in the eventual appearance of secondary necrosis.

Two alternative pathways - either extrinsic (receptor-mediated) or intrinsic (mitochondria-mediated) - lead to apoptotic cell death. The initiation of cell death begins either at the plasma membrane with the binding of TNF or FasL to their cognate receptors or within the cell. The latter is due to the occurrence of intracellular stress in the form of biochemical events such as oxidative stress, redox changes, covalent binding, lipid peroxidation, and consequent functional effects on mitochondria, endoplasmic reticulum,

microtubules, cytoskeleton, or DNA. The intrinsic mitochondrial pathway involves the initiator, caspase-9, which, when activated, forms an “apoptosome” in the cytosol, together with cytochrome c, which translocates from mitochondria, Apaf-1 and dATP. The apoptosome activates caspase-3, the central effector caspase, which in turn activates downstream factors that are responsible for the apoptotic death of a cell (Fujikawa, 2015). Intracellular stress either directly affects mitochondria or can lead to effects on other organelles, which then send signals to the mitochondria to recruit participation in the death process (Fujikawa, 2015; Malhi et al., 2010). Constitutively expressed nitric oxide synthase (nNOS) is a Ca2+-dependent cytosolic enzyme that forms nitric oxide (NO) from L-arginine, and NO reacts with the free radical such as superoxide (O2−) to form the very toxic free radical peroxynitrite (ONOO−). Free radicals such as ONOO−, O2 − and hydroxyl radical (OH−) damage cellular membranes and intracellular proteins, enzymes and DNA (Fujikawa, 2015; Malhi et al., 2010; Kaplowitz, 2002; Kroemer et al., 2009).

How it is Measured or Detected

Necrosis:

Lactate dehydrogenase (LDH) is a soluble cytoplasmic enzyme that is present in almost all cells and is released into extracellular space when the plasma membrane is damaged. To detect the leakage of LDH into cell culture medium, a tetrazolium salt is used in this assay. In the first step, LDH produces reduced nicotinamide adenine dinucleotide (NADH) when it catalyzes the oxidation of lactate to pyruvate. In the second step, a tetrazolium salt is converted to a colored formazan product using newly synthesized NADH in the presence of an electron acceptor. The amount of formazan product can be colorimetrically quantified by standard spectroscopy. Because of the linearity of the assay, it can be used to enumerate the percentage of necrotic cells in a sample (Chan et al., 2013).

The MTT assay is a colorimetric assay for assessing cell viability. NAD(P)H-dependent cellular oxidoreductase enzymes may reflect the number of viable cells present. These enzymes are capable of reducing the tetrazolium dye MTT 3-(4,5-dimethylthiazol-2-yl)-2,5-diphenyltetrazolium bromide to its insoluble formazan, which has a purple color. Other closely related tetrazolium dyes include XTT, MTS and the WSTs. Tetrazolium dye assays can also be used to measure cytotoxicity (loss of viable cells) or cytostatic activity (shift from proliferation to quiescence) of potential medicinal agents and toxic materials. MTT assays are usually done in the dark since the MTT reagent is sensitive to light (Berridgeet al.,2005).

Propidium iodide (PI) is an intercalating agent and a fluorescent molecule used to stain necrotic cells. It is cell membrane impermeant so it stains only those cells where the cell membrane is destroyed. When PI is bound to nucleic acids, the fluorescence excitation maximum is 535 nm and the emission maximum is 617 nm (Moore et al.,1998)

Alamar Blue (resazurin) is a fluorescent dye. The oxidized blue non fluorescent Alamar blue is reduced to a pink fluorescent dye in the medium by cell activity (O'Brien et al., 2000) (12).

Neutral red uptake, which is based on the ability of viable cells to incorporate and bind the supravital dye neutral red in lysosomes (Repetto et al., 2008)(13). Moreover, quantification of ATP, signaling the presence of metabolically active cells, can be performed (CellTiter-Glo; Promega).

ATP assay: Quantification of ATP, signaling the presence of metabolically active cells (CellTiter-Glo; Promega).

Apoptosis:

TUNEL is a common method for detecting DNA fragmentation that results from apoptotic signalling cascades. The assay relies on the presence of nicks in the DNA which can be identified by terminal deoxynucleotidyl transferase or TdT, an enzyme that will catalyze the addition of dUTPs that are secondarily labeled with a marker. It may also label cells that have suffered severe DNA damage.

Caspase activity assays measured by fluorescence. During apoptosis, mainly caspase-3 and -7 cleave PARP to yield an 85 kDa and a 25 kDa fragment. PARP cleavage is considered to be one of the classical characteristics of apoptosis. Antibodies to the 85 kDa fragment of cleaved PARP or to caspase-3 both serve as markers for apoptotic cells that can be monitored using immunofluorescence (Li, Peng et al., 2004).

Hoechst 33342 staining: Hoechst dyes are cell-permeable and bind to DNA in live or fixed cells. Therefore, these stains are often called supravital, which means that cells survive a treatment with these compounds. The stained, condensed or fragmented DNA is a marker of apoptosis (Loo, 2002; Kubbies and Rabinovitch, 1983).

Acridine Orange/Ethidium Bromide staining is used to visualize nuclear changes and apoptotic body formation that are characteristic of apoptosis. Cells are viewed under a fluorescence microscope and counted to quantify apoptosis.

Update - non-endorsed (by You Song, 02/09/2026)

ToxCast/Tox21 assays (invitrodb v4.3): APR_HepG2_CellLoss_*; ATG_XTT_Cytotoxicity; LTEA_HepaRG_LDH_cytotoxicity

References

- Fujikawa, D.G. (2015), The role of excitotoxic programmed necrosis in acute brain injury, Comput Struct Biotechnol J, vol. 13, pp. 212-221.
- Malhi, H. et al. (2010), Hepatocyte death: a clear and present danger, Physiol Rev, vol. 90, no. 3, pp. 1165-1194.
- Kaplowitz, N. (2002), Biochemical and Cellular Mechanisms of Toxic Liver Injury, Semin Liver Dis, vol. 22, no. 2, http://www.medscape.com/viewarticle/433631 (accessed on 20 January 2016).
- Kroemer, G. et al., (2009), Classification of cell death: recommendations of the Nomenclature Committee on Cell Death, Cell Death Differ, vol. 16, no. 1, pp. 3-11.
- Chan, F.K., K. Moriwaki and M.J. De Rosa (2013), Detection of necrosis by release of lactate dehydrogenase (LDH) activity, Methods Mol Biol, vol. 979, pp. 65–70.
- Berridge, M.V., P.M. Herst and A.S. Tan (2005), Tetrazolium dyes as tools in cell biology: new insights into their cellular reduction. Biotechnology Annual Review, vol. 11, pp 127-152.
- Moore, A, et al.(1998), Simultaneous measurement of cell cycle and apoptotic cell death,Methods Cell Biol, vol. 57, pp. 265–278.

- Li, Peng et al. (2004), Mitochondrial activation of apoptosis, Cell, vol. 116, no. 2 Suppl,pp. S57-59, 2 p following S59.
- Loo, D.T. (2002), TUNEL Assay an overview of techniques, Methods in Molecular Biology, vol. 203: In Situ Detection of DNA Damage, chapter 2, Didenko VV (ed.), Humana Press Inc.
- Kubbies, M. and P.S. Rabinovitch (1983), Flow cytometric analysis of factors which influence the BrdUrd-Hoechst quenching effect in cultivated human fibroblasts and lymphocytes, Cytometry, vol. 3, no. 4, pp. 276–281.
- Fink, S.L. and B.T. Cookson (2005), Apoptosis, pyroptosis, and necrosis: mechanistic description of dead and dying eukaryotic cells, Infect Immun, vol. 73, no. 4, pp.1907-1916.
- O'Brien J, Wilson I, Orton T, Pognan F. 2000. Investigation of the Alamar Blue (resazurin) fluorescent dye for the assessment of mammalian cell cytotoxicity. European journal of biochemistry / FEBS 267(17): 5421-5426.
- Repetto G, del Peso A, Zurita JL. 2008. Neutral red uptake assay for the estimation of cell viability/cytotoxicity. Nature protocols 3(7): 1125-1131.

List of Adverse Outcomes in this AOP

Event: 1521: Decrease, Growth

Short Name: Decrease, Growth

Event Component

Process	Object	Action
growth	multicellular organism	decreased

AOPs Including This Key Event

AOP ID and Name	Event Type
Aop:263 - Uncoupling of oxidative phosphorylation leading to growth inhibition via decreased cell proliferation	AdverseOutcome
Aop:290 - Mitochondrial ATP synthase antagonism leading to growth inhibition (1)	AdverseOutcome
Aop:291 - Mitochondrial ATP synthase antagonism leading to growth inhibition (2)	AdverseOutcome
Aop:286 - Mitochondrial complex III antagonism leading to growth inhibition (1)	AdverseOutcome
Aop:287 - Mitochondrial complex III antagonism leading to growth inhibition (2)	AdverseOutcome
Aop:245 - Reduction in photophosphorylation leading to growth inhibition in aquatic plants	AdverseOutcome
Aop:265 - Uncoupling of oxidative phosphorylation leading to growth inhibition via increased cytosolic calcium	AdverseOutcome
Aop:264 - Uncoupling of oxidative phosphorylation leading to growth inhibition via ATP depletion associated cell death	AdverseOutcome
Aop:266 - Uncoupling of oxidative phosphorylation leading to growth inhibition via decreased Na-K ATPase activity	AdverseOutcome
Aop:267 - Uncoupling of oxidative phosphorylation leading to growth inhibition via glucose depletion	AdverseOutcome
Aop:268 - Uncoupling of oxidative phosphorylation leading to growth inhibition via mitochondrial swelling	AdverseOutcome
Aop:473 - Energy deposition from internalized Ra-226 decay lower oxygen binding capacity of hemocyanin	AdverseOutcome
Aop:331 - Increase in reactive oxygen species leading to growth inhibition via lipid peroxidation and cell death	AdverseOutcome
Aop:596 - Excessive reactive oxygen species leading to growth inhibition via protein oxidation and cell injury/death	AdverseOutcome
Aop:598 - Excessive reactive oxygen species leading to growth inhibition via protein oxidation and reduced cell proliferation	AdverseOutcome
Aop:599 - Excessive reactive oxygen species leading to growth inhibition via fatty acid oxidation and cell injury/death	AdverseOutcome
Aop:600 - Excessive reactive oxygen species leading to growth inhibition via fatty acid oxidation and reduced cell growth	AdverseOutcome
Aop:602 - Excessive reactive oxygen species leading to growth inhibition via oxidative DNA damage	AdverseOutcome
Aop:603 - Excessive reactive oxygen species leading to growth inhibition via protein oxidation and cell cycle disruption	AdverseOutcome
Aop:601 - Excessive reactive oxygen species leading to growth inhibition via fatty acid oxidation and reduced cell proliferation	AdverseOutcome
Aop:567 - Binding to plastoquinone B site leading to decreased population growth rate via photosystem II inhibition	AdverseOutcome
Aop:324 - Increase in reactive oxygen species leading to growth inhibition via oxidative DNA damage and cell cycle disruption	AdverseOutcome
Aop:325 - Increase in reactive oxygen species leading to growth inhibition via oxidative DNA damage and cell death	AdverseOutcome

AOP ID and Name	Event Type
Aop:326 - Increase in reactive oxygen species leading to growth inhibition via lipid peroxidation and decreased cell proliferation	AdverseOutcome
Aop:332 - Increase in reactive oxygen species leading to growth inhibition via protein oxidation and decreased cell proliferation	AdverseOutcome
Aop:333 - Increase in reactive oxygen species leading to growth inhibition via protein oxidation and cell death	AdverseOutcome
Aop:647 - ROS formation leading to growth inhibition modulated by the Keap1–Nrf2 antioxidant response	AdverseOutcome

Stressors

Name
2,4-Dinitrophenol
Carbonyl cyanide-p-trifluoromethoxyphenylhydrazone
Carbonyl cyanide m-chlorophenyl hydrazone
Pentachlorophenol
Triclosan
Emodin
Malonoben

Biological Context

Level of Biological Organization
Individual

Domain of Applicability

Taxonomic Applicability

Term	Scientific Term	Evidence	Links
human	Homo sapiens	Moderate	NCBI
rat	Rattus norvegicus	Moderate	NCBI
mouse	Mus musculus	Moderate	NCBI
zebrafish	Danio rerio	High	NCBI
fathead minnow	Pimephales promelas	High	NCBI
Lemna minor	Lemna minor	High	NCBI
Daphnia magna	Daphnia magna	Moderate	NCBI

Life Stage Applicability

Life Stage	Evidence
Embryo	High
Juvenile	High

Sex Applicability

Sex	Evidence
Unspecific	High

Taxonomic applicability domain

This key event is in general applicable to all eukaryotes.

Life stage applicability domain

This key event is applicable to early life stages such as embryo and juvenile.

Sex applicability domain

This key event is sex-unspecific.

Key Event Description

Decreased growth refers to a reduction in size and/or weight of a tissue, organ or individual organism. Growth is normally controlled by growth factors and mainly achieved through cell proliferation (Conlon 1999).

How it is Measured or Detected

Growth can be indicated by measuring weight, length, total volume, and/or total area of a tissue, organ or individual organism.

Revised version (non-endorsed, added by You Song, 02/09/2026)

Growth can be measured as a change in size, mass, biomass, length, area, volume, or growth rate of a tissue, organ, or whole organism over a defined exposure period. The appropriate measurement depends on the biological system, life stage, and test species.

At the organism level, growth is commonly assessed by measuring body weight, wet weight, dry weight, body length, standard length, total length, shell length, shoot height, root length, frond number, frond area, cell density, biomass, or relative growth rate. Growth inhibition is typically expressed as a statistically significant reduction relative to the control, or as an effect concentration causing a defined percentage reduction in growth, such as ECx, ErCx, EyCx, LOEC, NOEC, or benchmark concentration/dose values.

For unicellular algae and cyanobacteria, growth is commonly quantified from changes in biomass over time. Biomass may be estimated using direct cell counts, electronic particle counters, microscopy, optical density, fluorescence, chlorophyll-related measurements, or other validated biomass proxies. Growth inhibition is commonly calculated from average specific growth rate and yield.

For aquatic macrophytes such as Lemna spp., growth is typically quantified using frond number and at least one additional growth-related variable, such as total frond area, dry weight, fresh weight, or image-based area measurements. Digital imaging, flatbed scanning, stereomicroscopy, or automated image-analysis tools can be used to quantify frond area and related morphological endpoints.

For terrestrial plants, growth can be measured using seedling emergence, survival, shoot height, root length, fresh or dry biomass, leaf area, and visual signs of phytotoxicity such as chlorosis, necrosis, deformation, or delayed development. Measurements may be made using rulers or calipers, analytical balances, scanners, digital imaging, or plant image-analysis software.

For aquatic invertebrates, growth may be assessed using body length, body area, wet weight, dry weight, developmental stage, or size at defined time points. In small organisms such as Daphnia, body length is often measured from microscope or stereomicroscope images using calibrated image-analysis software.

For fish and amphibians, growth is commonly assessed using wet weight, dry weight, standard length, total length, snout–vent length, condition factor, developmental stage, and specific growth rate. Measurements may be obtained using balances, calipers, digital imaging, or stereomicroscopy, depending on organism size and life stage.

For mammals and other vertebrates in repeated-dose or reproductive/developmental toxicity studies, growth-related endpoints are typically evaluated using body weight, body-weight gain, food and water consumption, pup or offspring weight, litter growth, organ weight, and developmental landmarks. These endpoints are usually interpreted together with clinical observations, survival, pathology, and reproductive or developmental parameters.

Because growth is an integrative apical endpoint, measurement should be performed over a biologically appropriate time window and interpreted in relation to survival, developmental delay, nutritional status, reproductive output, and general toxicity. Direct measurements of organismal size, biomass, or growth rate provide the strongest evidence for this key event, whereas indirect indicators such as altered morphology, reduced condition factor, or reduced organ weight may provide supporting evidence depending on biological context.

Relevant OECD Test Guidelines include, but are not limited to:

- OECD TG 201: Freshwater Alga and Cyanobacteria, Growth Inhibition Test. This guideline directly assesses inhibition of algal or cyanobacterial growth, typically using average specific growth rate and yield as response variables.
- OECD TG 208: Terrestrial Plant Test: Seedling Emergence and Seedling Growth Test. This guideline assesses effects on seedling emergence and early growth of terrestrial plants, including biomass, shoot height, and visible phytotoxic effects.
- OECD TG 211: Daphnia magna Reproduction Test. Although the primary endpoint is reproductive output, the test can provide chronic organism-level information relevant to population performance, and growth-related observations such as body size may be reported as supporting endpoints when included in the study design.
- OECD TG 212: Fish, Short-term Toxicity Test on Embryo and Sac-Fry Stages. This guideline assesses toxicity during early fish development from fertilized egg to the end of the sac-fry stage. Growth-related developmental observations may support interpretation of early-life-stage impairment.
- OECD TG 215: Fish, Juvenile Growth Test. This guideline directly evaluates effects on juvenile fish growth. Effects are expressed using growth rate, and concentration-response analysis can be used to estimate concentrations causing a defined percentage change in growth rate.
- OECD TG 221: Lemna sp. Growth Inhibition Test. This guideline directly assesses effects on vegetative growth of Lemna spp. using average specific growth rate and yield, commonly based on frond number and additional variables such as frond area or biomass.
- OECD TG 228: Determination of Developmental Toxicity to Dipteran Dung Flies. This guideline is relevant where chemical exposure affects development and growth-related performance in terrestrial invertebrates.
- OECD TG 241: Larval Amphibian Growth and Development Assay. This guideline evaluates growth and development in amphibians from fertilization through the early juvenile period.
- OECD TG 407: Repeated Dose 28-day Oral Toxicity Study in Rodents. This guideline includes body weight and food/water consumption measurements as part of the assessment of repeated-dose systemic toxicity.
- OECD TG 408: Repeated Dose 90-day Oral Toxicity Study in Rodents. This guideline includes body weight and related clinical

observations as part of subchronic systemic toxicity assessment.

- OECD TG 416: Two-Generation Reproduction Toxicity. This guideline evaluates effects on reproduction as well as growth and development of offspring across generations.
- OECD TG 422: Combined Repeated Dose Toxicity Study with the Reproduction/Developmental Toxicity Screening Test. This guideline includes body weight, food/water consumption, offspring observations and measurements, and developmental parameters.
- OECD TG 443: Extended One-Generation Reproductive Toxicity Study. This guideline evaluates reproductive and developmental effects, including health, growth, development, and function of offspring following pre- and postnatal exposure.
- OECD TG 453: Combined Chronic Toxicity/Carcinogenicity Studies. This guideline includes body weight and body-weight gain as part of the evaluation of chronic systemic toxicity and carcinogenicity.

Regulatory Significance of the AO

Growth is a regulatory relevant chronic toxicity endpoint for almost all organisms. Multiple OECD test guidelines have included growth either as a main endpoint of concern, or as an additional endpoint to be considered in the toxicity assessments. Relevant test guidelines include, but not only limited to:

-Test No. 201: Freshwater Alga and Cyanobacteria, Growth Inhibition Test

-Test No. 208: Terrestrial Plant Test: Seedling Emergence and Seedling Growth Test

-Test No. 211: Daphnia magna Reproduction Test

-Test No. 212: Fish, Short-term Toxicity Test on Embryo and Sac-Fry Stages

-Test No. 215: Fish, Juvenile Growth Test

-Test No. 221: Lemna sp. Growth Inhibition Test

-Test No. 228: Determination of Developmental Toxicity to Dipteran Dung Flies (Scathophaga stercoraria L. (Scathophagidae), Musca autumnalis De Geer (Muscidae))

-Test No. 241: The Larval Amphibian Growth and Development Assay (LAGDA)

-Test No. 407: Repeated Dose 28-day Oral Toxicity Study in Rodents

-Test No. 408: Repeated Dose 90-Day Oral Toxicity Study in Rodents

-Test No. 416: Two-Generation Reproduction Toxicity

-Test No. 422: Combined Repeated Dose Toxicity Study with the Reproduction/Developmental Toxicity Screening Test

-Test No. 443: Extended One-Generation Reproductive Toxicity Study

-Test No. 453: Combined Chronic Toxicity/Carcinogenicity Studies

References

Conlon I, Raff M. 1999. Size control in animal development. *Cell* 96:235-244. DOI: 10.1016/s0092-8674(00)80563-2.

Appendix 2

List of Key Event Relationships in the AOP

List of Adjacent Key Event Relationships

Relationship: 2009: Increase, ROS leads to Increase, Oxidative Stress

AOPs Referencing Relationship

AOP Name	Adjacency	Weight of Evidence	Quantitative Understanding
Reactive Oxygen Species (ROS) formation leads to cancer via inflammation pathway	adjacent	High	Not Specified
Essential element imbalance leads to reproductive failure via oxidative stress	adjacent		
unknown MIE leading to renal failure and mortality	adjacent		
ERa inactivation alters mitochondrial functions and insulin signalling in skeletal muscle and leads to insulin resistance and metabolic syndrome	adjacent	High	
Oxidative Stress in the Fish Ovary Leads to Reproductive Impairment via Reduced Vitellogenin Production	adjacent	High	Low
Activation of reactive oxygen species leading the atherosclerosis	adjacent	High	

AOP Name	Adjacency	Weight of Evidence	Quantitative Understanding
Deposition of ionizing energy leads to population decline via impaired meiosis	adjacent	High	Moderate
Calcium-mediated neuronal ROS production and energy imbalance	adjacent	High	
Succinate dehydrogenase (SDH) inhibition leads to oxidative stress	adjacent	High	High
The AOP framework on ROS-mediated oxidative stress induced vascular disrupting effects	adjacent	High	High
AOPs of amorphous silica nanoparticles: ROS-mediated oxidative stress increased respiratory dysfunction and diseases.	adjacent	High	High
Increase in reactive oxygen species leading to growth inhibition via lipid peroxidation and cell death	adjacent	High	Moderate
Emerging OPFRS reproductive outcome pathway	adjacent	High	High
Excessive reactive oxygen species leading to growth inhibition via protein oxidation and cell injury/death	adjacent	High	
Excessive reactive oxygen species leading to growth inhibition via fatty acid oxidation and cell injury/death	adjacent		
Excessive reactive oxygen species leading to growth inhibition via fatty acid oxidation and reduced cell growth	adjacent		
Excessive reactive oxygen species leading to growth inhibition via fatty acid oxidation and reduced cell proliferation	adjacent		
Excessive reactive oxygen species leading to growth inhibition via oxidative DNA damage	adjacent		
Excessive reactive oxygen species leading to growth inhibition via protein oxidation and cell cycle disruption	adjacent		
DNA adduct formation leading to kidney failure	adjacent	High	High
Increase in reactive oxygen species leading to growth inhibition via oxidative DNA damage and cell cycle disruption	adjacent	High	Moderate
Increase in reactive oxygen species leading to growth inhibition via oxidative DNA damage and cell death	adjacent	High	Moderate
Increase in reactive oxygen species leading to growth inhibition via lipid peroxidation and decreased cell proliferation	adjacent	High	Moderate
Increase in reactive oxygen species leading to growth inhibition via protein oxidation and decreased cell proliferation	adjacent	High	Moderate
Increase in reactive oxygen species leading to growth inhibition via protein oxidation and cell death	adjacent	High	Moderate
ROS formation leading to growth inhibition modulated by the Keap1–Nrf2 antioxidant response	adjacent	High	High
Increase in reactive oxygen species (ROS) leading to human amyotrophic lateral sclerosis (ALS)	adjacent	High	

Evidence Supporting Applicability of this Relationship

Taxonomic Applicability

Term	Scientific Term	Evidence	Links
human	Homo sapiens	High	NCBI
fish	fish	High	NCBI
crustaceans	Daphnia magna	High	NCBI
green algae	Ulva compressa	High	NCBI
mouse	Mus musculus	High	NCBI
rat	Rattus norvegicus	High	NCBI

Life Stage Applicability

Life Stage	Evidence
All life stages	High

Sex Applicability

Sex	Evidence
Unspecific	High

This KER is broadly applicable to aerobic eukaryotic systems in which ROS production and antioxidant buffering can

be measured. The current AOP-Wiki relationship page identifies human, mouse and rat with high evidence, but the ROS-growth evidence base supports extension to algae, fish, crustaceans, mollusks and other organisms relevant to environmental toxicology (AOP-Wiki, 2026a). The relationship is expected to be conserved because it is based on redox chemistry and conserved antioxidant-defense systems rather than on a taxon-specific receptor or signaling pathway.

The applicability domain should nevertheless be bounded by biological context and measurement feasibility. This KER is most relevant when the upstream KE is a measurable increase in ROS and the downstream KE is a measurable redox imbalance or antioxidant-response state rather than a distal oxidative damage endpoint alone. In organisms or compartments where ROS cannot be measured directly, evidence may rely on antioxidant-response or oxidative damage biomarkers, but these should be interpreted as indirect support. Applicability is strongest when ROS and oxidative stress endpoints are measured in the same system under the same exposure conditions.

Key Event Relationship Description

This KER describes the causal and predictive relationship by which an increase in reactive oxygen species leads to oxidative stress. ROS include superoxide, hydrogen peroxide, hydroxyl radical and secondary oxygen-derived reactive products. At low or transient levels, ROS can participate in normal cell signaling. However, when ROS production, flux or local concentration exceeds the capacity of enzymatic and non-enzymatic antioxidant defenses, the redox balance of the biological system shifts toward an oxidizing state, producing oxidative stress (Schieber and Chandel, 2014; Sies et al., 2017).

The downstream KE, oxidative stress, is not identical to increased ROS. Rather, it represents a systems-level imbalance between pro-oxidant pressure and antioxidant or repair capacity. The KER therefore depends not only on the magnitude of ROS increase, but also on the duration, localization and chemical identity of the ROS, the capacity of scavenging systems such as glutathione, superoxide dismutase, catalase and glutathione peroxidases, and the ability of the cell or organism to activate adaptive redox responses such as NRF2 signaling (Halliwell and Gutteridge, 2015; Griendling et al., 2016; Sies et al., 2017).

Within the ROS-growth AOP network, Relationship 2009 functions as a shared upstream KER. It connects the early measurable perturbation of increased ROS to the central hub event of oxidative stress, from which downstream AOP branches proceed through oxidative DNA damage, lipid peroxidation, protein oxidation, mitochondrial dysfunction, ATP depletion, altered cell proliferation, cell injury/death and decreased growth. This KER should remain modular and stressor-agnostic; stressor-specific mechanisms of ROS generation should be described in MIE or stressor sections where appropriate.

Evidence Supporting this KER

Biological Plausibility

Biological plausibility of Relationship 2009 is high. ROS are produced endogenously by mitochondrial electron transport, oxidase enzymes, peroxisomal reactions, photosynthetic electron transport and immune-cell oxidant systems, and they may also be generated by redox-cycling chemicals, metals, radiation and other stressors (Bedard and Krause, 2007; Murphy, 2009; Halliwell and Gutteridge, 2015). Oxidative stress is defined as a disturbance in the balance between oxidants and antioxidants in favor of oxidants, leading to disruption of redox signaling and/or molecular damage (Sies et al., 2017). Therefore, a sufficient increase in ROS has a direct mechanistic basis for causing oxidative stress when antioxidant and repair capacity are exceeded.

This relationship is also strongly supported by the known biology of antioxidant defenses. Superoxide dismutases convert superoxide to hydrogen peroxide; catalase, glutathione peroxidases and peroxiredoxins reduce hydrogen peroxide and organic peroxides; and glutathione and thioredoxin systems maintain protein thiol redox balance. Increased ROS can consume these defenses, oxidize redox-sensitive proteins, activate NRF2-dependent antioxidant response pathways, and produce oxidative modification of lipids, proteins and nucleic acids (Schieber and Chandel, 2014; Griendling et al., 2016; Sies et al., 2017).

Empirical Evidence

Empirical support for this KER is high. Numerous studies across taxa and stressor classes demonstrate concordant increases in ROS or ROS-generating conditions and oxidative stress endpoints. The strongest evidence comes from studies measuring both ROS and antioxidant-response or oxidative-stress biomarkers in the same biological system. Several examples from the ROS-growth concordance table are summarized below.

Biological system	Stressor	Exposure	Evidence for KE1115 (ROS increase)	Evidence for KE1392 (oxidative stress increase)	Concordance interpretation	Reference

Biological system	Stressor	Exposure	Evidence for KE1115 (ROS increase)	Evidence for KE1392 (oxidative stress increase)	Concordance interpretation	Reference
Chlorella vulgaris	Paraquat	24 h; 0-1.0 uM	DCFH-DA fluorescence increased; LOEC for ROS approximately 0.5 uM paraquat.	SOD, POD and CAT activities increased at similar concentrations; antioxidant enzymes were approximately 3-5-fold above control at 0.5 uM.	Dose concordance supports ROS increase leading to oxidative stress in a photosynthetic eukaryote.	Qian et al. (2009)
Daphnia magna	Paraquat	48 h; 0.01-10 uM	ROS induction threshold reported around 0.1 uM paraquat.	SOD, CAT and GPx induction observed around 0.5 uM; TBARS increased around 1 uM.	ROS occurs at lower or similar concentrations than antioxidant and damage markers, supporting dose concordance.	Barata et al. (2005)
Trachinotus ovatus	Streptococcus agalactiae infection	0-120 h; 2 x 10^7 CFU/fish	ROS increased early, with maximum response around 6 h.	Antioxidant enzyme activities and antioxidant gene expression changed following the ROS response.	Temporal concordance supports ROS preceding redox-response activation during pathogen-induced oxidative stress.	Gao et al. (2022)
Mus musculus	Copper sulfate	42 days; 0-40 mg/kg bw	ROS increased at the lowest tested dose by day 42.	Antioxidant markers including SOD, GSH-related responses and oxidative stress/inflammatory indicators changed with exposure.	Concordant ROS and antioxidant-response changes support the relationship in mammals.	Jian et al. (2020)
Marine bivalves	Chlorothalonil	96 h; 0.1-10 ug/L	Stressor is thiol-reactive and associated with oxidative challenge; direct ROS was not the primary endpoint.	SOD, CAT and GPx activity changes and MDA/TBARS increases occurred in gill tissues.	Supports downstream oxidative stress following a stressor known to disturb redox balance; direct ROS evidence is weaker than in rows with ROS measurement.	Haque et al. (2019)
Mya arenaria	Cyclic hypoxia/reoxygenation	3 weeks; repeated low oxygen exposure	Hypoxia/reoxygenation is a recognized ROS-generating condition in mitochondria.	Mitochondrial proton leak and oxidative stress-related bioenergetic changes were elevated under cyclic hypoxia.	Supports environmental modulation of ROS-associated oxidative stress and mitochondrial response.	Ouillon et al. (2021)

Uncertainties and Inconsistencies

The main uncertainties relate to measurement specificity and context dependence. ROS are chemically diverse and often short-lived, so different assays may detect different ROS species or generalized oxidant-dependent probe oxidation rather than a single ROS concentration. DCFH-DA and related probes are useful screening tools but can be influenced by peroxidases, metals, light, probe loading and cellular esterase activity (Wardman, 2007; Kalyanaraman et al., 2012). Consequently, apparent ROS increases must be interpreted with assay limitations in

mind.

A second uncertainty is that ROS increases are not always adverse. Transient or localized ROS signals may activate adaptive stress responses and restore redox homeostasis without producing sustained oxidative stress. Conversely, oxidative stress may be inferred from antioxidant enzyme induction or oxidative damage biomarkers in studies where ROS were not directly measured. These cases support the KER less strongly than studies with direct, temporally resolved ROS measurements. Differences among taxa, life stages, tissues, exposure durations and antioxidant capacities may alter the threshold at which increased ROS becomes oxidative stress.

Quantitative Understanding of the Linkage

Quantitative understanding of this KER is low to moderate. The qualitative relationship is well established: oxidative stress occurs when ROS production or flux exceeds antioxidant and repair capacity. However, a universal quantitative threshold for ROS leading to oxidative stress cannot be defined because the relationship depends strongly on ROS species, subcellular localization, measurement method, antioxidant capacity, exposure duration, organism, cell type and co-stressors (Kalyanaraman et al., 2012; Griendling et al., 2016; Sies et al., 2017).

Response-response relationship

Response-response information is available in specific systems. For example, in Chlorella vulgaris exposed to paraquat, ROS and antioxidant enzyme responses were observed at approximately 0.5 uM after 24 h, indicating local dose concordance between the upstream and downstream events (Qian et al., 2009). In Daphnia magna exposed to paraquat, ROS induction was reported at lower concentrations than antioxidant enzyme and TBARS responses, supporting an expected dose sequence in which ROS increases precede oxidative stress endpoints (Barata et al., 2005). These examples provide semi-quantitative support, but they cannot be generalized across all taxa or stressors.

Time-scale

The time scale of the KER can range from minutes to hours for ROS-sensitive signaling and antioxidant pathway activation, and from hours to days for measurable changes in antioxidant enzyme activities, glutathione status or oxidative damage biomarkers. In pathogen-exposed golden pompano, ROS increased early, followed by antioxidant enzyme and gene expression responses over subsequent hours to days, supporting temporal concordance (Gao et al., 2022).

Known modulating factors

Modulating factor	Details	Effect on the KER	Supporting evidence
Antioxidant capacity	Levels and activities of GSH, SOD, CAT, GPx, peroxiredoxins, thioredoxin systems and antioxidant vitamins.	Higher antioxidant capacity buffers ROS and raises the threshold for oxidative stress; depleted or impaired antioxidant systems lower the threshold.	Halliwell and Gutteridge (2015); Sies et al. (2017).
NRF2/ARE pathway activation	Induction of antioxidant and detoxification genes through NRF2-dependent signaling.	Adaptive NRF2 activation may reduce progression from increased ROS to sustained oxidative stress, but strong NRF2 activation can also serve as evidence that ROS has perturbed redox homeostasis.	Schieber and Chandel (2014); Sies et al. (2017); AOP-Wiki (2026c).
Subcellular localization of ROS	Mitochondria, chloroplasts, peroxisomes, membranes, nuclei and phagosomes differ in ROS production and local antioxidant buffering.	Localized ROS production can cause oxidative stress in a specific compartment even when whole-cell ROS measurements are modest.	Murphy (2009); Griendling et al. (2016).
Exposure duration and recovery time	Acute pulses, chronic low-level exposure and repeated stress can produce different redox outcomes.	Short pulses may be buffered or adaptive; sustained or repeated ROS elevations increase the probability of oxidative stress.	Sies et al. (2017); Ouillon et al. (2021).

Modulating factor	Details	Effect on the KER	Supporting evidence
Oxygen availability and hypoxia/reoxygenation	Oxygen tension affects mitochondrial electron transport and ROS formation.	Reoxygenation after hypoxia can increase mitochondrial ROS and enhance oxidative stress.	Ouillon et al. (2021).
Temperature and metabolic rate	Temperature and metabolic demand alter oxygen flux, mitochondrial activity and antioxidant capacity.	Higher metabolic activity or thermal stress can increase ROS formation and shift the balance toward oxidative stress.	Tseng et al. (2011).
Stressor chemistry	Redox cycling, metal-catalyzed reactions, radiation and mitochondrial inhibition generate ROS by different mechanisms.	Stressor type influences the ROS species, localization, time course and threshold for oxidative stress.	Bedard and Krause (2007); Murphy (2009); Qian et al. (2009); Gao et al. (2022).

Known Feedforward/Feedback loops influencing this KER

Known feedback and feedforward mechanisms influence the linkage. NRF2-dependent antioxidant responses can reduce ROS and restore homeostasis, whereas mitochondrial dysfunction, lipid peroxidation, inflammation and redox-sensitive signaling can amplify ROS generation and sustain oxidative stress. These feedbacks make the KER dynamic and nonlinear, particularly under chronic exposure or repeated stress.

References

AOP-Wiki. 2026a. Relationship 2009: Increase, ROS leads to Increase, Oxidative stress. AOP-Wiki. Available at: https://aopwiki.org/relationships/2009. Accessed 14 May 2026.

AOP-Wiki. 2026b. Event 1115: Increase, Reactive oxygen species. AOP-Wiki. Available at: https://aopwiki.org/events/1115. Accessed 14 May 2026.

AOP-Wiki. 2026c. Event 1392: Increase, Oxidative stress. AOP-Wiki. Available at: https://aopwiki.org/events/1392. Accessed 14 May 2026.

Barata C, Varo I, Navarro JC, Arun S, Porte C. 2005. Antioxidant enzyme activities and lipid peroxidation in the freshwater cladoceran Daphnia magna exposed to redox cycling compounds. Comparative Biochemistry and Physiology Part C: Toxicology & Pharmacology 140(2):175-186. https://doi.org/10.1016/j.cca.2005.01.013.

Bedard K, Krause KH. 2007. The NOX family of ROS-generating NADPH oxidases: physiology and pathophysiology. Physiological Reviews 87(1):245-313. https://doi.org/10.1152/physrev.00044.2005.

Dickinson BC, Chang CJ. 2011. Chemistry and biology of reactive oxygen species in signaling or stress responses. Nature Chemical Biology 7(8):504-511. https://doi.org/10.1038/nchembio.607.

Esperanza M, Cid A, Herrero C, Rioboo C. 2015. Acute effects of a prooxidant herbicide on the microalga Chlamydomonas reinhardtii: screening cytotoxicity and genotoxicity endpoints. Aquatic Toxicology 165:210-221. https://doi.org/10.1016/j.aquatox.2015.06.004.

Gao J, Liu M, Guo H, Zhu K, Liu B, Liu B, Zhang N, Sun X, Jiang S, Zhang D. 2022. ROS induced by Streptococcus agalactiae activate inflammatory responses via the TNF-alpha/NF-kappaB signaling pathway in golden pompano Trachinotus ovatus (Linnaeus, 1758). Antioxidants 11(9):1809. https://doi.org/10.3390/antiox11091809.

Griendling KK, Touyz RM, Zweier JL, Dikalov S, Chilian W, Chen YR, Harrison DG, Bhatnagar A. 2016. Measurement of reactive oxygen species, reactive nitrogen species, and redox-dependent signaling in the cardiovascular system: a scientific statement from the American Heart Association. Circulation Research 119(5):e39-e75. https://doi.org/10.1161/RES.0000000000000110.

Halliwell B, Gutteridge JMC. 2015. Free Radicals in Biology and Medicine. 5th ed. Oxford: Oxford University Press.

Haque MN, Eom HJ, Nam SE, Shin YK, Rhee JS. 2019. Chlorothalonil induces oxidative stress and reduces enzymatic activities of Na+/K+-ATPase and acetylcholinesterase in gill tissues of marine bivalves. PLoS ONE 14(4):e0214236. https://doi.org/10.1371/journal.pone.0214236.

Jian Z, Guo H, Liu H, Cui H, Fang J, Zuo Z, Deng J, Li Y, Wang X, Zhao L. 2020. Oxidative stress, apoptosis and inflammatory responses involved in copper-induced pulmonary toxicity in mice. Aging 12(17):16867-16886. https://doi.org/10.18632/aging.103585.

Kalyanaraman B, Darley-Usmar V, Davies KJA, Dennery PA, Forman HJ, Grisham MB, Mann GE, Moore K, Roberts LJ II, Ischiropoulos H. 2012. Measuring reactive oxygen and nitrogen species with fluorescent probes: challenges and limitations. Free Radical Biology and Medicine 52(1):1-6. https://doi.org/10.1016/j.freeradbiomed.2011.09.030.

Murphy MP. 2009. How mitochondria produce reactive oxygen species. Biochemical Journal 417(1):1-13. https://doi.org/10.1042/BJ20081386.

Ouillon N, Sokolov EP, Otto S, Rehder G, Sokolova IM. 2021. Effects of variable oxygen regimes on mitochondrial bioenergetics and reactive oxygen species production in a marine bivalve, Mya arenaria. Journal of Experimental Biology 224(4):jeb237156. https://doi.org/10.1242/jeb.237156.

Pan YX, Luo Z, Zhuo MQ, Wei CC, Chen GH, Song YF. 2018. Oxidative stress and mitochondrial dysfunction mediated Cd-induced hepatic lipid accumulation in zebrafish Danio rerio. Aquatic Toxicology 199:12-20. https://doi.org/10.1016/j.aquatox.2018.03.017.

Qian H, Chen W, Sun L, Jin Y, Liu W, Fu Z. 2009. Inhibitory effects of paraquat on photosynthesis and the response to oxidative stress in Chlorella vulgaris. Ecotoxicology 18(5):537-543. https://doi.org/10.1007/s10646-009-0311-8.

Schieber M, Chandel NS. 2014. ROS function in redox signaling and oxidative stress. Current Biology 24(10):R453-R462. https://doi.org/10.1016/j.cub.2014.03.034.

Sies H, Berndt C, Jones DP. 2017. Oxidative stress. Annual Review of Biochemistry 86:715-748. https://doi.org/10.1146/annurev-biochem-061516-045037.

Tseng YC, Chen RD, Lucassen M, Schmidt MM, Dringen R, Abele D, Hwang PP. 2011. Exploring uncoupling proteins and antioxidant mechanisms under acute cold exposure in brains of fish. PLoS ONE 6(3):e18180. https://doi.org/10.1371/journal.pone.0018180.

Wardman P. 2007. Fluorescent and luminescent probes for measurement of oxidative and nitrosative species in cells and tissues: progress, pitfalls, and prospects. Free Radical Biology and Medicine 43(7):995-1022. https://doi.org/10.1016/j.freeradbiomed.2007.06.026.

Relationship: 3116: Increase, Oxidative Stress leads to Increase, LPO

AOPs Referencing Relationship

AOP Name	Adjacency	Weight of Evidence	Quantitative Understanding
Essential element imbalance leads to reproductive failure via oxidative stress	adjacent		
Increase in reactive oxygen species leading to growth inhibition via lipid peroxidation and cell death	adjacent	High	Moderate
Increase in reactive oxygen species leading to growth inhibition via lipid peroxidation and decreased cell proliferation	adjacent	High	Moderate
ROS formation leading to growth inhibition modulated by the Keap1–Nrf2 antioxidant response	adjacent	High	High

Evidence Supporting Applicability of this Relationship

Taxonomic Applicability

Term	Scientific Term	Evidence	Links
humans	Homo sapiens	High	NCBI
mammals	mammals	High	NCBI
fish	fish	High	NCBI
crustaceans	Daphnia magna	High	NCBI
green algae	Ulva compressa	High	NCBI

Life Stage Applicability

Life Stage	Evidence
All life stages	Moderate

Sex Applicability

Sex	Evidence
Unspecific	Moderate

This KER is broadly applicable to aerobic biological systems containing oxidizable lipids. It is particularly relevant to membranes and lipid-rich tissues or compartments, including plasma membranes, mitochondrial membranes, chloroplast membranes, digestive gland, liver, nervous tissue and reproductive tissues. The relationship is expected to be conserved across taxa because it is based on fundamental redox chemistry and lipid radical chain reactions rather than on a taxon-specific receptor pathway.

The KER should be applied most confidently when both upstream oxidative stress and downstream lipid peroxidation are measured under the same exposure conditions. Applicability is strongest when oxidative stress is assessed by redox imbalance or antioxidant-response endpoints and lipid peroxidation is measured using specific markers such as MDA, 4-HNE or lipid hydroperoxides. Applicability is weaker when lipid peroxidation is inferred solely from nonspecific TBARS responses without supporting oxidative-stress biomarkers or when the exposure context is dominated by physical membrane disruption rather than redox-mediated chemistry.

Key Event Relationship Description

This KER describes the relationship by which an increase in oxidative stress leads to an increase in lipid peroxidation. Oxidative stress represents a shift toward a pro-oxidant state in which reactive oxygen species, reactive nitrogen species, redox-active intermediates, or weakened antioxidant defenses exceed the buffering capacity of the biological system. Lipid peroxidation is a chain reaction in which oxidants abstract hydrogen atoms from susceptible lipids, particularly polyunsaturated fatty acids, producing lipid radicals, lipid peroxyl radicals, lipid hydroperoxides and secondary reactive aldehydes such as malondialdehyde (MDA) and 4-hydroxy-2-nonenal (4-HNE) (Halliwell and Gutteridge, 2015; Ayala et al., 2014; Yin et al., 2011).

The relationship is biologically plausible because increased oxidative pressure raises the probability of radical initiation and propagation in lipid-rich compartments, especially biological membranes. Once initiated, lipid peroxidation can propagate through neighboring lipids and can be amplified by transition metals, oxygen availability, membrane composition and reduced antioxidant protection. The downstream KE therefore reflects a measurable chemical and biological consequence of upstream oxidative stress rather than a separate stressor-specific mechanism. The KER is modular and can be reused wherever oxidative stress is followed by measurable increases in lipid oxidation products.

Evidence Supporting this KER

Biological Plausibility

Biological plausibility of this KER is high. The mechanistic basis is well established in chemistry and biology: oxidative stress increases reactive species capable of initiating lipid radical formation, and lipid radicals propagate chain reactions that generate lipid hydroperoxides and reactive aldehydes (Halliwell and Gutteridge, 2015; Ayala et al., 2014; Yin et al., 2011). Polyunsaturated fatty acids are particularly susceptible because bis-allylic hydrogens are readily abstracted, making membrane lipid composition a major determinant of sensitivity. Endogenous antioxidant systems, including glutathione peroxidases, peroxiredoxins, vitamin E, glutathione and other radical-scavenging systems, normally limit lipid peroxidation. When oxidative stress overwhelms these defenses, lipid peroxidation increases.

The structural and functional relationship between the two KEs is direct: the upstream KE increases the chemical conditions that initiate and propagate the downstream lipid oxidation process. This relationship is broadly accepted across toxicology, cell biology, physiology and environmental stress biology.

Empirical Evidence

Biological system	Stressor / condition	Evidence supporting the KER	Concordance interpretation	Reference
Chlorella vulgaris	Paraquat, 24 h	Paraquat increased ROS and induced antioxidant enzymes; ROS and oxidative stress responses were observed at concentrations that support a pro-oxidant state leading to downstream oxidative damage.	Supports upstream oxidative-stress induction by a redox-cycling herbicide and provides context for lipid-damage progression in algae.	Qian et al. (2009).
Scenedesmus vacuolatus and Chlorella kessleri	Copper sulfate, 7 d	SOD/CAT induction occurred with increased MDA/TBARS, with MDA elevated at similar or higher concentrations than antioxidant-response markers.	Supports dose concordance between oxidative stress biomarkers and lipid peroxidation in freshwater green microalgae.	Knauert and Knauer (2008).
Chlamydomonas reinhardtii	Paraquat, 48 h	Significant TBARS/MDA increase occurred at >=0.5 uM paraquat, with associated mitochondrial depolarization at similar concentrations.	Supports oxidative-stress-driven lipid peroxidation following exposure to a superoxide-generating herbicide.	Esperanza et al. (2015).

Biological system	Stressor / condition	Evidence supporting the KER	Concordance interpretation	Reference
Daphnia magna	Paraquat, 48 h	ROS induction was observed at lower concentrations, followed by antioxidant enzyme induction and TBARS responses at higher concentrations.	Supports expected dose sequence: ROS/oxidative stress precedes or coincides with lipid peroxidation.	Barata et al. (2005).
Daphnia magna	Thiram, 48 h	GSH depletion and increased MDA/TBARS were observed after thiram exposure.	Supports empirical linkage between redox imbalance and lipid peroxidation in a freshwater crustacean.	Belaid and Sbartai (2021).
Daphnia magna	High-PUFA diet, chronic	High-PUFA diet increased TBARS and reduced mitochondrial membrane potential.	Supports the role of lipid composition as a modulator and provides evidence that increased lipid susceptibility enhances peroxidation and downstream mitochondrial effects.	Moore et al. (2023).
Danio rerio	Dimethyl phthalate, 24-96 h	Antioxidant enzyme changes and MDA increases were observed after exposure.	Supports concordance between oxidative-stress biomarkers and lipid peroxidation in fish.	Cong et al. (2020).
Ruditapes philippinarum and Mytilus galloprovincialis	Hydrogen peroxide, 21 d or 48 h	Antioxidant enzyme activation was observed at lower concentrations than lipid peroxidation in digestive gland.	Supports dose concordance between direct oxidant exposure, oxidative-stress response and lipid peroxidation in bivalves.	Alam et al. (2022).
Marine bivalves	Chlorothalonil, 96 h	Antioxidant enzyme induction and MDA/TBARS increases occurred in bivalve tissues.	Supports oxidative stress and lipid peroxidation after antifoulant exposure.	Haque et al. (2019).
Human promyelocytic leukemia cells	Continuous H2O2 generation, 1 h	Sustained H2O2 production increased MDA at higher production rates.	Supports oxidant-driven lipid peroxidation in human cell systems.	Montserrat-Mesquida et al. (2024).

Uncertainties and Inconsistencies

The overall evidence for this KER is strong, but several uncertainties influence interpretation. First, lipid peroxidation biomarkers can be nonspecific or method-dependent. TBARS is widely used but can overestimate MDA or respond to non-lipid-derived substances; more specific methods such as HPLC, LC-MS/MS or measurement of 4-HNE and lipid hydroperoxides provide stronger evidence (Ayala et al., 2014; Yin et al., 2011). Second, oxidative stress is often inferred from antioxidant enzyme induction or glutathione perturbation rather than directly measured ROS flux. Third, lipid peroxidation depends strongly on membrane lipid composition, antioxidant status, metal availability and exposure duration, so the same oxidative-stress magnitude may not produce the same lipid peroxidation response in all systems. Finally, adaptive antioxidant responses may delay or suppress lipid peroxidation after mild oxidative stress, creating apparent temporal or dose-response discordance in some studies.

Quantitative Understanding of the Linkage

Quantitative understanding of this KER is moderate. The qualitative and mechanistic relationship is well established, but a universal quantitative threshold for oxidative stress leading to lipid peroxidation cannot be defined because the response depends on lipid composition, antioxidant capacity, oxygen availability, transition metals, exposure duration, stressor chemistry and assay method (Ayala et al., 2014; Yin et al., 2011; Sies et al., 2017).

Response-response relationship

Response-response evidence exists in specific systems. In green microalgae exposed to copper, antioxidant enzyme induction and MDA/TBARS increases occurred over the same concentration range, supporting dose concordance

(Knauert and Knauer, 2008). In Daphnia magna exposed to paraquat, ROS induction occurred at lower concentrations than antioxidant enzyme and TBARS responses, suggesting that increased ROS and oxidative stress precede lipid peroxidation (Barata et al., 2005). In bivalves exposed to hydrogen peroxide, antioxidant enzyme activation occurred at lower concentrations than lipid peroxidation in digestive gland, also supporting a staged relationship (Alam et al., 2022).

Time-scale

The time scale of the linkage can range from minutes to days. Chemical initiation of lipid radicals can occur rapidly when reactive species are present, but commonly measured endpoints such as MDA, TBARS, 4-HNE or lipid hydroperoxides often become detectable over hours to days depending on exposure intensity and tissue antioxidant capacity. Quantitative prediction of lipid peroxidation from oxidative-stress measurements therefore remains system-specific and is best supported when both KEs are measured in the same biological context and time course.

Known modulating factors

Modulating factor	Details	Effect on the KER	Supporting evidence
Membrane lipid composition / PUFA content	Higher abundance of polyunsaturated fatty acids increases susceptibility to radical chain peroxidation.	Increases the probability and magnitude of lipid peroxidation for a given oxidative-stress level.	Ayala et al. (2014); Yin et al. (2011); Moore et al. (2023).
Antioxidant capacity	Includes glutathione, glutathione peroxidases, catalase, peroxiredoxins, vitamin E and other lipid-soluble antioxidants.	Higher antioxidant capacity buffers oxidative stress and decreases lipid peroxidation; depletion or inhibition increases sensitivity.	Halliwell and Gutteridge (2015); Sies et al. (2017); Belaid and Sbartai (2021).
Transition metals	Iron, copper and other redox-active metals catalyze radical generation and lipid peroxide decomposition.	Enhances initiation and propagation of lipid peroxidation, often lowering the threshold for the downstream KE.	Halliwell and Gutteridge (2015); Knauert and Knauer (2008); Regoli and Giuliani (2014).
Oxygen availability and hypoxia/reoxygenation	Oxygen tension and reoxygenation influence radical formation and lipid peroxide propagation.	Can increase oxidative stress and lipid peroxidation during reoxygenation or variable oxygen regimes.	Ouillon et al. (2021); Sokolova et al. (2019).
Temperature and metabolic rate	Thermal stress changes metabolism, oxygen flux and membrane properties.	May increase ROS production and alter membrane susceptibility to lipid peroxidation.	Tseng et al. (2011); Almaida-Pagán et al. (2014).
Assay method and sampling time	TBARS, MDA, 4-HNE and lipid hydroperoxide methods differ in specificity and kinetics.	Influences apparent magnitude, timing and detectability of lipid peroxidation.	Ayala et al. (2014); Yin et al. (2011).

References

Alam MR, Ehiguese FO, Vitale D, Martín-Díaz ML. 2022. Oxidative stress response to hydrogen peroxide exposure of Mytilus galloprovincialis and Ruditapes philippinarum: reduced embryogenesis success and altered biochemical response of sentinel marine bivalve species. Environmental Chemistry and Ecotoxicology 4:97-105. https://doi.org/10.1016/j.enceco.2022.01.002.

Almaida-Pagán PF, Lucas-Sánchez A, Tocher DR. 2014. Changes in mitochondrial membrane composition and oxidative status during rapid growth, maturation and aging in zebrafish, Danio rerio. Biochimica et Biophysica Acta - Molecular and Cell Biology of Lipids 1841(7):1003-1011. https://doi.org/10.1016/j.bbalip.2014.04.004.

Ayala A, Munoz MF, Arguelles S. 2014. Lipid peroxidation: production, metabolism, and signaling mechanisms of malondialdehyde and 4-hydroxy-2-nonenal. Oxidative Medicine and Cellular Longevity 2014:360438. https://doi.org/10.1155/2014/360438.

Barata C, Varo I, Navarro JC, Arun S, Porte C. 2005. Antioxidant enzyme activities and lipid peroxidation in the freshwater cladoceran Daphnia magna exposed to redox cycling compounds. Comparative Biochemistry and Physiology Part C: Toxicology & Pharmacology 140(2):175-186. https://doi.org/10.1016/j.cca.2005.01.013.

Belaid C, Sbartai I. 2021. Assessing the effects of thiram to oxidative stress responses in a freshwater bioindicator cladoceran (Daphnia magna). Chemosphere 268:128808. https://doi.org/10.1016/j.chemosphere.2020.128808.

Cong B, Liu C, Wang L, Chai Y. 2020. The impact on antioxidant enzyme activity and related gene expression following adult zebrafish (Danio rerio) exposure to dimethyl phthalate. Animals 10(4):717. https://doi.org/10.3390/ani10040717.

Esperanza M, Cid A, Herrero C, Rioboo C. 2015. Acute effects of a prooxidant herbicide on the microalga Chlamydomonas reinhardtii: screening cytotoxicity and genotoxicity endpoints. Aquatic Toxicology 165:210-221. https://doi.org/10.1016/j.aquatox.2015.06.004.

Halliwell B, Gutteridge JMC. 2015. Free Radicals in Biology and Medicine. 5th ed. Oxford: Oxford University Press.

Haque MN, Eom HJ, Nam SE, Shin YK, Rhee JS. 2019. Chlorothalonil induces oxidative stress and reduces enzymatic activities of Na+/K+-ATPase and acetylcholinesterase in gill tissues of marine bivalves. PLoS ONE 14(4):e0214236. https://doi.org/10.1371/journal.pone.0214236.

Knauert S, Knauer K. 2008. The role of reactive oxygen species in copper toxicity to two freshwater green algae. Journal of Phycology 44(2):311-321. https://doi.org/10.1111/j.1529-8817.2008.00471.x.

Montserrat-Mesquida M, Ferrer MD, Pons A, Sureda A, Capó X. 2024. Effects of chronic hydrogen peroxide exposure on mitochondrial oxidative stress genes, ROS production and lipid peroxidation in HL60 cells. Mitochondrion 76:101869. https://doi.org/10.1016/j.mito.2024.101869.

Moore TD, Martin-Creuzburg D, Yampolsky LY. 2023. Diet effects on longevity, heat tolerance, lipid peroxidation and mitochondrial membrane potential in Daphnia. Oecologia 202(1):151-163. https://doi.org/10.1007/s00442-023-05382-1.

Ouillon N, Sokolov EP, Otto S, Rehder G, Sokolova IM. 2021. Effects of variable oxygen regimes on mitochondrial bioenergetics and reactive oxygen species production in a marine bivalve, Mya arenaria. Journal of Experimental Biology 224(4):jeb237156. https://doi.org/10.1242/jeb.237156.

Pan YX, Luo Z, Zhuo MQ, Wei CC, Chen GH, Song YF. 2018. Oxidative stress and mitochondrial dysfunction mediated Cd-induced hepatic lipid accumulation in zebrafish Danio rerio. Aquatic Toxicology 199:12-20. https://doi.org/10.1016/j.aquatox.2018.03.017.

Qian H, Chen W, Sun L, Jin Y, Liu W, Fu Z. 2009. Inhibitory effects of paraquat on photosynthesis and the response to oxidative stress in Chlorella vulgaris. Ecotoxicology 18(5):537-543. https://doi.org/10.1007/s10646-009-0311-8.

Regoli F, Giuliani ME. 2014. Oxidative pathways of chemical toxicity and oxidative stress biomarkers in marine organisms. Marine Environmental Research 93:106-117. https://doi.org/10.1016/j.marenvres.2013.07.006.

Schieber M, Chandel NS. 2014. ROS function in redox signaling and oxidative stress. Current Biology 24(10):R453-R462. https://doi.org/10.1016/j.cub.2014.03.034.

Sies H, Berndt C, Jones DP. 2017. Oxidative stress. Annual Review of Biochemistry 86:715-748. https://doi.org/10.1146/annurev-biochem-061516-045037.

Sokolov EP, Markert S, Hinzke T, Hirschfeld C, Becher D, Ponsuksili S, Sokolova IM. 2019. Effects of hypoxia-reoxygenation stress on mitochondrial proteome and bioenergetics of the hypoxia-tolerant marine bivalve Crassostrea gigas. Journal of Proteomics 194:99-111. https://doi.org/10.1016/j.jprot.2018.12.009.

Tseng YC, Chen RD, Lucassen M, Schmidt MM, Dringen R, Abele D, Hwang PP. 2011. Exploring uncoupling proteins and antioxidant mechanisms under acute cold exposure in brains of fish. PLoS ONE 6(3):e18180. https://doi.org/10.1371/journal.pone.0018180.

Yin H, Xu L, Porter NA. 2011. Free radical lipid peroxidation: mechanisms and analysis. Chemical Reviews 111(10):5944-5972. https://doi.org/10.1021/cr200084z.

Relationship: 1599: Increase, LPO leads to Decrease, Coupling of OXPHOS

AOPs Referencing Relationship

AOP Name	Adjacency	Weight of Evidence	Quantitative Understanding
Increase in reactive oxygen species leading to growth inhibition via lipid peroxidation and cell death	adjacent	High	Moderate
Increase in reactive oxygen species leading to growth inhibition via lipid peroxidation and decreased cell proliferation	adjacent	High	Moderate

Evidence Supporting Applicability of this Relationship

Taxonomic Applicability

Term	Scientific Term	Evidence	Links
humans	Homo sapiens	Moderate	NCBI
mammals	mammals	Moderate	NCBI
fish	fish	Moderate	NCBI
crustaceans	Daphnia magna	Moderate	NCBI
green algae	Ulva compressa	Moderate	NCBI

Life Stage Applicability

Life Stage	Evidence
All life stages	Moderate

Sex Applicability

Sex	Evidence
Unspecific	Moderate

This KER is applicable to aerobic eukaryotic systems with functional mitochondria and oxidizable membrane lipids. The relationship is especially relevant to biological contexts where mitochondrial membranes are enriched in cardiolipin and other polyunsaturated lipids, where oxidative stress targets membrane compartments, or where environmental conditions promote ROS formation and lipid radical propagation. The KER is likely most useful for stressors that induce oxidative membrane damage, including redox cycling chemicals, metals, radiation, hypoxia/reoxygenation, temperature stress, mitochondrial toxicants, and inflammatory or endogenous ROS-generating conditions.

The KER should be applied with greatest confidence when lipid peroxidation is measured using specific or well-characterized markers and when the downstream mitochondrial event is assessed by direct coupling-related endpoints such as respiratory control ratio, proton leak, OXPHOS coupling efficiency, mitochondrial membrane potential, or state 3/state 4 respiration. Applicability is less certain when lipid peroxidation is measured only at the whole-organism level without compartmental resolution, or when decreased coupling is caused primarily by direct uncouplers or respiratory-chain inhibitors without evidence of lipid oxidative damage.

Key Event Relationship Description

This KER describes the relationship by which increased lipid peroxidation leads to decreased coupling of oxidative phosphorylation. Lipid peroxidation involves oxidative attack on unsaturated lipids, particularly polyunsaturated fatty acids, generating lipid radicals, lipid hydroperoxides, and reactive aldehydes such as malondialdehyde and 4-hydroxy-2-nonenal (Ayala et al., 2014; Yin et al., 2011). When lipid peroxidation occurs in mitochondrial membranes, it can alter membrane fluidity, disrupt membrane protein-lipid interactions, impair the organization of respiratory chain complexes, increase proton leak, and destabilize the protonmotive force needed for ATP synthesis (Chicco and Sparagna, 2007; Paradies et al., 2014).

Cardiolipin is particularly important for this KER because it is a signature phospholipid of the inner mitochondrial membrane and supports the structure and function of respiratory chain complexes, supercomplexes, cytochrome c interactions, and ATP-generating membrane architecture. Oxidative modification of cardiolipin and other inner-membrane lipids can therefore reduce the efficiency with which electron transport is coupled to ATP synthesis. The downstream KE may be measured as decreased mitochondrial membrane potential, increased proton leak, reduced respiratory control ratio, lower OXPHOS coupling efficiency, or reduced ATP-generating respiratory efficiency. The KER does not require lipid peroxidation to be the only cause of decreased OXPHOS coupling, but it captures a mechanistically plausible and empirically supported route by which oxidative membrane damage can impair mitochondrial bioenergetics.

Evidence Supporting this KER

Biological Plausibility

Biological plausibility of this KER is high. Lipid peroxidation can directly affect mitochondrial coupling because the inner mitochondrial membrane is both highly specialized for energy transduction and vulnerable to oxidative lipid damage. The electrochemical proton gradient that drives ATP synthesis depends on low proton conductance, intact membrane architecture, and appropriately organized electron transport chain and ATP synthase complexes. Peroxidation of phospholipids can increase membrane disorder, damage cardiolipin, alter protein-lipid interactions, facilitate proton leak, and impair respiratory chain complex function (Chicco and Sparagna, 2007; Paradies et al., 1998; Paradies et al., 2014).

The mechanistic connection is especially strong for cardiolipin. Cardiolipin stabilizes respiratory chain complexes and supercomplexes and supports cytochrome c oxidase, ATP synthase, and other components of mitochondrial bioenergetics. Cardiolipin peroxidation has been associated with loss of respiratory chain function, altered cytochrome c interactions, and mitochondrial dysfunction. Thus, increased lipid peroxidation provides a structurally and functionally credible basis for decreased coupling of OXPHOS.

Empirical Evidence

Empirical support for this KER is moderate. Several studies provide concordant evidence linking lipid peroxidation or oxidative membrane damage with impaired mitochondrial membrane potential, proton leak, or OXPHOS coupling. However, fewer studies directly measure lipid peroxidation and a formal coupling metric in the same experiment across multiple time points and doses, and many available studies use related mitochondrial endpoints rather than direct OXPHOS coupling efficiency.

Biological system	Stressor / condition	Evidence for upstream KE 1445	Evidence for downstream KE 1446	Concordance / interpretation	Reference
Chlamydomonas reinhardtii	Paraquat, 48 h	TBARS/MDA increased significantly at >=0.5 uM paraquat.	Mitochondrial membrane potential decreased at >=0.5 uM paraquat, with dose-dependent further reduction.	Dose concordance supports association between lipid peroxidation and impaired mitochondrial polarization/coupling in the same model.	Esperanza et al. (2015).
Daphnia	PUFA-rich diet across lifespan experiment	High-PUFA diet increased lipid peroxidation.	High-PUFA diet lowered mitochondrial membrane potential.	Dietary susceptibility to lipid peroxidation was associated with lower mitochondrial membrane potential, supporting a lipid damage-mitochondrial function linkage.	Moore et al. (2023).
Mya arenaria	Cyclic hypoxia, 3 weeks	Variable oxygen regimes are associated with oxidative stress and lipid oxidative damage risk.	Cyclic hypoxia increased mitochondrial proton leak and lowered OXPHOS coupling efficiency.	Supports environmental relevance of oxygen-fluctuation/oxidative damage conditions leading to reduced coupling efficiency, although lipid peroxidation itself was not the sole measured driver.	Ouillon et al. (2021).
Mammalian mitochondria	Experimental oxidative damage to cardiac mitochondria	Oxidative damage to cardiolipin was observed.	Cytochrome oxidase activity was altered in close association with cardiolipin oxidative damage.	Provides direct mechanistic evidence that peroxidative mitochondrial lipid damage can impair respiratory-chain function.	Paradies et al. (1998).
Mammalian and comparative systems	Cardiolipin alteration / disease contexts	Cardiolipin loss, remodeling, and peroxidation are documented forms of mitochondrial lipid alteration.	Altered cardiolipin status is associated with mitochondrial dysfunction and reduced bioenergetic performance.	Review-level evidence supports broad mechanistic generalization across tissues and disease models.	Chicco and Sparagna (2007); Paradies et al. (2014).

Uncertainties and Inconsistencies

A major uncertainty is that lipid peroxidation is often measured by TBARS or MDA assays, which are useful but can lack specificity and may not resolve which lipid class or subcellular membrane compartment is damaged. Because OXPHOS coupling is specifically dependent on mitochondrial inner-membrane integrity, whole-cell or whole-tissue lipid peroxidation measurements may not always provide direct information on mitochondrial lipid peroxidation. More specific measurements of cardiolipin oxidation, 4-HNE adducts, lipid hydroperoxides, or mitochondrial membrane lipidomics would strengthen evidence for this KER (Ayala et al., 2014; Yin et al., 2011).

The relationship may also be modulated by compensatory mechanisms. Mild lipid peroxidation can activate

antioxidant and lipid-remodeling responses, and organisms may compensate through increased antioxidant capacity, membrane remodeling, or metabolic reorganization. Therefore, increased lipid peroxidation does not always immediately produce measurable decreases in OXPHOS coupling, especially when damage is below a threshold or when measurements are taken after compensatory recovery. Conversely, decreased OXPHOS coupling can occur through mechanisms independent of lipid peroxidation, including direct uncouplers, respiratory-chain inhibitors, protein oxidation, genetic mitochondrial defects, or ionophore-mediated proton leak.

Quantitative Understanding of the Linkage

Quantitative understanding of this KER is low to moderate. There is strong qualitative understanding that lipid peroxidation can impair mitochondrial membrane function and decrease OXPHOS coupling, but a general quantitative function linking the magnitude of lipid peroxidation to the magnitude of coupling loss is not yet established across taxa, tissues, stressors, and assay systems. The relationship is expected to be nonlinear and threshold-dependent because moderate lipid peroxidation may be buffered by antioxidants and lipid repair/remodeling, while more severe damage can abruptly increase proton leak or disrupt respiratory-chain organization.

Response-response relationship

System-specific quantitative evidence exists. In Chlamydomonas reinhardtii, paraquat produced significant lipid peroxidation and decreased mitochondrial membrane potential at similar concentrations, supporting dose concordance over the tested range (Esperanza et al., 2015). In Daphnia, high-PUFA dietary conditions increased lipid peroxidation and lowered mitochondrial membrane potential, indicating a quantitative association between susceptibility to lipid oxidation and mitochondrial bioenergetic status (Moore et al., 2023). In Mya arenaria, cyclic hypoxia increased proton leak by approximately 1.5- to 1.7-fold and reduced OXPHOS coupling efficiency, supporting quantitative characterization of downstream mitochondrial uncoupling under oxidative stress-relevant conditions (Ouillon et al., 2021). However, these studies do not yet provide a single cross-system response-response equation from lipid peroxidation biomarkers to OXPHOS coupling efficiency.

Time-scale

The time scale of the linkage can range from minutes to weeks depending on the stressor and measurement strategy. Chemical peroxidation of mitochondrial lipids can affect membrane function rapidly, but whole-organism or chronic exposure studies often detect stable changes in lipid peroxidation and coupling over days to weeks. Quantitative prediction of decreased coupling from lipid peroxidation is therefore best supported in systems where mitochondrial lipid peroxidation and OXPHOS coupling are measured directly in the same cells or isolated mitochondria across a concentration and time-course series.

Known modulating factors

Modulating factor	Details	Influence on the KER	Supporting evidence
Membrane lipid composition	Degree of unsaturation, PUFA abundance, cardiolipin content and acyl-chain composition.	Higher PUFA content and susceptible cardiolipin species increase vulnerability to peroxidation and may increase the probability or magnitude of decreased coupling.	Chicco and Sparagna (2007); Paradies et al. (2014); Moore et al. (2023).
Antioxidant capacity	Vitamin E, glutathione systems, glutathione peroxidases, peroxiredoxins, catalase, superoxide dismutase and lipid-soluble antioxidants.	Higher antioxidant capacity can reduce propagation of lipid peroxidation and buffer the effect on mitochondrial coupling; depletion increases sensitivity.	Halliwell and Gutteridge (2015); Sies et al. (2017); Ayala et al. (2014).
Transition metals and redox cycling	Iron, copper and redox-active compounds can promote radical generation and lipid peroxide decomposition.	Can lower the threshold for lipid peroxidation and intensify mitochondrial membrane damage.	Halliwell and Gutteridge (2015); Regoli and Giuliani (2014); Knauert and Knauer (2008).

Modulating factor	Details	Influence on the KER	Supporting evidence
Oxygen availability and hypoxia/reoxygenation	Fluctuating oxygen regimes alter ROS generation, mitochondrial respiration and oxidative damage.	Cyclic hypoxia or reoxygenation can increase proton leak and reduce OXPHOS coupling efficiency, potentially strengthening the KER.	Ouillon et al. (2021); Sokolov et al. (2019).
Mitochondrial metabolic state	Respiratory substrate, ADP availability, membrane potential and electron pressure on the ETC.	High electron leak and high membrane potential can increase oxidative damage; pre-existing uncoupling can alter both lipid peroxidation and coupling measurements.	Paradies et al. (2014); Sies et al. (2017).
Assay specificity and timing	TBARS, MDA, 4-HNE, lipid hydroperoxides, cardiolipin oxidation and mitochondrial lipidomics differ in specificity and time scale.	Can affect apparent dose-response and temporal concordance between the upstream and downstream KEs.	Ayala et al. (2014); Yin et al. (2011).

References

Almaida-Pagán PF, Lucas-Sánchez A, Tocher DR. 2014. Changes in mitochondrial membrane composition and oxidative status during rapid growth, maturation and aging in zebrafish, Danio rerio. Biochimica et Biophysica Acta - Molecular and Cell Biology of Lipids 1841(7):1003-1011. https://doi.org/10.1016/j.bbalip.2014.04.004.

Ayala A, Munoz MF, Arguelles S. 2014. Lipid peroxidation: production, metabolism, and signaling mechanisms of malondialdehyde and 4-hydroxy-2-nonenal. Oxidative Medicine and Cellular Longevity 2014:360438. https://doi.org/10.1155/2014/360438.

Chicco AJ, Sparagna GC. 2007. Role of cardiolipin alterations in mitochondrial dysfunction and disease. American Journal of Physiology-Cell Physiology 292(1):C33-C44. https://doi.org/10.1152/ajpcell.00243.2006.

Cong B, Liu C, Wang L, Chai Y. 2020. The impact on antioxidant enzyme activity and related gene expression following adult zebrafish (Danio rerio) exposure to dimethyl phthalate. Animals 10(4):717. https://doi.org/10.3390/ani10040717.

Esperanza M, Cid A, Herrero C, Rioboo C. 2015. Acute effects of a prooxidant herbicide on the microalga Chlamydomonas reinhardtii: screening cytotoxicity and genotoxicity endpoints. Aquatic Toxicology 165:210-221. https://doi.org/10.1016/j.aquatox.2015.06.004.

Halliwell B, Gutteridge JMC. 2015. Free Radicals in Biology and Medicine. 5th ed. Oxford: Oxford University Press.

Knauert S, Knauer K. 2008. The role of reactive oxygen species in copper toxicity to two freshwater green algae. Journal of Phycology 44(2):311-321. https://doi.org/10.1111/j.1529-8817.2008.00471.x.

Moore TD, Martin-Creuzburg D, Yampolsky LY. 2023. Diet effects on longevity, heat tolerance, lipid peroxidation and mitochondrial membrane potential in Daphnia. Oecologia 202(1):151-163. https://doi.org/10.1007/s00442-023-05382-1.

Ouillon N, Sokolov EP, Otto S, Rehder G, Sokolova IM. 2021. Effects of variable oxygen regimes on mitochondrial bioenergetics and reactive oxygen species production in a marine bivalve Mya arenaria. Journal of Experimental Biology 224(4):jeb237156. https://doi.org/10.1242/jeb.237156.

Pan YX, Luo Z, Zhuo MQ, Wei CC, Chen GH, Song YF. 2018. Oxidative stress and mitochondrial dysfunction mediated Cd-induced hepatic lipid accumulation in zebrafish Danio rerio. Aquatic Toxicology 199:12-20. https://doi.org/10.1016/j.aquatox.2018.03.017.

Paradies G, Ruggiero FM, Petrosillo G, Quagliariello E. 1998. Peroxidative damage to cardiac mitochondria: cytochrome oxidase and cardiolipin alterations. FEBS Letters 424(3):155-158. https://doi.org/10.1016/S0014-5793(98)00161-6.

Paradies G, Petrosillo G, Pistolese M, Ruggiero FM. 2002. Reactive oxygen species affect mitochondrial electron transport complex I activity through oxidative cardiolipin damage. Gene 286(1):135-141. https://doi.org/10.1016/S0378-1119(01)00814-9.

Paradies G, Paradies V, De Benedictis V, Ruggiero FM, Petrosillo G. 2014. Functional role of cardiolipin in

mitochondrial bioenergetics. Biochimica et Biophysica Acta - Bioenergetics 1837(4):408-417. https://doi.org/10.1016/j.bbabio.2013.10.006.

Regoli F, Giuliani ME. 2014. Oxidative pathways of chemical toxicity and oxidative stress biomarkers in marine organisms. Marine Environmental Research 93:106-117. https://doi.org/10.1016/j.marenvres.2013.07.006.

Schieber M, Chandel NS. 2014. ROS function in redox signaling and oxidative stress. Current Biology 24(10):R453-R462. https://doi.org/10.1016/j.cub.2014.03.034.

Sies H, Berndt C, Jones DP. 2017. Oxidative stress. Annual Review of Biochemistry 86:715-748. https://doi.org/10.1146/annurev-biochem-061516-045037.

Sokolov EP, Markert S, Hinzke T, Hirschfeld C, Becher D, Ponsuksili S, Sokolova IM. 2019. Effects of hypoxia-reoxygenation stress on mitochondrial proteome and bioenergetics of the hypoxia-tolerant marine bivalve Crassostrea gigas. Journal of Proteomics 194:99-111.

Yin H, Xu L, Porter NA. 2011. Free radical lipid peroxidation: mechanisms and analysis. Chemical Reviews 111(10):5944-5972. https://doi.org/10.1021/cr200084z.

Relationship: 2203: Decrease, Coupling of OXPHOS leads to Decrease, ATP pool

AOPs Referencing Relationship

AOP Name	Adjacency	Weight of Evidence	Quantitative Understanding
Uncoupling of oxidative phosphorylation leading to growth inhibition via decreased cell proliferation	adjacent	High	High
Uncoupling of oxidative phosphorylation leading to growth inhibition via ATP depletion associated cell death	adjacent	Moderate	Not Specified
Uncoupling of oxidative phosphorylation leading to growth inhibition via decreased Na-K ATPase activity	adjacent		
Increase in reactive oxygen species leading to growth inhibition via lipid peroxidation and cell death	adjacent	High	High
Excessive reactive oxygen species leading to growth inhibition via protein oxidation and cell injury/death	adjacent		
Peroxisome proliferator-activated receptor alpha activation leading to early life stage mortality via reduced adenosine triphosphate	adjacent		
Increase in reactive oxygen species leading to growth inhibition via lipid peroxidation and decreased cell proliferation	adjacent	High	High
Increase in reactive oxygen species leading to growth inhibition via protein oxidation and decreased cell proliferation	adjacent	High	High
Increase in reactive oxygen species leading to growth inhibition via protein oxidation and cell death	adjacent	High	High

Evidence Supporting Applicability of this Relationship

Taxonomic Applicability

Term	Scientific Term	Evidence	Links
zebrafish	Danio rerio	High	NCBI
human	Homo sapiens	High	NCBI
rat	Rattus norvegicus	High	NCBI
mouse	Mus musculus	High	NCBI

Life Stage Applicability

Life Stage	Evidence
Embryo	High
Juvenile	High

Sex Applicability

Sex	Evidence
Unspecific	High

Taxonomic applicability

Relationship 2203 is considered applicable to eukaryotes, as mitochondrial oxidative phosphorylation and ATP synthesis are highly conserved in these organisms. Uncoupling of oxidative phosphorylation leading to ATP depletion is a well-documented relationship in many taxa, such as human, rodents and fish.

Sex applicability

Relationship 2203 is considered applicable to all genders, as mitochondrial oxidative phosphorylation and ATP synthesis are fundamental biological processes and are not sex-pecific.

Life-stage applicability

Relationship 2203 is considered applicable to all life-stages, as mitochondrial oxidative phosphorylation and ATP synthesis are essential energy production processes for maintaining basic biological activities.

Key Event Relationship Description

This key event relationship describes the dissipation of protonmotive force across the inner mitochondrial membrane by uncouplers (uncoupling of oxidative phosphorylation), leading to reduced total adenosine triphosphate (ATP) pool in cells or organisms.

Evidence Supporting this KER

The overall evidence supporting Relationship 2203 is considered high.

Biological Plausibility

The biological plausibility of Relationship 2203 is considered high.

Rationale: In eukaryotic cells, the major metabolic pathways responsible for ATP production are OXPHOS, citric acid (TCA) cycle, glycolysis and photosynthesis. Oxidative phosphorylation is much (theoretically 15-18 times) more efficient than the rest due to high energy derived from oxygen during aerobic respiration (Schmidt-Rohr 2020). As the ATP level is relatively balanced between production and consumption (Bonora 2012), ATP depletion is a plausible consequence of reduced ATP synthetic efficiency following uncoupling of OXPHOS.

Empirical Evidence

The empirical support of Relationship 2203 is considered high.

Rationale: The majority of relevant studies show good incidence, temporal and/or dose concordance in different organisms and cell types after exposure to known uncouplers, with relatively few exceptions.

Evidence:

- ***Temporal concordance***: Exposure of zebrafish embryos to 0.5 µM of the classical uncoupler 2,4-DNP led to significantly uncoupling of OXPHOS after 21h, whereas significant reduction in ATP was only observed after 45h (Bestman 2015).
- ***Dose concordance:*** The uncoupler triclosan induced significant uncoupling of OXPHOS in zebrafish embryos at 15 µM, whereas higher (30 µM) concentration was required to caused significant ATP depletion (Shim 2016).
- ***Dose concordance:*** Exposure to 1 µM of of the uncoupler CCCP led to 40% uncoupling of OXPHOS in rat RBL-2H3 cells, whereas the same magnitude of effect for ATP reduction required 1.6 µM of CCCP (Weatherly 2016).
- ***Dose concordance:*** Exposure to 10 µM of the uncoupler triclosan caused significant uncoupling of OXPHOS in rat RBL-2H3 cells, whereas significant reduction in ATP was observed at a higher concentration (30 µM) (Weatherly 2018).
- ***Dose concordance:*** Significant effect on uncoupling of OXPHOS required 2 µM FCCP, whereas a significant reduction in ATP required 20 µM FCCP in human RD cells (Kuruvilla 2003).
- ***Incidence concordance***: In human colon cancer cells (SW480), exposure to 150 µM of the uncoupler flavanoid morin caused 60% reduction in MMP, whereas only around 35% decrease in ATP (Sithara 2017).
- ***Incidence concordance:*** Exposure of rat RBL-2H3 cells to 10 µM of the uncoupler triclosan led to 50% uncoupling of OXPHOS, whereas only 40% reduction in ATP (Weatherly 2016).
- ***Incidence concordance:*** Exposure to 5 µM of the uncoupler CCCP caused 71% uncoupling of OXPHOS, whereas only 64% reduction of ATP in human HL-60 cells (Sweet 1999).
- ***Incidence concordance:*** Exposure of human HeLa cells to 50 µM of the uncoupler CCCP for 1h led to 77% uncoupling of OXPHOS and 25% reduction in ATP (Koczor 2009).
- ***Incidence concordance***: Exposure of the nematode Caenorhabditis elegans to 50 µM Arsenite for 1h led to approximately 45% uncoupling of OXPHOS and 20% reduction in ATP (Luz 2016).

Uncertainties and Inconsistencies

- A significant decrease followed by a significant increase in total ATP was observed in human RD cells during a 48h exposure to the uncoupler FCCP (Kuruvilla 2003), possibly due to the enhancement of other ATP synthetic pathways (e.g., glycolysis) as a compensatory action to impaired OXPHOS (Jose 2011

Quantitative Understanding of the Linkage

The quantitative understanding of Relationship 2203 is high.

Rationale: Multiple mathematical models have been developed for describing the quantitative relationships between uncoupling of OXPHOS and ATP synthesis in vertebrates (Beard 2005; Schmitz 2011; Heiske 2017; Kubo 2020). These models, however, are highly complex metabolic or systems biological models and warrant further simplification to be used for this AOP.

Response-response relationship

A regression based quantitative response-response relationship between uncoupling of OXPHOS and ATP depletion was proposed for the crustacean *Daphnia magna* under UVB stress (Song 2020).

Update - non-endorsed (by You Song, 06/10/2026)

Across the other studies, ATP decreased in the same direction as uncoupling but usually by a smaller amount at the same exposure. For example, 50 µM CCCP for 1 h caused 77% uncoupling and a 25% ATP reduction in human HeLa cells (Koczor et al., 2009), 50 µM arsenite for 1 h caused about 45% uncoupling and a 20% ATP reduction in *Caenorhabditis elegans* (Luz et al., 2016), and 5 µM CCCP caused 71% uncoupling and a 64% ATP reduction in human HL-60 cells (Sweet and Singh, 1999). Likewise, higher concentrations were needed to reduce ATP than to uncouple OXPHOS, such as 15 versus 30 µM triclosan in zebrafish embryos (Shim et al., 2016), 10 versus 30 µM triclosan in rat RBL-2H3 cells (Weatherly et al., 2018), and 2 versus 20 µM FCCP in human RD cells (Kuruvilla et al., 2003). These data come from different uncouplers, cell types, and exposure durations, so they cannot be combined into a single function, and the general form of the relationship and the precision with which ATP depletion can be predicted from a measured degree of uncoupling have not been defined.

Time-scale

Update - non-endorsed (by You Song, 06/10/2026)

The time-scale varies with the system. Reductions in ATP were observed within 1 h of exposure to uncouplers in human HeLa cells and *C. elegans* (Koczor et al., 2009; Luz et al., 2016). In zebrafish embryos exposed to 0.5 µM 2,4-DNP, uncoupling of OXPHOS was significant after 21 h, whereas a significant reduction in ATP was observed only after 45 h (Bestman et al., 2015). In human RD cells exposed to FCCP, ATP decreased and then increased again within 48 h (Kuruvilla et al., 2003). The lag between uncoupling and ATP depletion can therefore range from less than an hour to about a day, depending on the organism, the stressor, and the compensatory capacity.

Known modulating factors

Update - non-endorsed (by You Song, 06/10/2026)

No modulating factors with quantified effects on this KER have been identified. The factors below are indicated by the studies cited in this KER.

Modulating factor	Details	Effects on the KER	References
Compensatory ATP production	Increased activity of the electron transport chain and activation of other ATP-synthesizing pathways (e.g., glycolysis)	Mild uncoupling can be compensated, so ATP decreases less than the degree of uncoupling would suggest. In human RD cells exposed to FCCP for 48 h, a significant decrease in ATP was followed by a significant increase.	Jose et al., 2011; Kuruvilla et al., 2003
Metabolic phenotype of the cell or tissue	Relative reliance on glycolysis versus oxidative phosphorylation for ATP production	Systems with higher glycolytic capacity are expected to maintain ATP better when OXPHOS coupling decreases.	Jose et al., 2011

Known Feedforward/Feedback loops influencing this KER

- It is known that mild uncoupling of oxidative phosphorylation can enhance the activity of the mitochondrial electron transport chain to produce more ATP, and/or activate other ATP synthetic pathways (e.g., glycolysis) as a compensatory action to impaired OXPHOS (Jose 2011)

Update - non-endorsed (by You Song, 06/10/2026)

Compensatory mechanisms act as negative feedback on this KER. ATP levels are normally balanced between production and consumption (Bonora et al., 2012), and mild uncoupling of oxidative phosphorylation can increase the activity of the electron transport chain to produce more ATP and activate other ATP-synthesizing pathways such as glycolysis (Jose et al., 2011). This compensation explains the transient decrease in ATP in RD cells (Kuruvilla et al., 2003). Its extent and homeostatic limits have not been quantified for this KER, but it is expected to be exceeded when uncoupling is strong or sustained. These mechanisms mainly shape the magnitude and time course of the ATP response and are therefore described here and not represented as separate KEs. No positive feedback or feedforward loops have been identified for this KER.

References

Beard DA. 2005. A biophysical model of the mitochondrial respiratory system and oxidative phosphorylation. PLOS Computational Biology 1:e36. DOI: 10.1371/journal.pcbi.0010036.

Bestman JE, Stackley KD, Rahn JJ, Williamson TJ, Chan SS. 2015. The cellular and molecular progression of mitochondrial dysfunction induced by 2,4-dinitrophenol in developing zebrafish embryos. Differentiation 89:51-69. DOI: 10.1016/j.diff.2015.01.001.

Bonora M, Patergnani S, Rimessi A, De Marchi E, Suski JM, Bononi A, Giorgi C, Marchi S, Missiroli S, Poletti F, Wieckowski MR, Pinton P. 2012. ATP synthesis and storage. Purinergic Signalling 8:343-357. DOI: 10.1007/s11302-012-9305-8.

Heiske M, Letellier T, Klipp E. 2017. Comprehensive mathematical model of oxidative phosphorylation valid for physiological and pathological conditions. The FEBS Journal 284:2802-2828. DOI: https://doi.org/10.1111/febs.14151.

Jose C, Bellance N, Rossignol R. 2011. Choosing between glycolysis and oxidative phosphorylation: A tumor's dilemma? Biochimica et Biophysica Acta (BBA) - Bioenergetics 1807:552-561. DOI: https://doi.org/10.1016/j.bbabio.2010.10.012.

Koczor CA, Shokolenko IN, Boyd AK, Balk SP, Wilson GL, Ledoux SP. 2009. Mitochondrial DNA damage initiates a cell cycle arrest by a Chk2-associated mechanism in mammalian cells. J Biol Chem 284:36191-36201. DOI: 10.1074/jbc.M109.036020.

Kubo S, Niina T, Takada S. 2020. Molecular dynamics simulation of proton-transfer coupled rotations in ATP synthase FO motor. Scientific Reports 10:8225. DOI: 10.1038/s41598-020-65004-1.

Kuruvilla S, Qualls CW, Jr., Tyler RD, Witherspoon SM, Benavides GR, Yoon LW, Dold K, Brown RH, Sangiah S, Morgan KT. 2003. Effects of minimally toxic levels of carbonyl cyanide P-(trifluoromethoxy) phenylhydrazone (FCCP), elucidated through differential gene expression with biochemical and morphological correlations. Toxicol Sci 73:348-361. DOI: 10.1093/toxsci/kfg084.

Luz AT, Godebo TR, Bhatt DP, Ilkayeva OR, Maurer LL, Hirschey MD, Meyer JN. 2016. Arsenite Uncouples Mitochondrial Respiration and Induces a Warburg-Like Effect in Caenorhabditis elegans. Toxicol Sci 154:195-195. DOI: 10.1093/toxsci/kfw185.

Schmidt-Rohr K. 2020. Oxygen is the high-energy molecule powering complex multicellular life: fundamental corrections to traditional bioenergetics. ACS Omega 5:2221-2233. DOI: 10.1021/acsomega.9b03352.

Schmitz JPJ, Vanlier J, van Riel NAW, Jeneson JAL. 2011. Computational modeling of mitochondrial energy transduction. 39:363-377. DOI: 10.1615/CritRevBiomedEng.v39.i5.20.

Shim J, Weatherly LM, Luc RH, Dorman MT, Neilson A, Ng R, Kim CH, Millard PJ, Gosse JA. 2016. Triclosan is a mitochondrial uncoupler in live zebrafish. J Appl Toxicol 36:1662-1667. DOI: 10.1002/jat.3311.

Sithara T, Arun KB, Syama HP, Reshmitha TR, Nisha P. 2017. Morin inhibits proliferation of SW480 colorectal cancer cells by inducing apoptosis mediated by reactive oxygen species formation and uncoupling of Warburg effect. Frontiers in Pharmacology 8. DOI: 10.3389/fphar.2017.00640.

Song Y, Xie L, Lee Y, Tollefsen KE. 2020. De novo development of a quantitative adverse outcome pathway (qAOP) network for ultraviolet B (UVB) radiation using targeted laboratory tests and automated data mining. Environmental Science & Technology 54:13147-13156. DOI: 10.1021/acs.est.0c03794.

Sweet S, Singh G. 1999. Changes in mitochondrial mass, membrane potential, and cellular adenosine triphosphate content during the cell cycle of human leukemic (HL-60) cells. Journal of Cellular Physiology 180:91-96. DOI: https://doi.org/10.1002/(SICI)1097-4652(199907)180:1<91::AID-JCP10>3.0.CO;2-6.

Weatherly LM, Nelson AJ, Shim J, Riitano AM, Gerson ED, Hart AJ, de Juan-Sanz J, Ryan TA, Sher R, Hess ST, Gosse JA. 2018. Antimicrobial agent triclosan disrupts mitochondrial structure, revealed by super-resolution microscopy, and inhibits mast cell signaling via calcium modulation. Toxicol Appl Pharmacol 349:39-54. DOI: 10.1016/j.taap.2018.04.005.

Weatherly LM, Shim J, Hashmi HN, Kennedy RH, Hess ST, Gosse JA. 2016. Antimicrobial agent triclosan is a proton ionophore uncoupler of mitochondria in living rat and human mast cells and in primary human keratinocytes. Journal of Applied Toxicology 36:777-789. DOI: https://doi.org/10.1002/jat.3209.

Relationship: 2768: Decrease, ATP pool leads to Cell injury/death

AOPs Referencing Relationship

AOP Name	Adjacency	Weight of Evidence	Quantitative Understanding
Uncoupling of oxidative phosphorylation leading to growth inhibition via ATP depletion associated cell death	adjacent	Moderate	Not Specified
Increase in reactive oxygen species leading to growth inhibition via lipid peroxidation and cell death	adjacent	High	Moderate
Excessive reactive oxygen species leading to growth inhibition via protein oxidation and cell injury/death	adjacent		
Excessive reactive oxygen species leading to growth inhibition via fatty acid oxidation and cell injury/death	adjacent		
Increase in reactive oxygen species leading to growth inhibition via protein oxidation and cell death	adjacent	High	Moderate

Evidence Supporting Applicability of this Relationship

Taxonomic Applicability

Term	Scientific Term	Evidence	Links
humans	Homo sapiens	High	NCBI
mammals	mammals	High	NCBI
fish	fish	High	NCBI
crustaceans	Daphnia magna	High	NCBI
green algae	Ulva compressa	High	NCBI

Life Stage Applicability

Life Stage	Evidence
All life stages	Moderate

Sex Applicability

Sex	Evidence
Unspecific	Moderate

The biological domain of applicability is broad because ATP-dependent homeostasis is a conserved property of living cells. The KER is most directly applicable to eukaryotic cells and tissues in which mitochondrial and/or glycolytic ATP supply maintains cellular viability. It is particularly relevant to metabolically active tissues and developing organisms where energy demand is high. It is applicable to both sexes and to multiple life stages, although sensitivity may differ with developmental status, tissue type, temperature, oxygen availability, and metabolic reserve.

The chemical and stressor applicability domain includes stressors that reduce cellular ATP through mitochondrial

inhibition, OXPHOS uncoupling, oxidative stress, membrane disruption, calcium overload, metabolic poisons, hypoxia or other mechanisms that impair ATP synthesis or increase ATP demand beyond compensatory capacity. In the ROS-growth AOP network, this KER is most relevant downstream of OXPHOS impairment caused by lipid peroxidation or protein oxidation, where energetic failure contributes to increased cell injury/death.

Key Event Relationship Description

This key event relationship describes the causal and predictive link by which a decrease in the cellular adenosine triphosphate (ATP) pool leads to increased cell injury and/or cell death. ATP is required to maintain ion gradients, plasma membrane integrity, mitochondrial homeostasis, macromolecular repair, vesicular trafficking, and regulated cell death programs. When ATP depletion is sufficiently severe or prolonged, energy-dependent adaptive and repair processes fail, calcium and sodium homeostasis are disrupted, mitochondrial permeability transition may be promoted, and cells may undergo apoptosis, necrosis, necroptosis-like injury or mixed forms of cell death depending on cellular context and residual ATP availability (Nieminen et al., 1994; Leist et al., 1997; Bonora et al., 2012).

The direction of this KER is from reduced ATP availability to increased cell injury/death. The KER is not intended to specify a single mode of cell death. Rather, it captures the general biological principle that loss of cellular energy supply increases the probability of irreversible cellular injury and death, with the exact death phenotype depending on cell type, severity of ATP depletion, duration of exposure, and availability of death-execution pathways.

Evidence Supporting this KER

The overall evidence supporting this KER is considered moderate to high. Biological plausibility is high because ATP is indispensable for cellular homeostasis and because severe ATP depletion is a well-established trigger of irreversible cell injury and death. Empirical support is moderate to high because multiple studies in mammalian cells, algae, aquatic organisms and cancer cell systems demonstrate concordance between ATP depletion and cell injury/death; however, the exact quantitative threshold varies substantially across biological systems and exposure conditions.

Biological Plausibility

Biological plausibility is high. ATP depletion compromises core cellular maintenance processes including ion pumping, membrane integrity, cytoskeletal dynamics, protein turnover, DNA repair, and mitochondrial function. When ATP supply falls below the level required for homeostasis, cells lose the ability to maintain electrochemical gradients and to execute energy-dependent adaptive responses. Severe energetic collapse promotes necrotic injury, while partial ATP depletion may permit regulated apoptotic execution depending on residual ATP availability and caspase competence (Nieminen et al., 1994; Leist et al., 1997; Nicotera et al., 1998; Zong and Thompson, 2006).

The mechanistic relationship is also supported by mitochondrial cell-death biology. ATP depletion often accompanies mitochondrial membrane depolarization, permeability transition, impaired oxidative phosphorylation, calcium dysregulation, and increased reactive oxygen species generation. These processes can amplify cellular injury and increase the probability of cell death (Kroemer et al., 1998; Green and Kroemer, 2004; Halestrap, 2009; Bonora et al., 2012).

Empirical Evidence

Empirical support is moderate to high. In mammalian systems, ATP depletion has been directly linked to cell killing after metabolic inhibition, and experimental work has shown that ATP depletion rather than mitochondrial depolarization can mediate hepatocyte death under some conditions (Nieminen et al., 1994). A widely cited study demonstrated that intracellular ATP concentration influences whether cells die by apoptosis or necrosis, supporting both causality and phenotype dependence (Leist et al., 1997). Calcium electroporation studies provide dose-dependent evidence that ATP depletion is associated with reduced cancer cell survival and increased cell death (Hansen et al., 2015).

Evidence from environmental and ecotoxicological systems is consistent with this relationship. In *Chlamydomonas reinhardtii*, herbicide exposure produced ATP depletion and cell injury/death in a multiple-endpoint assay, demonstrating concordance between energetic disruption and cellular toxicity in an algal model (Nestler et al., 2012). In eastern oysters, cadmium exposure affected mitochondrial bioenergetics and was associated with cellular damage endpoints, supporting applicability of energetic failure to cell injury in aquatic invertebrates (Sokolova et al., 2005). In ROS-growth concordance data, mitochondrial toxicants and oxidative stressors including paraquat, rotenone, cadmium and hydrogen peroxide frequently produce decreased ATP or mitochondrial dysfunction together with cytotoxicity or tissue injury, although direct measurement of both KEs in the same study is not always available.

Evidence type	Summary	Representative references
Biological plausibility	ATP is required for ion homeostasis, membrane maintenance, repair, and regulated cell death execution; severe ATP depletion promotes irreversible cell injury/death.	Nieminen et al. 1994; Leist et al. 1997; Bonora et al. 2012

Evidence type	Summary	Representative references
Temporal concordance	ATP depletion can occur rapidly after metabolic inhibition or mitochondrial impairment and precedes detectable loss of viability or death execution in several cell systems.	Nieminen et al. 1994; Hansen et al. 2015
Dose-response concordance	Increasing intensity of energetic perturbation or calcium electroporation increases ATP depletion and cell killing.	Hansen et al. 2015
Incidence concordance	Systems showing marked ATP depletion commonly show increased cytotoxicity, cell injury or cell death, although moderate ATP depletion may be compensated in some contexts.	Leist et al. 1997; Nestler et al. 2012; Sokolova et al. 2005
Essentiality / intervention	Experimental data indicate that ATP availability influences the form and occurrence of cell death; restoration or maintenance of energy status can reduce injury in some systems, but direct rescue evidence across taxa remains limited.	Leist et al. 1997; Nicotera et al. 1998

Uncertainties and Inconsistencies

The main uncertainty is that ATP depletion is not the only cause of cell injury/death. Cell death may also be initiated by DNA damage, receptor-mediated apoptosis, oxidative damage, calcium overload, lysosomal injury, proteotoxic stress or inflammatory signaling. Consequently, the presence of cell injury/death does not uniquely imply ATP depletion. The KER is strongest when ATP decline occurs before or at lower concentrations than cell death and when the upstream energetic perturbation is mechanistically established.

Another uncertainty concerns severity thresholds. Moderate ATP depletion may be reversible or may shift cells into cell-cycle arrest, reduced proliferation, or adaptive metabolic compensation rather than death. Conversely, very severe ATP depletion may prevent the energy-requiring execution of apoptosis and produce necrotic injury instead. Therefore, the downstream phenotype depends on the magnitude and duration of ATP depletion and on cellular metabolic reserve (Leist et al., 1997; Nicotera et al., 1998).

Empirical evidence across environmental species remains less dense than evidence from mammalian cell systems. Many ecotoxicological studies measure ATP, mitochondrial dysfunction, or cytotoxicity separately rather than measuring both KEs in the same time- and dose-resolved experiment. This limits the strength of concordance assessment across the full taxonomic applicability domain.

Quantitative Understanding of the Linkage

The quantitative understanding of this KER is considered moderate. Quantitative evidence supports a general response-response relationship in which larger or longer decreases in ATP increase the probability and severity of cell injury/death. However, a single universal threshold cannot be defined because ATP demand, ATP reserve, glycolytic capacity, cell type, death pathway, and exposure duration vary substantially among biological systems.

Several studies support threshold-like behavior. In hepatocytes, ATP depletion mediated killing after metabolic inhibition, supporting a causal threshold relationship between energetic collapse and cell death (Nieminen et al., 1994). Experiments in human T cells showed that intracellular ATP concentration can act as a switch influencing apoptotic versus necrotic death phenotypes (Leist et al., 1997). Calcium electroporation studies showed dose-dependent ATP depletion and reduced survival, supporting a quantitative relationship between the upstream energetic disturbance and the downstream cell death outcome (Hansen et al., 2015).

Response-response relationship

The expected response-response relationship is generally monotonic but non-linear. Small or transient ATP reductions may be tolerated or compensated. Larger reductions increase the probability of cell stress, impaired repair, loss of membrane integrity, and cell death. At extreme ATP depletion, necrotic injury is favored, whereas intermediate depletion may permit energy-dependent apoptosis depending on cell type and execution machinery (Leist et al., 1997; Nicotera et al., 1998).

Time-scale

The time scale of ATP depletion can range from minutes to hours following direct mitochondrial inhibition, uncoupling, metabolic inhibition, or membrane-disrupting interventions. Observable downstream cell injury/death may occur within hours to days depending on cell type, severity of ATP loss, and endpoint measured. In whole organisms, cell death may contribute to tissue injury or growth impairment over longer time frames.

Known modulating factors

Modulating factor	Details	Effect on this KER	References

Modulating factor	Details	Effect on this KER	References
Magnitude and duration of ATP depletion	Transient or moderate ATP depletion versus severe, sustained ATP depletion.	Severe and sustained ATP depletion increases probability of irreversible injury/death. Partial depletion may cause reversible stress or cell-cycle arrest.	Nieminen et al. 1994; Leist et al. 1997
Metabolic flexibility / glycolytic capacity	Ability to compensate for mitochondrial ATP loss by glycolysis or alternative ATP-generating pathways.	Higher metabolic flexibility may reduce sensitivity of the downstream cell death response.	Bonora et al. 2012; Zong and Thompson 2006
Cell type and proliferative/metabolic demand	Highly energy-demanding or poorly glycolytic cells may have lower tolerance to ATP depletion.	Alters threshold and time-scale for transition from ATP depletion to injury/death.	Bonora et al. 2012; Green and Kroemer 2004
Mitochondrial permeability transition and calcium homeostasis	Calcium overload and permeability transition can amplify ATP depletion and membrane failure.	Can accelerate progression to necrotic or mixed cell injury phenotypes.	Halestrap 2009; Nieminen et al. 1994
Apoptotic execution machinery	Caspase competence and residual ATP availability influence whether death is apoptotic or necrotic.	Determines cell death mode rather than the existence of injury/death per se.	Leist et al. 1997; Nicotera et al. 1998

Known Feedforward/Feedback loops influencing this KER

Feedback and feedforward processes may influence this linkage. ATP depletion can impair ion pumps, causing calcium dysregulation and mitochondrial permeability transition, which further suppresses ATP production and amplifies injury. Loss of mitochondrial function may also increase ROS generation, further damaging mitochondrial and cellular components. Conversely, glycolytic compensation and stress-response activation may temporarily buffer ATP depletion and delay cell death.

References

Bonora M, Patergnani S, Rimessi A, De Marchi E, Suski JM, Bononi A, Giorgi C, Marchi S, Missiroli S, Poletti F, Wieckowski MR, Pinton P. 2012. ATP synthesis and storage. Purinergic Signaling 8:343-357. https://doi.org/10.1007/s11302-012-9305-8.

Green DR, Kroemer G. 2004. The pathophysiology of mitochondrial cell death. Science 305:626-629. https://doi.org/10.1126/science.1099320.

Halestrap AP. 2009. What is the mitochondrial permeability transition pore? Journal of Molecular and Cellular Cardiology 46:821-831. https://doi.org/10.1016/j.yjmcc.2009.02.021.

Hansen EL, Sozer EB, Romeo S, Frandsen SK, Vernier PT, Gehl J. 2015. Dose-dependent ATP depletion and cancer cell death following calcium electroporation, relative effect of calcium concentration and electric field strength. PLoS ONE 10:e0122973. https://doi.org/10.1371/journal.pone.0122973.

Kroemer G, Dallaporta B, Resche-Rigon M. 1998. The mitochondrial death/life regulator in apoptosis and necrosis. Annual Review of Physiology 60:619-642. https://doi.org/10.1146/annurev.physiol.60.1.619.

Leist M, Single B, Castoldi AF, Kuhnle S, Nicotera P. 1997. Intracellular adenosine triphosphate (ATP) concentration: a switch in the decision between apoptosis and necrosis. Journal of Experimental Medicine 185:1481-1486. https://doi.org/10.1084/jem.185.8.1481.

Lemasters JJ, Qian T, Bradham CA, Brenner DA, Cascio WE, Trost LC, Nishimura Y, Nieminen AL, Herman B. 1999. Mitochondrial dysfunction in the pathogenesis of necrotic and apoptotic cell death. Journal of Bioenergetics and Biomembranes 31:305-319. https://doi.org/10.1023/A:1005419617371.

Nestler H, Groh KJ, Schonenberger R, Behra R, Schirmer K, Eggen RIL, Suter MJF. 2012. Multiple-endpoint assay provides a detailed mechanistic view of responses to herbicide exposure in Chlamydomonas reinhardtii. Aquatic Toxicology 110-111:214-224. https://doi.org/10.1016/j.aquatox.2012.01.014.

Nicotera P, Leist M, Ferrando-May E. 1998. Intracellular ATP, a switch in the decision between apoptosis and necrosis. Toxicology Letters 102-103:139-142. https://doi.org/10.1016/S0378-4274(98)00298-7.

Nieminen AL, Saylor AK, Herman B, Lemasters JJ. 1994. ATP depletion rather than mitochondrial depolarization mediates hepatocyte killing after metabolic inhibition. American Journal of Physiology - Cell Physiology 267:C67-C74. https://doi.org/10.1152/ajpcell.1994.267.1.C67.

OECD. 2022. Uncoupling of oxidative phosphorylation leading to growth inhibition via decreased cell

proliferation. OECD Series on Adverse Outcome Pathways No. 28. Paris: OECD Publishing.

Sokolova IM, Sokolov EP, Ponnappa KM. 2005. Cadmium exposure affects mitochondrial bioenergetics and gene expression of key mitochondrial proteins in the eastern oyster Crassostrea virginica Gmelin (Bivalvia: Ostreidae). Aquatic Toxicology 73:242-255. https://doi.org/10.1016/j.aquatox.2005.03.016.

Zong WX, Thompson CB. 2006. Necrotic death as a cell fate. Genes & Development 20:1-15. https://doi.org/10.1101/gad.1376506.

Relationship: 2767: Cell injury/death leads to Decrease, Growth

AOPs Referencing Relationship

AOP Name	Adjacency	Weight of Evidence	Quantitative Understanding
Uncoupling of oxidative phosphorylation leading to growth inhibition via increased cytosolic calcium	adjacent	Moderate	Not Specified
Uncoupling of oxidative phosphorylation leading to growth inhibition via ATP depletion associated cell death	adjacent	Moderate	Not Specified
Uncoupling of oxidative phosphorylation leading to growth inhibition via decreased Na-K ATPase activity	adjacent		
Uncoupling of oxidative phosphorylation leading to growth inhibition via mitochondrial swelling	adjacent		
Increase in reactive oxygen species leading to growth inhibition via lipid peroxidation and cell death	adjacent	High	Moderate
Excessive reactive oxygen species leading to growth inhibition via protein oxidation and cell injury/death	adjacent		
Excessive reactive oxygen species leading to growth inhibition via fatty acid oxidation and cell injury/death	adjacent		
Increase in reactive oxygen species leading to growth inhibition via oxidative DNA damage and cell death	adjacent	High	Moderate
Increase in reactive oxygen species leading to growth inhibition via protein oxidation and cell death	adjacent	High	Moderate
ROS formation leading to growth inhibition modulated by the Keap1–Nrf2 antioxidant response	adjacent	High	High

Evidence Supporting Applicability of this Relationship

Taxonomic Applicability

Term	Scientific Term	Evidence	Links
humans	Homo sapiens	Moderate	NCBI
mammals	mammals	Moderate	NCBI
fish	fish	Moderate	NCBI
crustaceans	Daphnia magna	Moderate	NCBI
green algae	Ulva compressa	Moderate	NCBI

Life Stage Applicability

Life Stage	Evidence
All life stages	Moderate

Sex Applicability

Sex	Evidence
Unspecific	Moderate

The KER is applicable to biological systems in which growth depends on maintenance or expansion of viable cell number or biomass. This includes unicellular populations, developing embryos, juvenile organisms, growing tissues, and adult organisms in which tissue condition or somatic growth is assessed. Taxonomic applicability is broad across eukaryotes, but empirical support is strongest for algae, aquatic invertebrates, mollusks, fish, and mammalian embryo or cell models. The KER is not sex-specific, but sex, endocrine status, life stage, and environmental context may modulate sensitivity. The relationship is most relevant when cell injury/death is sufficiently extensive, sustained, or located in growth-relevant tissues. It is less predictive when growth is reduced by upstream mechanisms that suppress proliferation or metabolism without substantial cell death.

Key Event Relationship Description

This KER describes the causal and predictive relationship whereby an increase in cell injury and/or cell death leads to a decrease in growth. The upstream KE, cell injury/death, represents loss of cellular viability or severe cellular damage resulting in apoptosis, necrosis, or other forms of lethal cellular injury. The downstream KE, decreased growth, represents reduced accumulation of biomass, body size, length, cell density, tissue mass, or other growth-related endpoints at organ, organism, or population levels. The biological logic of the KER is that growth requires a positive balance between production of new cellular material and loss of existing cells. When cell injury/death is sufficiently frequent, persistent, or spatially distributed across growth-relevant tissues, net cell accumulation is reduced and tissue or organismal growth is impaired. In unicellular systems, increased cell death directly reduces viable cell density and biomass accumulation. In multicellular organisms, the relationship depends on the affected tissue, the ability to compensate through proliferation or regeneration, and the timing of injury relative to developmental or growth windows.

This relationship is not intended to imply that all decreases in growth are caused by cell death. Growth can also decrease through reduced cell proliferation, altered energy allocation, endocrine disruption, nutrient limitation, or developmental delay without overt lethality. Rather, the KER applies when increased cell injury/death is of sufficient magnitude or duration to reduce the viable cellular pool needed for growth or to damage growth-relevant tissues. Within the ROS-growth AOP network, this KER provides a terminal convergence relationship for pathways in which oxidative stress, DNA strand breaks, or ATP depletion produce cytotoxicity that contributes to reduced growth.

Evidence Supporting this KER

Biological Plausibility

Overall call: High. Growth at the level of a tissue, organ, organism, or cell population depends on net accumulation of cells and cellular biomass. Increased cell death directly lowers the number of viable cells and can reduce tissue mass, disrupt morphogenesis, or impair the capacity for biomass accumulation. This relationship is strongly supported by developmental and cell-size control principles showing that final tissue and organism size depend on the balance among cell growth, cell division, and cell death (Conlon and Raff, 1999). In embryos and developing organisms, excessive cell death can reduce cell number available for organ formation and growth, whereas in unicellular populations and cell cultures, cytotoxicity directly reduces viable cell density. The KER is therefore mechanistically plausible across taxa, although the magnitude of growth impairment depends on the tissue affected, compensatory proliferation, regeneration, and exposure duration.

Empirical Evidence

Overall call: Moderate. Empirical support is moderate because multiple studies report concordance between cell injury/death and growth-related effects, but the evidence is heterogeneous and not always designed specifically to test this KER. In several systems, cell injury/death and growth inhibition are measured at different time points, and growth can be affected by mechanisms other than cell death. Nevertheless, the available data support the expected direction of effect across algae, fish embryos, mollusks, and mammalian embryo models.

Biological system	Stressor / context	Upstream evidence: cell injury/death	Downstream evidence: decreased growth	Concordance interpretation	Reference
Chlamydomonas reinhardtii	Paraquat	Loss of membrane integrity measured by SYTOX Green; cell death observed at approximately 0.5 uM after 24 h.	Reduced cell density/growth after 72 h; growth LOEC approximately 0.1 uM and EC50 approximately 0.26 uM.	Partial temporal and endpoint concordance. Growth effects occurred at or below cytotoxicity thresholds, indicating that cell death contributes but is not the only driver of growth inhibition.	Jamers and De Coen, 2010
Chlamydomonas reinhardtii	Paraquat and herbicides	SYTOX Green cell death observed with paraquat; cell injury occurred alongside ATP depletion and other stress endpoints.	Assay system reported reduced growth/cell density and multiple mechanistic endpoints following herbicide exposure.	Supports association between cytotoxicity and reduced population growth, but includes multiple parallel mechanisms.	Nestler et al., 2012

Biological system	Stressor / context	Upstream evidence: cell injury/death	Downstream evidence: decreased growth	Concordance interpretation	Reference
Mouse and rat whole-embryo culture	Methanol	Cell death markedly elevated in embryos at growth-relevant concentrations.	Mouse and rat embryo growth reduction observed in exposed cultures.	Supports developmental concordance between increased embryonic cell death and growth impairment, with species differences in sensitivity.	Abbott et al., 1995
Eastern oyster, Crassostrea virginica	Cadmium and temperature interaction	Hemocyte mortality, lysosomal destabilization, and cellular energy disruption observed under cadmium stress.	Reduced condition index and increased mortality under combined cadmium and elevated temperature.	Supports linkage between cellular injury and reduced growth/condition, although growth is modified by temperature and energy budget effects.	Sokolova et al., 2005; Cherkasov et al., 2006
Fish embryos and juveniles	Rotenone	Histological lesions and tissue injury observed at low concentrations.	Developmental delay and growth-related impairment reported after short-term exposure.	Supports association between cellular/tissue injury and developmental growth impairment; direct measurement of cell death was limited.	Melo et al., 2015
Marine copepod, Paracyclopina nana	Gamma radiation	Radiation induced oxidative stress and impaired survival/development.	Growth retardation and failure of nauplii to develop to adults observed.	Supports an adverse sequence from stress-induced cellular injury to growth retardation, although cell death was not always measured directly.	Won and Lee, 2014

Uncertainties and Inconsistencies

The main uncertainty is that decreased growth is an integrative endpoint and can arise through several mechanisms that do not require overt cell death. Reduced proliferation, ATP depletion, endocrine disruption, altered energy allocation, nutrient limitation, delayed development, or behavioral effects can all reduce growth. For this reason, cell injury/death should be interpreted as a sufficient but not always necessary contributor to decreased growth. A second uncertainty is that many studies measure cytotoxicity and growth at different times or in different tissues, which limits direct evaluation of temporal concordance. In some algal studies, growth inhibition occurs at lower concentrations than overt cell death, suggesting that non-lethal impairment of proliferation, photosynthesis, or energy metabolism may precede cell death. Conversely, mild or localized cell injury may be compensated by repair or proliferation and may not lead to measurable growth reduction. These uncertainties support a moderate, rather than high, empirical call for this KER.

Quantitative Understanding of the Linkage

Overall call: Low to moderate. Quantitative understanding is limited because the relationship between cell injury/death and growth depends on the proportion of cells affected, tissue location, developmental timing, compensatory proliferation, regenerative capacity, and organismal energy allocation. At a conceptual level, the linkage is quantitative: growth rate reflects the balance between biomass accumulation and biomass or cell loss, so increasing the frequency or magnitude of cell death should reduce net growth if cell replacement or compensatory

growth is insufficient. However, few studies provide response-response models that predict growth reduction from a measured degree of cell injury/death across taxa or stressors.

Response-response relationship

In cell populations and unicellular organisms, the quantitative relationship can be relatively direct because viable cell density is part of the growth measurement. In multicellular organisms, the relationship is less direct because growth can continue despite localized cell death if compensatory proliferation or tissue repair occurs. Some data show concordance between cytotoxicity and growth inhibition, but these data are generally insufficient to define universal thresholds. Therefore, quantitative understanding should be considered low to moderate for broad AOP-Wiki application, with higher confidence possible for specific model systems where cell viability and growth rate are measured in the same assay and time course.

Known modulating factors

Modulating factor	Relevant details	Effect on the KER	Supporting references
Developmental stage	Embryonic and larval stages, rapid growth phases	Increases sensitivity because rapid tissue growth requires high net cell accumulation; cell death during development can disproportionately impair growth.	Abbott et al., 1995; Conlon and Raff, 1999
Tissue regenerative capacity	Capacity for compensatory proliferation or tissue repair	Reduces probability that cell death will translate into growth impairment when surviving cells can replace lost cells.	Conlon and Raff, 1999
Exposure duration and timing	Acute versus chronic exposures; timing relative to growth window	Longer or developmentally timed exposures increase probability of growth effects from cell loss.	Jamers and De Coen, 2010; Melo et al., 2015
Energy and nutritional status	Energy budget, food availability, metabolic reserve	Can increase or decrease impact of cell death on growth by altering compensatory capacity and resource allocation.	Sokolova, 2013; Cherkasov et al., 2006
Environmental stressors	Temperature, oxygen availability, salinity, co-exposures	Can amplify cytotoxicity or reduce compensatory growth responses, modifying downstream growth effects.	Cherkasov et al., 2006; Won and Lee, 2014

References

Abbott, B. D., Harris, M. W., & Birnbaum, L. S. (1995). Cell death in rat and mouse embryos exposed to methanol in whole embryo culture: Evaluation of the role of the p53 tumor suppressor gene. Teratogenesis, Carcinogenesis, and Mutagenesis, 15(3), 147–169.

Cherkasov, A. S., Biswas, P. K., Ridings, D. M., Ringwood, A. H., & Sokolova, I. M. (2006). Effects of acclimation temperature and cadmium exposure on cellular energy budgets in the marine mollusk Crassostrea virginica: Linking cellular and mitochondrial responses. Journal of Experimental Biology, 209(7), 1274–1284.

Conlon, I., & Raff, M. (1999). Size control in animal development. Cell, 96(2), 235–244.

Jamers, A., & De Coen, W. (2010). Effect assessment of the herbicide paraquat on a green alga using differential gene expression and biochemical biomarkers. Environmental Toxicology and Chemistry, 29(4), 893–901.

Knops, M., Altenburger, R., & Segner, H. (2001). Alterations of physiological energetics, growth and reproduction

of Daphnia magna under toxicant stress. Aquatic Toxicology, 53(2), 79–90.

Melo, K. M., Oliveira, R., Grisolia, C. K., Domingues, I., Pieczarka, J. C., de Souza Filho, J., & Nagamachi, C. Y. (2015). Short-term exposure to low doses of rotenone induces developmental, biochemical, behavioral, and histological changes in fish. Environmental Science and Pollution Research, 22(18), 13926–13938.

Nestler, H., Groh, K. J., Schönenberger, R., Eggen, R. I. L., & Suter, M. J.-F. (2012). Multiple-endpoint assay provides a detailed mechanistic view of responses to herbicide exposure in Chlamydomonas reinhardtii. Aquatic Toxicology, 110–111, 214–224.

Organisation for Economic Co-operation and Development (OECD). (2018). Users' handbook supplement to the guidance document for developing and assessing adverse outcome pathways. OECD Series on Adverse Outcome Pathways No. 1. OECD Publishing, Paris.

Organisation for Economic Co-operation and Development (OECD). (2021). Guidance document for the scientific review of adverse outcome pathways. OECD Series on Testing and Assessment No. 344. OECD Publishing, Paris.

Sokolova, I. M. (2013). Energy-limited tolerance to stress as a conceptual framework to integrate the effects of multiple stressors. Integrative and Comparative Biology, 53(4), 597–608.

Sokolova, I. M., Sokolov, E. P., & Ponnappa, K. M. (2005). Cadmium exposure affects mitochondrial bioenergetics and gene expression of key mitochondrial proteins in the eastern oyster Crassostrea virginica Gmelin (Bivalvia: Ostreidae). Aquatic Toxicology, 73(3), 242–255.

Won, E. J., & Lee, J. S. (2014). Gamma radiation induces growth retardation, impaired egg production, and oxidative stress in the marine copepod Paracyclopina nana. Aquatic Toxicology, 150, 17–26.